

| | | | |
|--|--|--|-----------|
| 1. Report No. UM-HSRI-BI-73-3-1 | 2. Government Accession No. | 3. Recipient's Catalog No. | |
| 4. Title and Subtitle Crash test device development; Repeatable Pete | | 5. Report Date June 1973 | |
| | | 6. Performing Organization Code | |
| 7. Author(s) James H. McElhaney, Ph.D. | | 8. Performing Organization Report No. UM-HSRI-BI-73-3-1 | |
| 9. Performing Organization Name and Address Highway Safety Research Institute University of Michigan Huron Parkway and Baxter Road Ann Arbor, Michigan 48105 | | 10. Work Unit No. | |
| | | 11. Contract or Grant No. | |
| | | 13. Type of Report and Period Covered Final Report | |
| 12. Sponsoring Agency Name and Address Motor Vehicle Manufacturers Association 320 New Center Building Detroit, Michigan 48202 | | 14. Sponsoring Agency Code | |
| 15. Supplementary Notes | | | |
| <p>16. Abstract</p> <p>This report describes the development and performance of a new crash test device aptly named, "Repeatable Pete." The general goal of the project was the development of an adequate crash test device to aid in the evaluation of the injury reducing potential of automotive passenger restraint systems. The general design criteria were:</p> <ol style="list-style-type: none"> 1. Repeatability of test results 2. Reproducibility of test results 3. Human-like responses in a moderate automotive crash environment 4. Non-frangibility <p>Biomechanical data describing the dynamic impact responses of unembalmed cadavers was used as the basis for humanlike performance.</p> <p>New and uniquely repeatable joints were developed. A urethane head and chest with more humanlike dynamic response was also developed. Self-skinning urethane foam was used extensively. Great care was used throughout to insure proper isolation of metal components.</p> <p>Extensive sled testing of two devices was done to verify performance.</p> | | | |
| 17. Key Words CRASH TEST DEVICE ANTHROPOMETRIC DUMMY REPEATABILITY REPRODUCIBILITY SLED TESTING | | 18. Distribution Statement UNLIMITED | |
| 19. Security Classif. (of this report) UNCLASSIFIED | 20. Security Classif. (of this page) UNCLASSIFIED | 21. No. of Pages 146 | 22. Price |

UM-HSRI-BI-73-3

FINAL REPORT
CRASH TEST DEVICE DEVELOPMENT
Repeatable Pete
June 1973

By:

James H. McElhaney, Ph.D.
Head, Biomechanics Department



Frontispiece
Some achieve greatness through their own efforts,
others have greatness thrust upon them,
"a friend."

ACKNOWLEDGEMENTS

This project was supported by the Motor Vehicle Manufacturers Association (MVMA). However, the opinions, findings and conclusions expressed in this report are those of the author and not necessarily those of MVMA. In addition,

- a. Approval of the final report is not to be construed as acceptance by MVMA of the test device (Repeatable Pete) as a compliance dummy for evaluating the safety performance of automotive restraint systems.
- b. Approval of the final report is not to be construed as acceptance by MVMA of the geometric, inertial, and biomechanical performance requirements set forth in the report as being representative of a 50th percentile adult male.
- c. Approval of the final report is not to be construed as acceptance by MVMA of the system performance of Repeatable Pete being less, equal, or better than any other dummy.
- d. Approval of the final report is not to be construed as acceptance by MVMA of the system performance of Repeatable Pete being characteristic of the 50th percentile adult male.

SUMMARY

This report describes the development and performance of a new crash test device aptly named, "Repeatable Pete." The general goal of the project was the development of an adequate crash test device to aid in the evaluation of the injury reducing potential of automotive passenger restraint systems. The general design criteria were:

1. Repeatability of Test Results
2. Reproducibility of Test Results
3. Human-like responses in a moderate automotive crash environment
4. Non-Frangibility

Biomechanical data describing the dynamic impact responses of un-embalmed cadavers was used as the basis for humanlike performance.

New and uniquely repeatable joints were developed. A urethane head and chest with more humanlike dynamic response was also developed. Self-skinning urethane foam was used extensively. Great care was used throughout to insure proper isolation of metal components.

Extensive sled testing of two devices was done to verify performance.

TABLE OF CONTENTS

| | Page |
|---|------|
| 1.0 GENERAL DESIGN CONSIDERATIONS | 1 |
| 1.1 <u>Accomplishments to Date</u> | 2 |
| 1.2 <u>Additional Requirements</u> | 3 |
| 1.3 <u>Humanlike Responses</u> | 3 |
| 1.4 <u>Durability, Simplicity and Ease of Manufacture</u> | 4 |
| 1.5 <u>Redesign</u> | 4 |
| 1.6 <u>Coordination with other Projects</u> | 4 |
| 2.0 OVERALL SPECIFICATIONS | 5 |
| 2.1 <u>Size and Shape</u> | 5 |
| 2.2 <u>Segment Weights and Centers of Gravity and Moments of Inertia</u> | 5 |
| 2.2.1 Weights | 6 |
| 2.2.2 Center of Gravity | 6 |
| 2.2.3 Moments of Inertia | 6 |
| 2.3 <u>Ranges of Motion</u> | 18 |
| 3.0 HEAD, MECHANICAL PROPERTIES | 20 |
| 3.1 <u>Static Stiffness</u> | 20 |
| 3.2 <u>Impact Response</u> | 20 |
| 3.3 <u>Repeatability</u> | 21 |
| 3.4 <u>Driving Point Impedance, Dynamic Stiffness and Dynamic Damping</u> | 21 |
| 3.5 <u>Scalp</u> | 21 |
| 3.6 <u>Instrumentation</u> | 51 |
| 4.0 TORSO | 52 |
| 4.1 <u>Static Stiffness</u> | 52 |
| 4.2 <u>Dynamic Stiffness and Damping</u> | 52 |

TABLE OF CONTENTS (continued)

| | Page |
|--|------|
| 4.3 <u>Repeatability</u> | 53 |
| 4.4 <u>Chest Design</u> | 53 |
| 4.5 <u>Instrumentation</u> | 53 |
| 4.5.1 Accelerometers | 53 |
| 4.5.2 Chest Displacement Transducer | 60 |
| 5.0 NECK | 60 |
| 6.0 PELVIS | 61 |
| 6.1 <u>Geometry</u> | 61 |
| 6.2 <u>Ranges of Motion</u> | 61 |
| 7.0 SPINE | 71 |
| 8.0 JOINTS | 71 |
| 8.1 <u>Design Features</u> | 71 |
| 8.2 <u>Life Tests</u> | 71 |
| 9.0 LIMBS | 72 |
| 9.1 <u>Patella</u> | 72 |
| 9.2 <u>Femur Loads</u> | 72 |
| 9.3 <u>Seating Position</u> | 72 |
| 10.0 SYSTEM PERFORMANCE | 86 |
| 10.1 <u>Sled Test Program</u> | 86 |
| 10.1.1 Introduction | 86 |
| 10.1.2 Mode I: Lap- and Torso-Belted Tests | 86 |
| 10.1.3 Mode II: Pre-inflated Airbag Tests | 89 |
| 10.1.4 Mode III: Dash/Windshield Impact Tests | 95 |
| 10.1.5 Mode IV: Steering Wheel Impact Tests | 95 |
| 10.2 <u>Instrumentation and Data Acquisition</u> | 101 |

TABLE OF CONTENTS (continued)

| | Page |
|---|------|
| 10.2.1 Accelerometer Data | 105 |
| 10.2.2 High Speed Motion Pictures | 105 |
| 10.2.3 Graph-Check Sequence Photographs | 105 |
| 10.3 <u>Sled Test Results</u> | 106 |
| 10.3.1 Mode I Test Results | 108 |
| 10.3.2 Mode II Test Results | 112 |
| 10.3.3 Mode III Test Results | 117 |
| 10.3.4 Mode IV Test Results | 123 |
| 11.0 MAINTENANCE MANUAL | 128 |
| 11.1 <u>Introduction</u> | 128 |
| 11.2 <u>Instrument Mounting</u> | 128 |
| 11.2.1 Head | 128 |
| 11.2.2 Chest | 129 |
| 11.2.3 Upper Leg | 130 |
| 11.3 <u>Assembly Procedure</u> | 130 |
| 11.3.1 Head | 130 |
| 11.3.2 Neck | 131 |
| 11.3.3 Covering | 131 |
| 11.3.4 Arm Assembly | 132 |
| 11.3.5 Leg Assembly | 135 |
| 11.3.6 Torso | 136 |
| 11.3.7 Joint Assembly Procedure | 138 |
| Appendix A | |
| Appendix B | |
| Appendix C | |

TABLE OF FIGURES

| | Page |
|--|------|
| Figure 1. Body Dimensions Side View | 7 |
| Figure 2. Body Dimensions Front View | 8 |
| Figure 3. Pivot Locations Side View | 9 |
| Figure 4. Pivot Locations Front View | 10 |
| Figure 5. Ranges of Motion | 15 |
| Figure 6. Center of Gravity Determination | 16 |
| Figure 7. Moment of Inertia Measurement | 17 |
| Figure 8. Human Skull Load-Deflection Curves, L-R Loading, 12 Tests | 24 |
| Figure 9. Human Skull Load-Deflection Curves, A-P Loading 12 Tests | 25 |
| Figure 10. Composite Force-Time Curves for Cadaver Front Head Impacts with Rigid Impactor | 26 |
| Figure 11. Composite Acceleration-Time Curves from A-P Accelerometer for Cadaver Front Head Impacts with Rigid Impactor | 27 |
| Figure 12. Composite Acceleration-Time Curves from S-I Accelerometer for Cadaver Front Head Impacts with Rigid Impactor | 28 |
| Figure 13. Composite Force-Time Curves for Cadaver Front Head Impacts with Padded Impactor | 29 |
| Figure 14. Composite Acceleration-Time Curves from A-P Accelerometer for Cadaver Front Head Impacts with Padded Impactor | 30 |
| Figure 15. Composite Acceleration-Time Curves from S-I Accelerometer for Cadaver Front Head Impacts with Padded Impactor | 31 |
| Figure 16. Composite Force-Time Curves for Cadaver Side Head Impacts with Rigid Impactors | 32 |
| Figure 17. Composite Acceleration-Time Curves from L-R Accelerometer for Cadaver Side Head Impacts with Rigid Impactor | 33 |

TABLE OF FIGURES (continued)

| | Page |
|---|------|
| Figure 18. Composite Acceleration-Time Curves from S-I Accelerometer for Cadaver Side Head Impacts with Rigid Impactor | 34 |
| Figure 19. Composite Force-Time Curves for Cadaver Side Head Impacts with Padded Impactor | 35 |
| Figure 20. Composite Acceleration-Time Curves from L-R Accelerometer for Cadaver Side Head Impacts with Padded Impactor | 36 |
| Figure 21. Composite Acceleration-Time Curves from S-I Accelerometer for Cadaver Side Head Impacts with Padded Impactor | 37 |
| Figure 22. Mechanical Impedance of Heads (Frontal) | 38 |
| Figure 23. Mechanical Impedance of Heads (Parietal) | 39 |
| Figure 24. Typical Setup for Front Head Impact with Rigid Impactor | 40 |
| Figure 25. Typical Setup for Front Head Impact with Rigid Impactor | 41 |
| Figure 26. Typical Setup for Side Head Impact with Rigid Impactor | 42 |
| Figure 27. Typical Setup for Side Head Impact with Rigid Impactor | 43 |
| Figure 28. Typical Setup for Padded Impact | 44 |
| Figure 29. Typical Setup for Padded Impact | 45 |
| Figure 30. Static Head Compression Test | 46 |
| Figure 31. Driving Point Impedance Test | 47 |
| Figure 32. Front View HSRI Head and Neck | 48 |
| Figure 33. Side View HSRI Head and Neck | 49 |
| Figure 34. Rear View HSRI Head and Neck | 50 |
| Figure 35. HSRI One Piece Chest | 54 |
| Figure 36. Chest Displacement Transducer | 55 |
| Figure 37. Chest Displacement Transducer Installed in Chest | 56 |

TABLE OF FIGURES (continued)

| | Page |
|--|------|
| Figure 38. Composite Load-Deflection Curves for Cadaver Front Chest Impacts | 57 |
| Figure 39. GM Blunt Impact Performance Corridors and HSRI Data on Chest Impacts | 58 |
| Figure 40. Human Chest Impacts | 59 |
| Figure 41. HSRI Dummy Neck | 62 |
| Figure 42. Comparison of Resultant Linear Head Accelerations for the HSRI Neck and Human Volunteers in Flexion | 63 |
| Figure 43. Comparison of Neck Moment for the HSRI Neck and Human Volunteers in Flexion | 64 |
| Figure 44. Comparison of Head Angular Accelerations and Range of Angular Motion for the HSRI Neck and Human Volunteers in Flexion | 65 |
| Figure 45. Comparison of Head Angular Accelerations and Range of Angular Motion for the HSRI Neck, Human Volunteers, and Cadavers in Extension | 66 |
| Figure 46. Resultant Linear Head Accelerations for the HSRI Neck in Extension for 5g (A-33) and 9.5g (A-30) Input Accelerations | 67 |
| Figure 47. Comparison of Neck Moment for the HSRI Neck, Human Volunteers, and Cadavers in Extension | 68 |
| Figure 48. Pelvis | 69 |
| Figure 49. Rear Assembly "Repeatable Pete." | 70 |
| Figure 50. Typical Joint Assembly | 75 |
| Figure 51. Typical Joint Components | 76 |
| Figure 52. Typical Joint Assembly | 77 |
| Figure 53. Typical Wrist and Ankle Joint | 78 |
| Figure 54. Joint Springs | 79 |
| Figure 55. Life Test of Knee Joint | 80 |
| Figure 56. Typical Setup for Joint Fatigue Testing | 81 |

TABLE OF FIGURES (continued)

| | Page |
|--|------|
| Figure 57. Section through Self-Skinning Urethane Foam Forearm | 82 |
| Figure 58. Knee Joint Assembly | 83 |
| Figure 59. Front Assembly "Repeatable Pete" | 84 |
| Figure 60. Dummy Seating Positions | 85 |
| Figure 61. Mode I: Pre-Test Configuration (Foot Straps not shown) | 87 |
| Figure 62. Mode I: Dummy Positioning Fixture | 88 |
| Figure 63. Mode II: Pre-Test Configuration of Body Buck with Airbag Preinflated | 90 |
| Figure 64. Mode II: Pre-Test Configuration | 91 |
| Figure 65. Mode II: Pre-Test Configuration of Deflated Bag, Knee Catcher and Support Panel | 93 |
| Figure 66. Airbag Pre-Inflation | 94 |
| Figure 67. Mode III: Pre-Test Configuration | 96 |
| Figure 68. Mode III: Post-Test Configuration of Windshield and Support Frame | 97 |
| Figure 69. Mode III: Post-Test Configuration | 98 |
| Figure 70. Mode III: Post-Test Configuration | 99 |
| Figure 71. Mode III: Dummy Head after Six Windshield Impacts | 100 |
| Figure 72. Steering Column Test Set-Up | 102 |
| Figure 73. Mode IV: Pre-Test Configuration | 103 |
| Figure 74. Mode IV: Post-Test Configuration | 104 |
| Figure 75. Mode I: Sequence Photo of Impact | 109 |
| Figure 76. Mode II: Sequence Photo of Impact | 114 |
| Figure 77. Mode II: Moment of Impact | 115 |
| Figure 78. Mode III: Sequence Photo of Impact | 118 |

TABLE OF FIGURES (continued)

| | Page |
|--|------|
| Figure 79. Mode III: Moment of Impact | 119 |
| Figure 80. Mode IV: Sequence Photo of Impact | 124 |

LIST OF TABLES

| | Page |
|---|------|
| Table 1. Body Dimensions | 11 |
| Table 2. Segment Weights, C.G. Locations and Moments of Inertia | 12 |
| Table 3. Pivot Locations - Inches | 13 |
| Table 4. 50th Percentile Male Ranges of Motions and Terminology | 14 |
| Table 5. Measured Segment Weights, C.G. Locations, and Moments of Inertia | 19 |
| Table 6. Description of Cadavers | 22 |
| Table 7. Dummy # 1 Joint Torque Specifications | 73 |
| Table 8. Dummy # 2 Joint Torque Specifications | 74 |
| Table 9. Dummy Performance Summary | 107 |
| Table 10. Data Summary: Lap- And Torso-Belted Tests | 110 |
| Table 11. Data Summary: Pre-Inflated Airbag Tests | 116 |
| Table 12. Data Summary: Dash/Windshield Impact Tests | 120 |
| Table 13. Data Summary: Steering Wheel Impact Tests | 125 |

LIST OF DRAWINGS

| Drawing Number | Title | Page |
|----------------|---|------------|
| 101-624-B | Mounting Triaxial Accelerometer Endevco Model | 140 |
| 101-625-B | #1 Retainer & Accelerometer Support for Endevco | 141 |
| 101-670-B | Foot | 142 |
| 101-674-B | Neck Assembly | 143 |
| 101-723-B | Mount- Triaxial Accelerometer - Setra | 144 |
| 101-724-B | Mounting - Triaxial Accelerometer - Setra | 145 |
| 101-727-B | Mounting Bracket-Head for Setra | 146 |
| 100-975-D | Shoulder Assembly | Appendix C |
| 100-998-C | Adapter - Neck - Assembly | Appendix C |
| 101-675-D | Head Assembly | Appendix C |
| 101-704-D | Hip Joint Assembly | Appendix C |
| 101-729-D | Spine Assembly - Upper | Appendix C |
| 101-742-C | Lower Spine Assembly | Appendix C |

CRASH TEST DEVICE PERFORMANCE REQUIREMENTS

1.0 GENERAL DESIGN CONSIDERATIONS

The general goal of this project was the production of an adequate crash test device to aid in the evaluation of the injury reducing potential of automotive passenger restraint systems. To be considered adequate, a crash test device must provide repeatable and reproducible results within acceptable limits. In addition, its performance must be correlatable with that of a standard human under similar loading. This does not mean that the device must necessarily behave like a human but the test results from use of the device must provide sufficient information to enable the prediction of real world system performance.

Unfortunately the human is subject to a wide variety of traumatic injuries. Many of the mechanical parameters and biomechanical factors that describe those injuries are unknown and some may be unknowable. Based on this fact and contemporary crash test evaluation procedures, the crash test device described here uses currently accepted methods of evaluating performance. Therefore, since the performance criteria have been established from human volunteer and/or human surrogates and since this crash test device will be utilized in a broad range of automotive crash environments, its dynamic performance was matched to unembalmed cadaver performance.

A further consideration has been cost. While the cost of a frangible crash test device would be acceptable for certain research purposes, the large number of tests required for engineering development require a non-frangible device.

Thus, an adequate crash test device for automotive restraint system performance evaluation must possess the following properties:

1. Repeatability of test results
2. Reproducibility of test results
3. Human like responses in a moderate automotive crash environment
4. Non-frangibility in a moderate automotive crash environment.

A moderate automotive crash environment is considered to be a 30 mph barrier crash. Human like responses have been developed from the published bio-mechanical literature and other recognized sources available to HSRI. Unfortunately, available funds did not permit any Biomechanical research to be performed under the terms of this project.

In the following sections the design criteria and performance of the crash test device "Repeatable Pete" will be discussed.

1.1 Accomplishments to Date

The following accomplishments have been achieved under the existing contract:

1. A head has been developed that performs in a humanlike manner when impacted with a rigid or padded striker in the front and side. This head, through a unique c.g. triax-accelerometer mounting design, offers c.g. accelerations correlatable with current cadaver measurements and head injury criteria.

2. A neck has been developed that meets the Mertz criteria. This neck is simple, inexpensive and durable.

3. A spine consisting of rigid metal blocks isolated from each other by butyl rubber shock pads in the thoracic region and a cast urethane lumbar region has been developed.

4. New joints for all locations have been developed. These joints have been life tested on a dynamic torsion testing machine designed for this purpose. They are rugged and long lived. They are preset at the factory and unless damaged, require no further adjustments.

5. A new method of applying skin and soft tissue has been developed using self-skinning urethane. This material is much stronger than current materials and more humanlike and is used in the arms and legs.

6. A new flexible urethane chest and abdomen has been developed that matches the dynamic responses of unembalmed cadavers when impacted in anterior-posterior direction as tested at HSRI.

1.2 Additional Requirements

Within the limitations of the current contract and adequate crash test device has not been developed. It is felt, however, that an adequate test device can be developed in a one year continuation program. The following additional tasks remain:

1. Redesign to provide more humanlike responses, particularly the spine and pelvis responses.

2. Redesign to make a more durable, simpler and more easily manufactured device.

3. Redesign to correct deficiencies after the extensive prototype sled testing accomplished in the current period.

1.3 Humanlike Responses

The HSRI crash test device has been designed to match the dynamic responses of the human head, neck and thorax. The thorax specifications are limited to the dynamic load-deflection characteristics of the front middle section, however. New biomechanical information has been developed at HSRI regarding the human thorax's characteristics when loaded from the side, additional human neck responses, abdominal characteristics and human spin characteristics. It is proposed to continue this project to incorporate these human characteristics into the existing design.

1.4 Durability, Simplicity and Ease of Manufacture

Much has been learned about the special fabrication methods required for this device. Unfortunately, time limitations have not permitted several of these new methods to be totally incorporated in the current design. Special moulding methods for rigid urethane, self-skinning urethane foam and butyl rubber parts have been developed. Additional attention however, should be given to developing more durable, simpler and more easily manufactured parts with the same performance level.

1.5 Redesign

Time limitations have prevented a second iteration in the testing and redesign cycle. This second iteration is required to correct certain small but important deficiencies established during the extensive prototype sled testing accomplished in the current period.

In addition, NHTSA has developed a set of dummy specifications. Since this project was initiated prior to the NHTSA announcement, "Repeatable Pete" does not meet the NHTSA dummy specifications. It is felt that the NHTSA specifications are obsolete in light of the new Biomechanical information available and the demonstrated performance of HSRI's "Repeatable Pete."

1.6 Coordination with other Projects

A sensitivity study and an improved joint structure project have been proposed by HSRI for FY 1974 efforts. Identification of those dummy parameters that most influence performance can be accomplished by suitable exercising of existing mathematical models of the vehicle occupant. These two projects will provide valuable information which should be coordinated with additional crash test device development.

2.0 OVERALL SPECIFICATIONS

Because human beings vary so widely in weight, external dimensions and ranges of motion, the 50th percentile male specifications have been agreed upon somewhat arbitrarily for the purposes of this program.

2.1 Size and Shape

"Repeatable Pete" generally conforms with the dimensions of the 50th percentile male as defined by the so-called "Golden Shells." These shells are seated figures sculptured to toleranced dimensions. The source document for these dimensions was, "Weight, Height and Selected Body Dimension of Adults 1960-62." Report series 11, number 8, National Center for Health Statistics, Public Health Service, HEW. At the time of the "Golden Shell" development, data on the thorax and abdominal dimensions were lacking. The missing dimensions were arrived at by S. W. Alderson and confirmed for the SAE Crash Dummy Sub-Committee by H. T. E. Hertzberg by extrapolation of data from Air Force personnel. A newer document, "Skinfolds, Body Girths, Bio-cromial Diameter and Selected Anthropometric Indices of Adults, United States, 1960-62," Report series 11, number 35, National Center for Health Statistics, Public Health Service, H.E.W., showed that the extrapolated thorax and abdomen values were somewhat low but acceptable. For the dimensions of the 50th percentile male form thus established, refer to Figures 1 and 2 and Table 1.

2.2 Segment Weights and Centers of Gravity and Moments of Inertia

The correct segment weight distribution and segment centers of gravity were developed by Alderson Research Laboratories by means of phantoms. Each phantom was built by first constructing a mold of the "Golden Shell" and registering the closest fitting human skeleton which could be obtained into

the mold. Lungs, premolded of material approximating the specific gravity of their human counterpart, were also registered. Fat equivalent material was built up in the buttocks and abdominal regions and finally a plastic non-hydroscopic material, having a specific gravity of 1.0 to simulate average tissue, was poured to complete the phantom.

2.2.1 Weights

The segment weights are based on those developed by Alderson Research Laboratories. The segmenting of the above described phantom is based on following those locations which are practical for a crash test device. The segment weights are listed in Table 2 and identified in Figure 3.

2.2.2 Center of Gravity

Centers of gravity were determined by suspending a segment successively from two points located in the plane of symmetry, as shown in Figure 4. The intersection of the two resulting vertical axes located the horizontal axis upon which the center of gravity is located, at its point of intersection with the plane of symmetry. Locations of the centers of gravity are given in Table 5 as the distance of the C.G. from the center of rotation when the segment is suspended vertically from its specified center of rotation (Figure 3).

2.2.3 Moments of Inertia

Moments of inertia about the specified points of rotation were obtained by suspending the segment at its center of rotation by means of a pair of needle bearings, and allowed to oscillate freely through a small angle. Period of oscillation was obtained by an optical switch consisting of a pin-light source and photovoltaic detector. A needle placed on the segment in line with the point of suspension and C.G. when the segment was suspended, activated the optical switch as the segment passed through its vertical position.

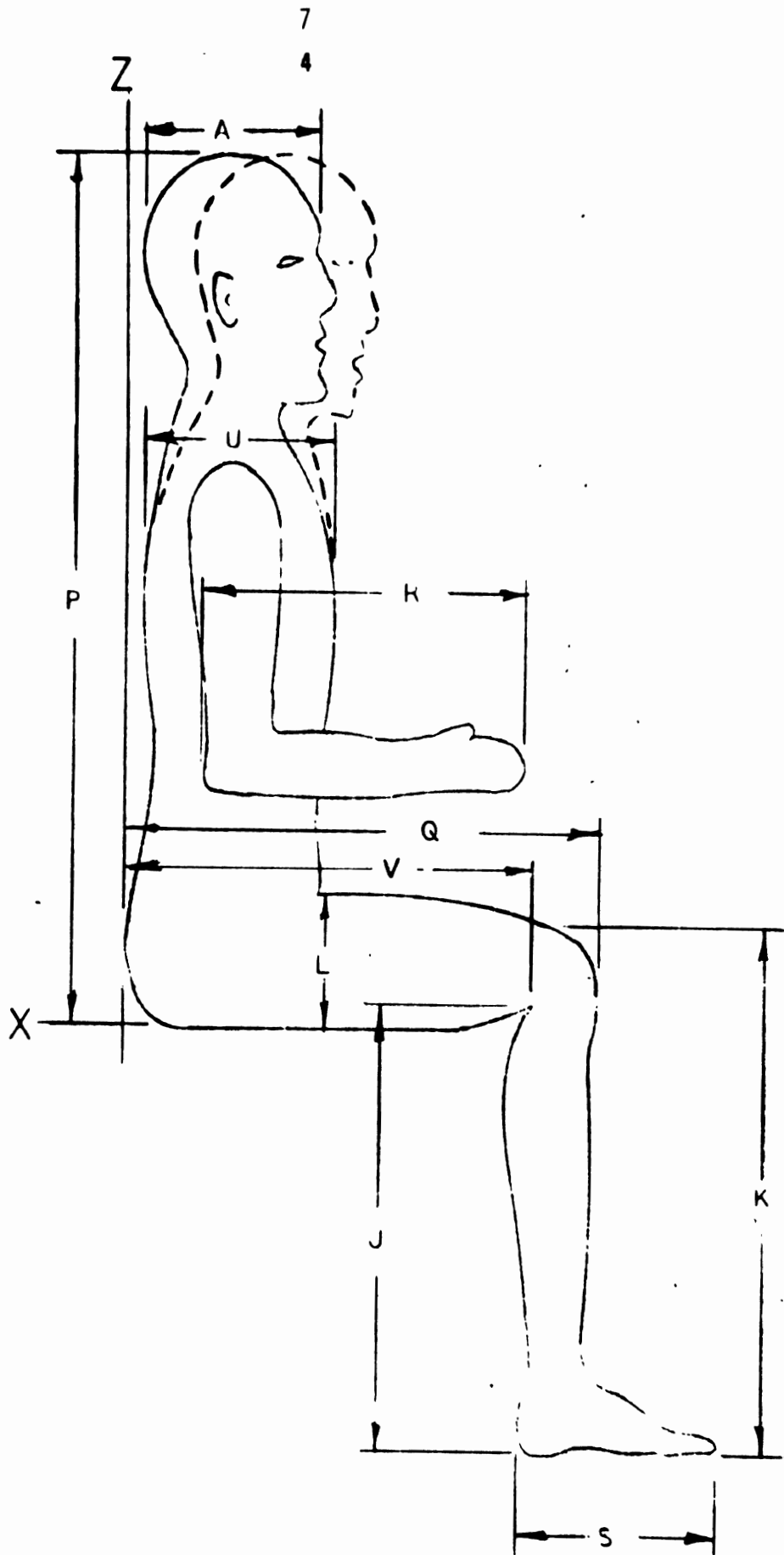


FIGURE 1. BODY DIMENSIONS SIDE VIEW

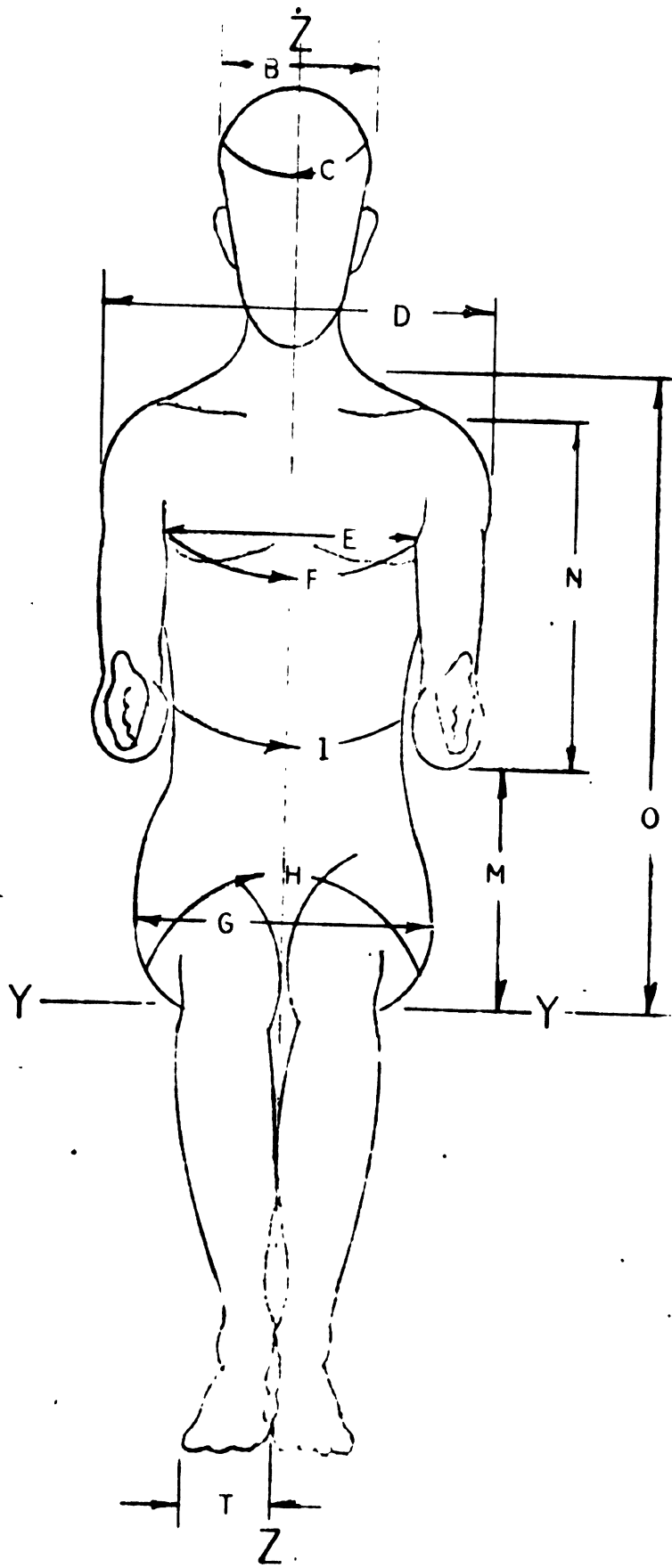


FIGURE 2. BODY DIMENSIONS FRONT VIEW

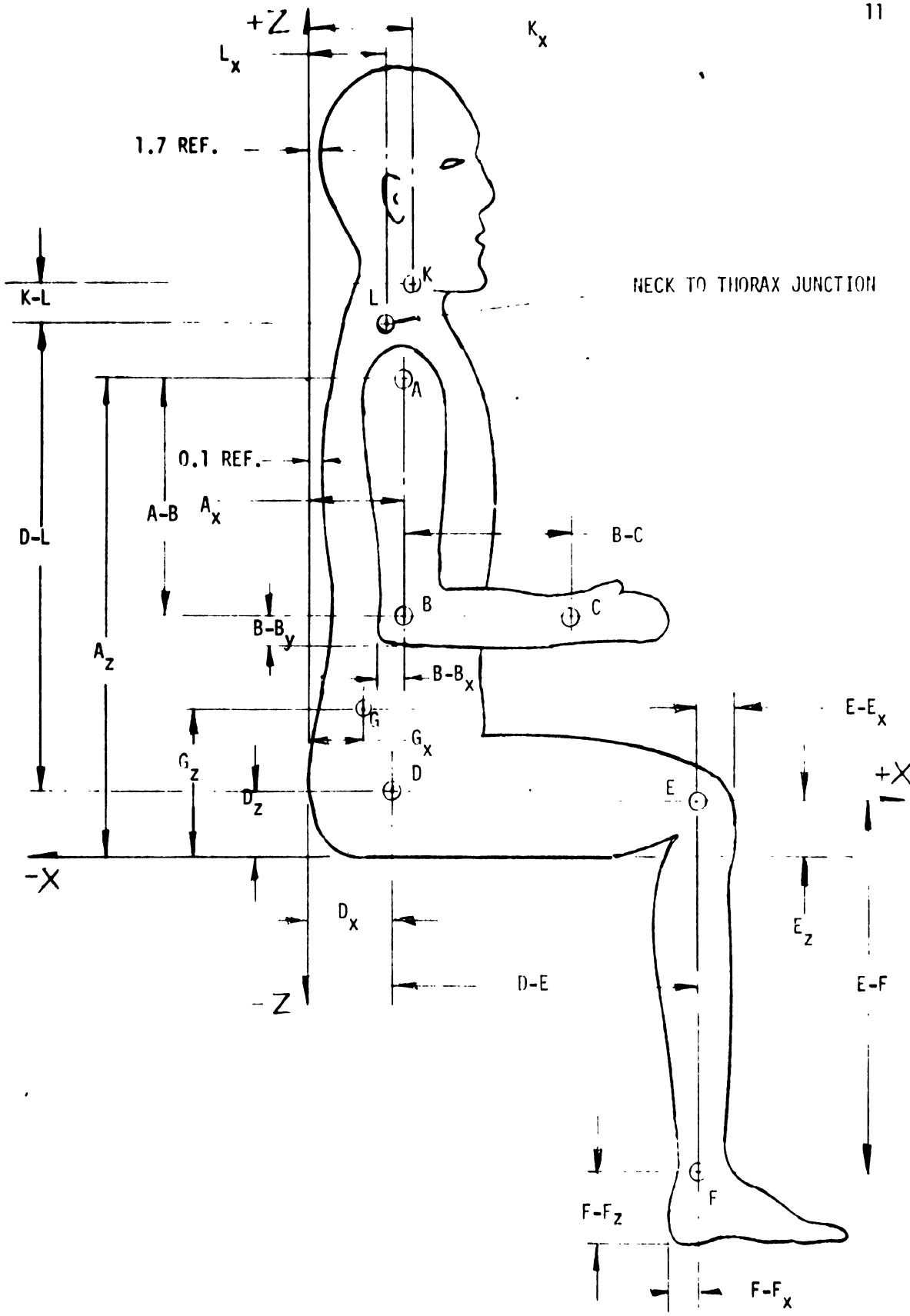


FIGURE 3. PIVOT LOCATIONS SIDE VIEW

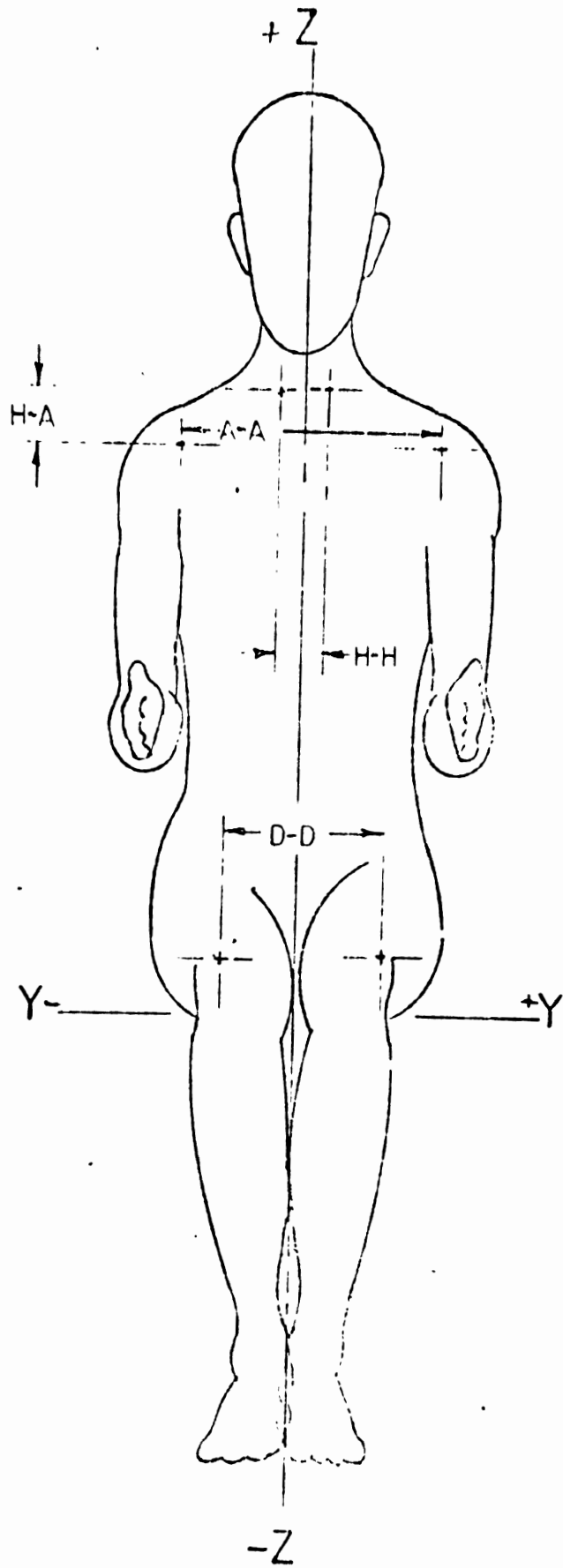


FIGURE 4. PIVOT LOCATIONS FRONT VIEW

TABLE 1. BODY DIMENSIONS

| Letter Designation | Description | Dimension Inches | Figure |
|--------------------|---------------------------------|------------------|--------|
| A | Head Length | 7.7±0.2 | 1 |
| B | Head Breadth | 6.1±0.2 | 2 |
| C | Head Circumference | 22.5±0.5 | 2 |
| D | Shoulder Breadth-(Bi-deltoid) | 17.9±0.4 | 2 |
| E | Chest Breadth | 12.5±0.3 | 2 |
| F | Chest Circumference | 37.7±1.0 | 2 |
| G | Hip Breadth, Sitting | 15.1±0.4 | 2 |
| H | Hip Circumference, Sitting | 41.5±1.0 | 2 |
| I | Waist Circumference, Sitting | 33.0±1.0 | 2 |
| J | Popliteal Height, Sitting | 17.3±0.2 | 1 |
| K | Knee Height, Sitting | 21.4±0.3 | 1 |
| L | Thigh Clearance Height, Sitting | 5.7±0.3 | 1 |
| M | Elbow Rest Height | 9.5±0.5 | 2 |
| N | Shoulder-Elbow Length | 14.1±0.3 | 2 |
| O | Mid-Shoulder Height | 24.3±0.5 | 2 |
| P | Sitting Height, Erect | 35.7±0.5 | 1 |
| Q | Buttock-Knee Length | 23.3±0.3 | 1 |
| R | Elbow-Fingertip Length | 18.7±0.5 | 1 |
| S | Foot Length | 10.5±0.2 | 1 |
| T | Foot Breadth | 3.8±0.3 | 2 |
| U | Chest Depth | 9.0±0.4 | 1 |
| V | Buttock-Popliteal Length | 19.5±0.3 | 1 |

TABLE 2. SEGMENT WEIGHTS, C.G. LOCATIONS AND MOMENTS OF INERTIA

| Segment | Weight Each Lbs.&Tol. | Weight Total Lbs. | Ref. Axis for C.G. and J | Center of Gravity | | |
|---|-----------------------------|-------------------------|--------------------------------|-------------------|----------------|----------------------------|
| | | | | X from Ref. | Z from Ref. | J in # sec ² |
| Head | 11.6 ±.3 | - | K | -0.2±.1 | +4.9±.2 | 0.97±.09 |
| Head and Neck | 13.6±.4 | 13.6 | L | +2.1±.1 | +5.9±.4 | 1.85±.17 |
| Foot | 2.7±.2 | 5.4 | F | +2.1±.1 | -1.8±.1 | 0.10±.01 |
| Lower Leg | 8.1±.4 | 16.2 | E | -0.5±.1 | -7.7±.5 | 1.73±.16 |
| Upper Leg | 12.3±.6 | 24.6 | E | -6.1±.4 | -0.1±.1 | 1.60±.14 |
| Upper Leg - Hip | 21.7 Ref | - | D | +5.6±.3 | -1.0±.1 | 3.42±.31 |
| Pelvic Region | 38.4±1.5 | 38.4 | G | +2.0±.1 | -4.5±.3 | 4.22±.38 |
| Abdomen | 7.6 Ref | - | G | +1.8±.1 | +1.3±.1 | 0.27±.02 |
| Shoulder, Thorax, and Abdomen | 49.7±2.0 | 49.7 | G | +1.6±.1 | +7.2±.4 | 10.10±.95 |
| Upper Arm | 3.9±.2 | 7.8 | A | -0.1±.1 | -5.2±.3 | 0.51±.04 |
| Forearm | 3.0±.2 | 6.0 | B | +4.0±.2 | 0.0±.1 | 0.24±.02 |
| Hand | 1.4±.2 | 2.8 | C | +2.9±.2 | - | 0.032±.003 |
| Total Body | - | 7.0 164.5 | X-Y Origin | +9.7±.6 | +9.1±.6 | -- |
| Moment of Inertia Total Body About C.G. | | | | | | 74.18±6.68 |

TABLE 3. PIVOT LOCATIONS - INCHES

| | Feature | Dim. |
|------------------|------------------------------------|---------|
| A _z | Shoulder Height | 21.5±.3 |
| A-A | Shoulder Width: Center-to-Center | 15.0±.3 |
| A _x | Shoulder-to-Back Line | 4.1±.3 |
| A-B | Shoulder-Elbow | 10.5±.2 |
| B-C | Elbow-Wrist | 9.9±.2 |
| B-B _x | Elbow-to-Back | 1.5±.2 |
| B-B _y | Elbow-to-Underside | 1.8±.2 |
| D _z | Hip Height | 3.5±.3 |
| D _x | Hip-to-Back Line | 5.5±.3 |
| D-E | Hip-Knee | 15.5±.2 |
| E _z | Knee-to-Seat | 3.0±.2 |
| E-E _x | Knee-to-Front | 2.2±.2 |
| E-F | Knee-to-Ankle | 16.2±.2 |
| F-F _z | Ankle-to-Floor | 3.0±.2 |
| F-F _x | Ankle-to-Heel Back | 2.6±.2 |
| G _z | Lumbar-to-Seat | 9.0±.3 |
| G _x | Lumbar-to-Back-Line | 3.3±.2 |
| D-D | Hip Center-to-Center (SAE Pelvis) | 6.9±.3 |
| H-A | Sterno-Clavicular-to-Shoulder | 0.7±.1 |
| L _x | Neck-to-Back Line | 3.9±.2 |
| D-L | Hip-to-Neck | 20.0±.3 |
| K _x | Head-to-Back-Line | 5.8±.2 |
| K-L | Head-Neck | 3.1±.1 |
| H-H | Sterno-Clavicular Center-to-Center | 1.4±.2 |

TABLE 4. 50th PERCENTILE MALE RANGES OF MOTIONS AND TERMINOLOGY

| Letter Designation | Title | Angle, Degree |
|--------------------|---------------------------------------|---------------|
| | Head with Respect to Torso | |
| B | Flexion | 60+10 |
| A | Hyperextension | 95°+10° |
| C | Lateral Flexion | ±40±10 |
| | Shoulder Girdle with Respect to Torso | |
| E | Anterior-Posterior Excursion | ±10 |
| F | Elevation | 20+10 |
| AG | Depression | 10+10 |
| | Upper Arm of Shoulder | |
| G | Abduction | 0 |
| H | Abduction | 135 }+10 |
| I | Medial Rotation | 90 |
| J | Lateral Rotation | 0 }+10 |
| K | Flexion | 180 |
| L | Hyperextension | 60 }+10 |
| | Forearm at Elbow | |
| M | Flexion | 135 min |
| | Hand at Wrist | |
| P | Palmar Flexion | 90+10 |
| Q | Dorsiflexion | 60+10 |
| | Thigh at hip | |
| R | Flexion | 120 min |
| S | Hyperextension | 45+10 |
| U | Medial Rotation | 50 |
| T | Lateral Rotation | 50 }+10 |
| W | Abduction | 10 |
| V | Abduction | 50 }+10 |
| | Lower Leg at Knee | |
| X | Flexion | 135 min |
| | Foot at Ankle | |
| Z | Plantar Flexion | 45 }+10 |
| Y | Dorsiflexion | 30 |
| | Long Axis of Torso | |
| AC | Flexion | 40 min |
| AE | Hyperextension | 30+5 |
| AD | Lateral Flexion | 35+10 |
| AE | Rotation | 35+10 |

NOTE: The movements are described and measured from a referenced "anatomical position," which is defined as: "An erect standing posture with the palm surfaces of the hands positioned anteriorly (in supination.)"

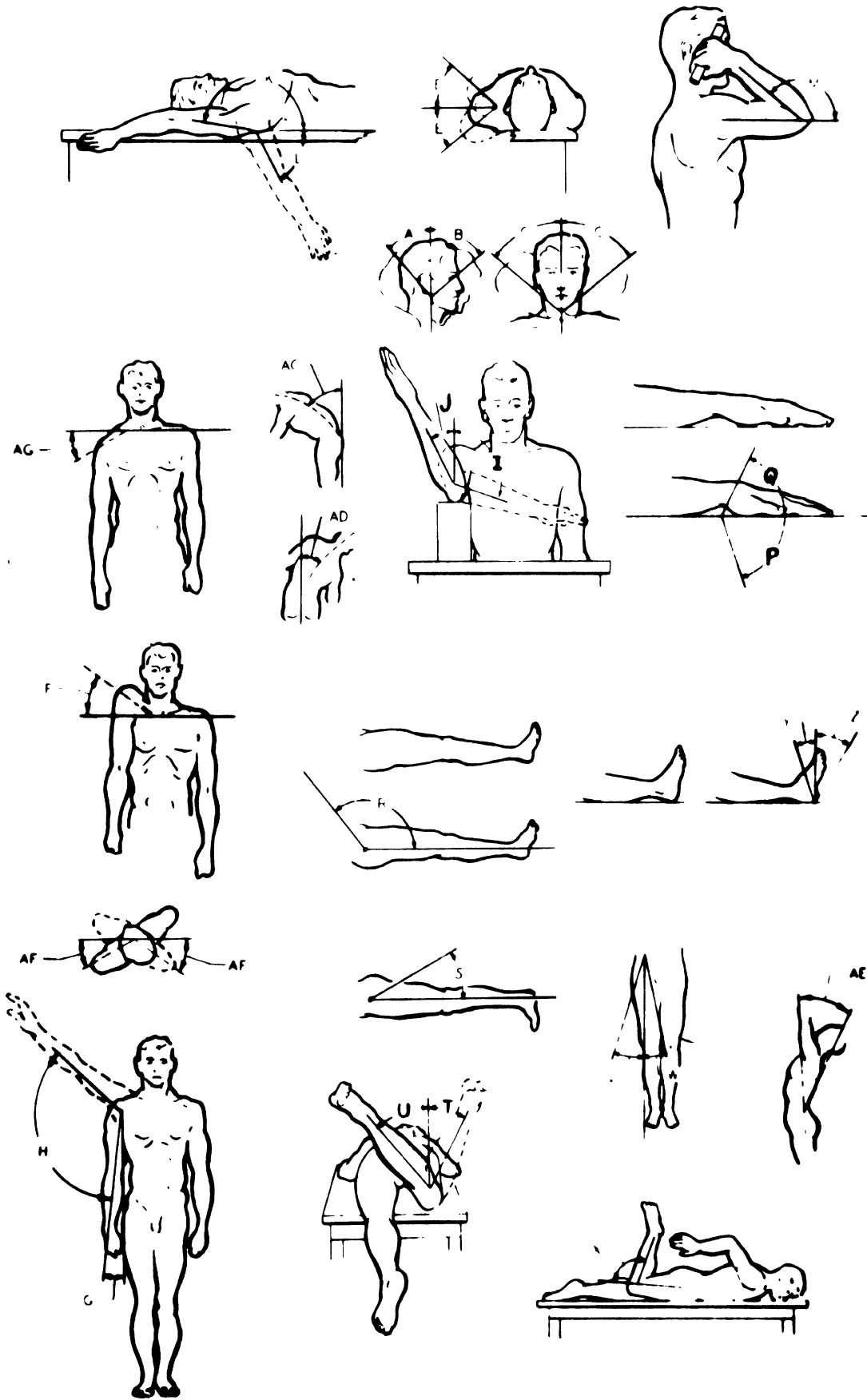


FIGURE 5. RANGES OF MOTION

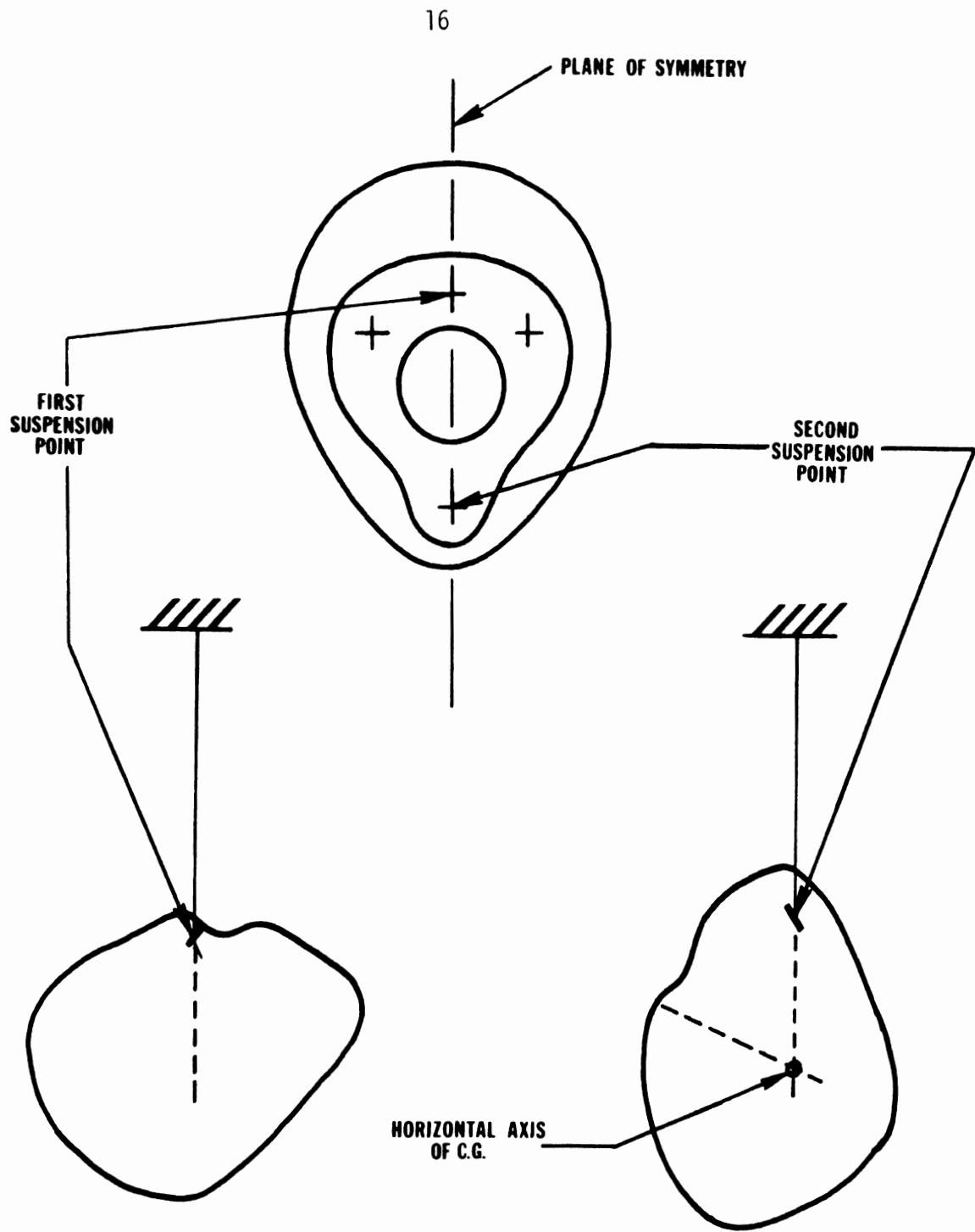


FIGURE 6

CENTER OF GRAVITY DETERMINATION

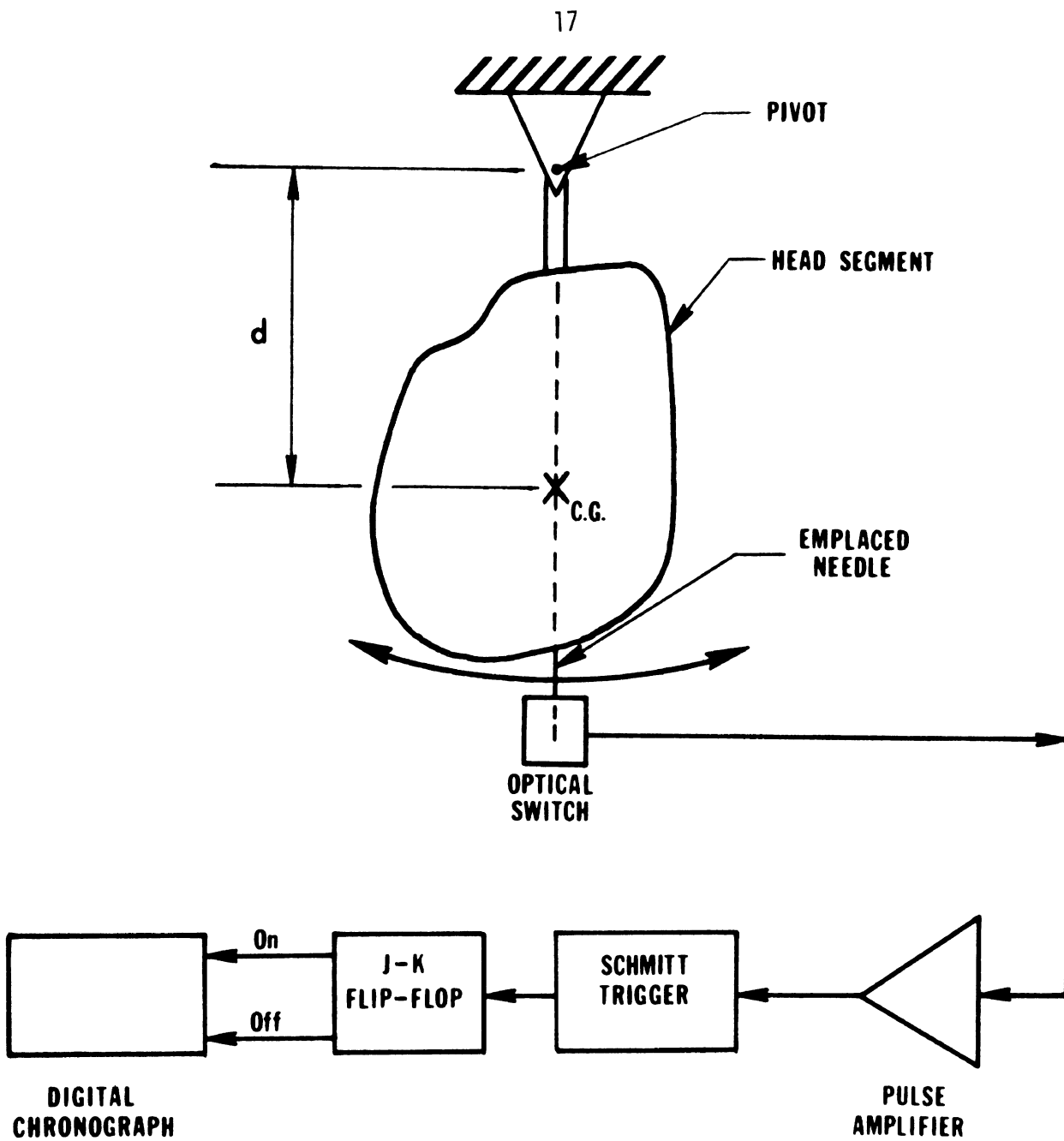


FIGURE 7

MOMENT OF INERTIA MEASUREMENT

When the needle passed through vertical, a digital chronograph was gated on; when the needle reached its maximum amplitude and returned through its vertical position, the chronograph was shut off, thus recording one-half the period. The measurement configuration is shown schematically in Figure 6.

The period of the segment oscillation for small amplitude is

$$T = 2\pi \frac{I}{mgd} \text{ seconds,}$$

where I is the rotational inertia, (in-lb-sec²)

mg is the segment weight acting at the C.G., (lbs)

d is the distance from the point of suspension to the C.G. (in).

Solving for the rotational inertia,

$$I = \frac{T^2 mgd}{4\pi^2} \text{ (in-lb-sec}^2\text{),}$$

where all the quantities on the right are directly measurable, when the segment C.G. is known.

Moments of inertia were computed from the above equation with the measured values of period, weight and equivalent simple pendulum lengths.

Accuracies of the measurements are approximately between 0.1% and 0.5%; round-off was to three significant figures.

Table 5 contains typical values of the segment weight C.G. location and moments of inertia. The definition of a particular segment is somewhat arbitrary. Our segment specification and parting line is also included.

2.3 Ranges of Motion

The ranges of motion of the crash test device conform to those listed in Table 4 and identified in Figure 5. These ranges of motion correspond to those which are contained in the current SAE J963 standard except that hand rotation, hand pronation and supination and foot inversion and eversion have been eliminated.

TABLE 5. MEASURED SEGMENT WEIGHTS, C.G. LOCATIONS, AND MOMENTS OF INERTIA

| SEGMENT, AND DEFINING ELEMENTS | WEIGHT (lbs) | REF. AXIS FOR C.G. AND J | C.G. FROM POINT OF ROTATION (in) | J (In-lbs-sec ²) |
|--|-----------------|--------------------------------|--|---------------------------------|
| Head, with Endevco accelerometer, mounting plate per DWG. No. 101-678-C, rubber neck element per DWG. No. 101-622-A, and aluminum spacer per DWG. No. 101-659-A. | 11.25 | K | 4.8 | 0.920 |
| Head & Neck, head as above, plus rubber neck elements per DWG. No. 101-663-A, aluminum spacer per DWG. No. 101-659-A, and neck mounting plate per DWG. No. 100-991-B. | 13.4 | L | 7.125 | 1.92 |
| Upper arm, includes shoulder pivot, elbow clevis, and all of elbow rotating elements. | 4.125 | A | 5.5 | 0.465 |
| Forearm, includes 1 7/8-in by 3/4 dia extension added to elbow pivot, all joint components except elbow clevis, and all wrist joint components except hand pivot. | 2.72 | B | 4.3 | 0.230 |
| Upper leg, includes knee clevis, knee cover, femur load cell, cast thigh, hip pivot, and three expanding bolts, with pin in hip pivot. | 11.95 | E | 5.7 | 1.66 |
| Lower leg, includes skin casting plus tube, all knee joint components, all ankle joint components, and steel spring stops. | 7.7 | E | 7.1 | 1.68 |
| Foot, includes ankle pivot. | 2.65 | F | 2.8 | 0.980 |
| Hand, includes wrist pivot. | 1.25 | C | 2.7 | 0.03 |

3.0 HEAD, MECHANICAL PROPERTIES

The crash test device has been designed and constructed to match the following mechanical properties of fresh cadaver heads. These properties have been measured in our laboratory and the same equipment and instrumentation procedures have been used for the comparative tests. A discussion of these test procedures is given in the Appendix.

The final head design consists of a solid skull cast of Uralite 3121 covered with a softer Uralite 3110 available from the Hexcel corporation. Figures 32, 33, and 34 show various views of the head and neck.

3.1 Static Stiffness

The static load-deformation characteristics of a significant number of fresh intact cadaver heads have been determined. The results are shown in Figures 8 and 9. The crash test device head has been designed so that its static stiffness falls within this band.

3.2 Impact Response

Since the head injury criteria specified in MVSS 208 rates the acceleration history of the head during impact, the impact response of the head of the crash test device should be similar to that of the human for a variety of impulse magnitudes, durations and directions for this criteria to be meaningful. Consequently a head impact performance criteria has been as the basic performance criteria for the crash test device head. Figures 10 through 21 show load and acceleration time histories for impacts to fresh cadaver heads in the left-right and anterior-posterior direction. The crash test device head has been designed so that its impact response falls within the bands of these curves. For comparison some of the data from Hodgson's and Thomas' work described in DOT-HS-800-583 final report is also included.

The HSRI test results have been specified instead of Hodgson's and Thomas' because:

1. Fresh cadavers were used.
2. The same equipment and instrumentation is available to test the crash test device.
3. The same impact velocity and impactor was used for all tests in the test band.
4. Both rigid and padded impact data is available.

These comments are in no way meant to fault the work of Hodgson and Thomas, but point out differences that make the HSRI data more suitable for this purpose. Figures 24 through 29 show typical test setups.

3.3 Repeatability

A major design consideration for this crash test device head is repeatability and reproducibility of test results. To verify repeatability at the component level all final qualifying impact tests have been performed six times. Less than 5% variation between the mean value of the peak load and acceleration components for the six tests and the outlier were observed. Tests were performed in both the anterior-posterior and left-right directions.

3.4 Driving Point Impedance, Dynamic Stiffness and Dynamic Damping

The driving point impedance, dynamic stiffness and dynamic damping have been determined for six fresh intact cadaver heads. The results are shown in Figures 22 and 23 for the anterior-posterior and left-right directions. Comparisons are also presented with the Sierra aluminum head. Similar measurements have been made on this crash test device head for comparative purposes.

3.5 Scalp

The mechanical properties of scalp have been determined in a variety of ways. For the purpose of selected scalp-like materials the work reported in:

TABLE 6 DESCRIPTION OF CADAVERS

| No. | Sex | Age | Height | Body | | | H | Circ. | Brain | Chest | Days | Cause of Death | Comments | |
|-----|-----|-----|--------|-------|------|-----|-----|-------|-------|-------|------|----------------|---|-------------------------------|
| | | | | Wt. | Wt. | W | | | | | | | | L |
| C1 | F | 48 | 5'2" | 129 | 10.6 | 6.2 | 8.0 | 5.2 | 23.0 | 3.25 | 32.1 | 3 | Cancer of Abdomen | |
| C2 | M | 66 | 5'3" | 79.2 | 9.7 | 6.0 | 6.8 | 5.7 | 21.0 | 2.75 | 29.7 | 6 | Cancer of Prostate | |
| C3 | M | 50 | 5'8" | 176 | 10.3 | 6.0 | 8.1 | 5.9 | 23.0 | 2.93 | 35.0 | 8 | Cardiac Arrest | Left Cranium Hydrocephalic |
| C4 | M | 78 | 5'9" | 158.8 | 11.1 | 6.1 | 7.7 | 6.3 | 23.0 | 3.15 | 34.1 | 5 | Multiple Myeloma | |
| C5 | M | 84 | 5'6" | 92.8 | 8.9 | 5.7 | 7.5 | 5.9 | 21.5 | 3.02 | 29.3 | 8 | Pneumonia | |
| C6 | M | 72 | 5'8" | 126.5 | 10.3 | 5.8 | 7.8 | 5.7 | 22.5 | 2.96 | 32.1 | 3 | Congestive Heart Failure | |
| C7 | M | 64 | 5'7" | 112.0 | 9.7 | 6.2 | 8.1 | 5.8 | 23.0 | 2.93 | 32.0 | 7 | Metastatic Nemanoma | |
| C8 | M | 72 | 5'7" | 112.4 | 10.1 | 6.2 | 7.8 | 5.8 | 22.5 | 2.83 | 31.7 | 5 | Asphyxiation | |
| C9 | M | 99 | 5'8.5" | 148.5 | 10.8 | 6.6 | 7.7 | 6.3 | 23.0 | 2.97 | 32.7 | 1 | Cerebral Vascular Accident | |
| C10 | M | 70 | 5'3" | 92.4 | 9.3 | 6.0 | 7.5 | 6.8 | 21.6 | 3.07 | 30.0 | 5 | Coronary Occlusion | |
| C11 | M | 70 | 5'6" | 123.8 | 10.7 | 5.9 | 6.8 | 5.4 | 21.0 | 3.09 | 34.1 | 2 | Acute Coronary | |
| C12 | M | 72 | 5'2" | 84.7 | 7.9 | 5.6 | 7.3 | 5.3 | 20.5 | 3.01 | 29.3 | 2 | Lobar Pneumonia Bilateral | Legs and Arms Bent Up |
| C13 | M | 85 | 5'7" | 135.7 | 10.7 | 6.0 | 7.7 | 5.5 | 22.3 | 2.74 | 33.1 | 9 | Pneumonitis | |
| C14 | M | 73 | - | - | 10.8 | 6.0 | 7.8 | 4.9 | 22.0 | 3.00 | 31.3 | 3 | Unknown | Double Amputee |
| C15 | M | 65 | 5'2" | 77 | 8.3 | 4.5 | 6.3 | 4.4 | 20.0 | 2.94 | 30.1 | 3 | Bilateral Extensive Bronchopneumonia, Fibrosis, Emphysema | |
| C16 | M | 88 | 5'8" | 149.4 | 10.9 | 6.3 | 8.4 | 5.5 | 23.6 | 3.11 | 37.1 | 4 | Unknown | |
| C17 | M | 49 | 5'11" | 155.0 | 11.3 | 6.2 | 7.3 | 5.9 | 22.3 | 2.81 | 38.2 | 2 | Acute Myocardial Infarction | |
| C18 | F | 65 | 5'3.5" | 100.0 | 9.6 | 5.4 | 6.8 | 4.8 | 20.3 | 2.97 | 30.8 | 3 | Generalized Carcinomatosis | |

TABLE 6 DESCRIPTION OF CADAVERS (Cont'd)

| No. | Sex | Age | Height | Body | | Wt. lbs. | Wt. lbs. | L in. | H in. | Circ. in. | Brain | | Chest in. | Days Dead | Cause of Death | Comments |
|-----|-----|-----|--------|----------|----------|----------|----------|-------|-------|-----------|-------|---|-------------------------|-----------|----------------|----------|
| | | | | Wt. lbs. | Wt. lbs. | | | | | | | | | | | |
| C19 | M | 52 | 5'10" | 203.0 | 11.7 | 6.3 | 7.9 | 5.5 | 22.5 | 3.12 | 42.0 | 3 | Coronary Heart Disease | | | |
| C20 | F | 75 | 4'8" | 88.0 | 9.3 | 6.2 | 8.1 | 5.6 | 20.8 | 3.11 | 28.5 | 5 | Coronary Thrombosis | | | |
| C21 | M | 62 | 6'0" | 113.0 | 10.5 | 6.1 | 7.7 | 4.7 | 21.5 | 2.89 | 31.7 | 2 | Coronary Heart Disease | | | |
| C22 | M | 63 | 5'7" | 128.0 | 11.0 | 6.1 | 7.4 | 5.3 | 22.0 | 2.84 | 33.3 | 1 | Cardiosenic Shock | | | |
| C23 | M | 58 | 5'10" | 155.0 | 12.1 | 6.1 | 8.0 | 6.3 | 23.0 | 3.11 | 39.5 | 3 | Aspiration of Pneumonia | | | |

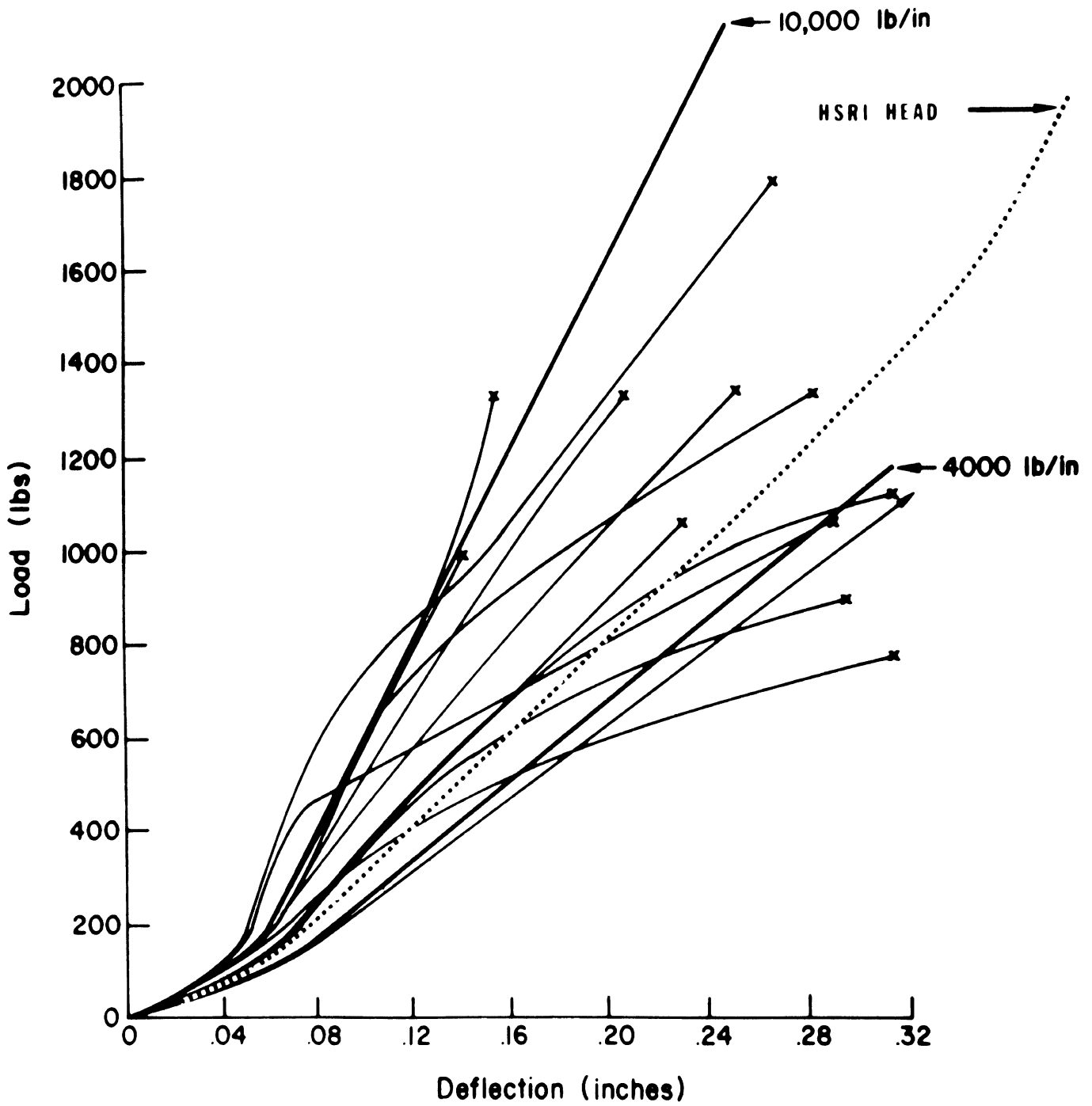


FIGURE 8 HUMAN SKULL LOAD-DEFLECTION CURVES,
L-R LOADING, 12 TESTS.

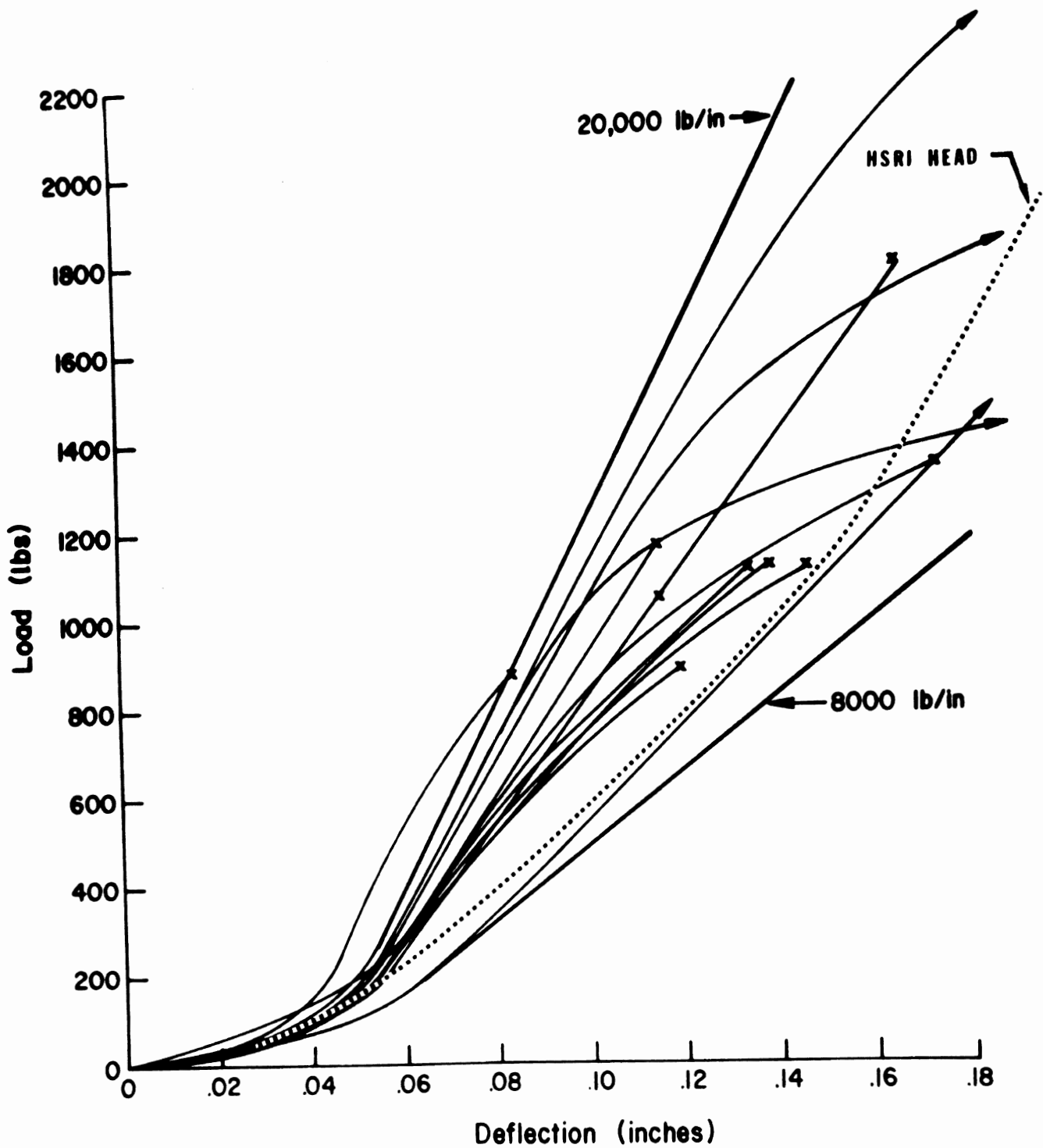


FIGURE 9 HUMAN SKULL LOAD-DEFLECTION CURVES,
A-P LOADING, 12 TESTS.

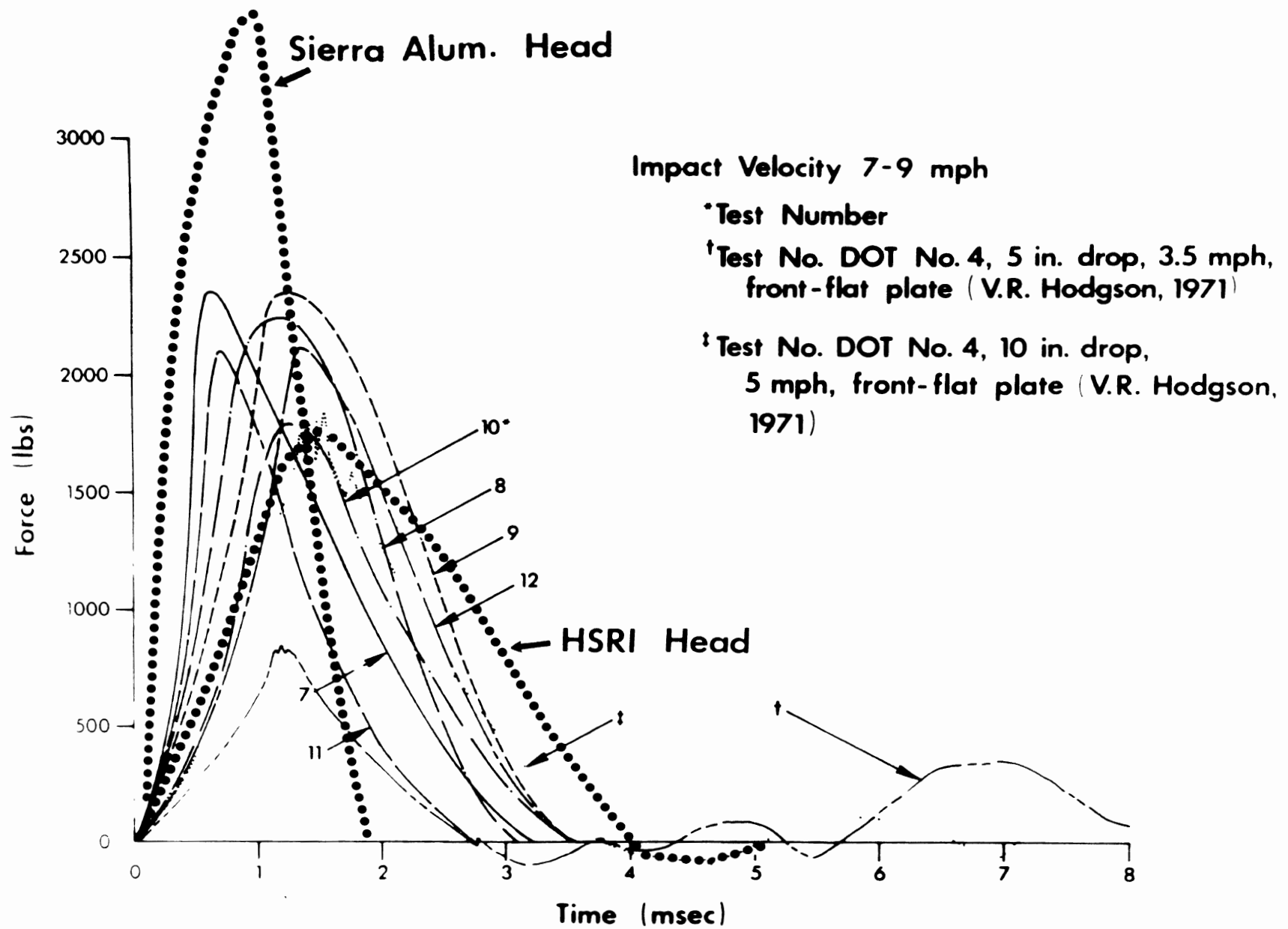


FIGURE 10 COMPOSITE FORCE-TIME CURVES FOR CADAVER FRONT HEAD IMPACTS WITH RIGID IMPACTOR.

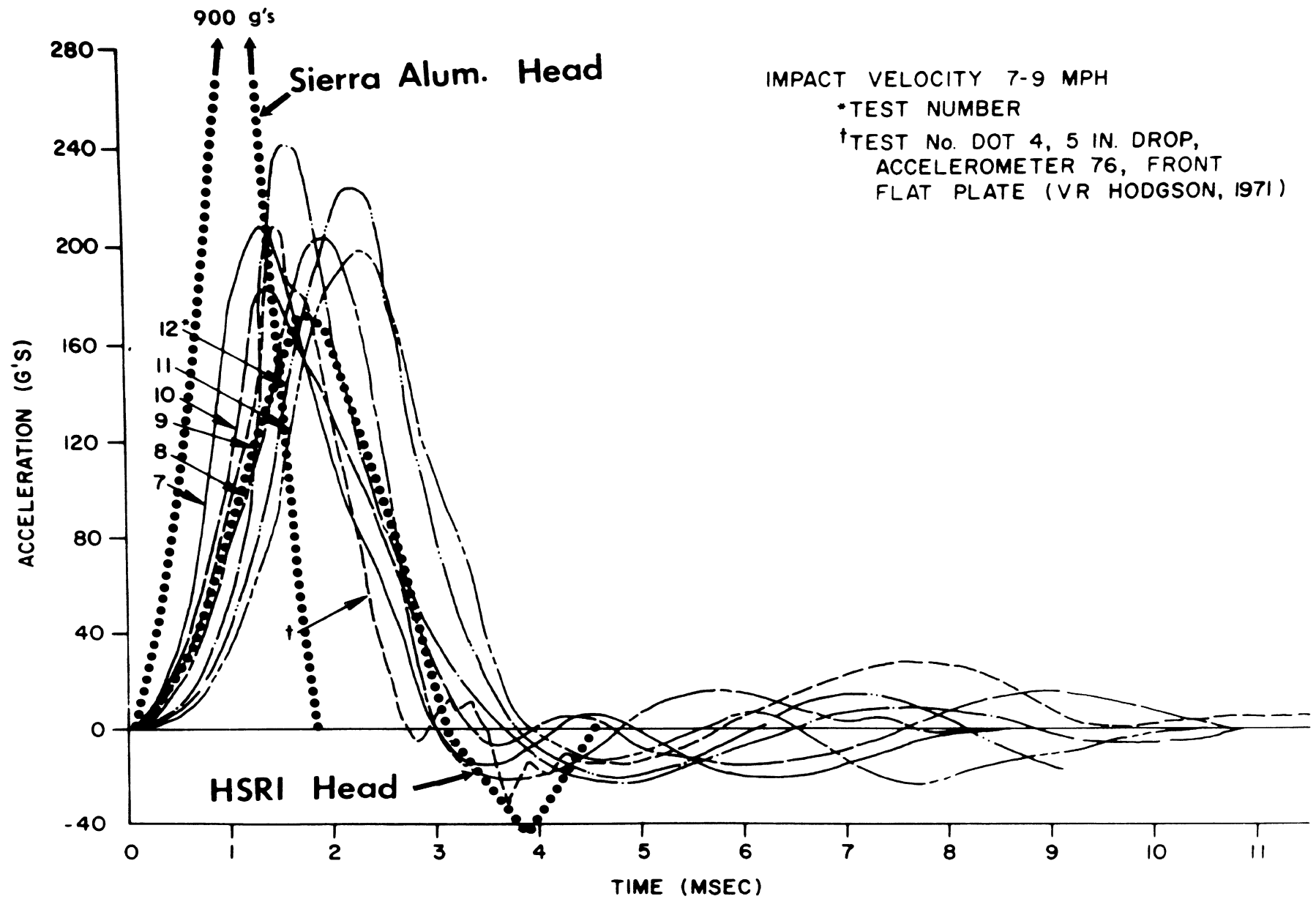


FIGURE 11 COMPOSITE ACCELERATION-TIME CURVES FROM A-P ACCELEROMETER FOR CADAVER FRONT HEAD IMPACTS WITH RIGID IMPACTOR.

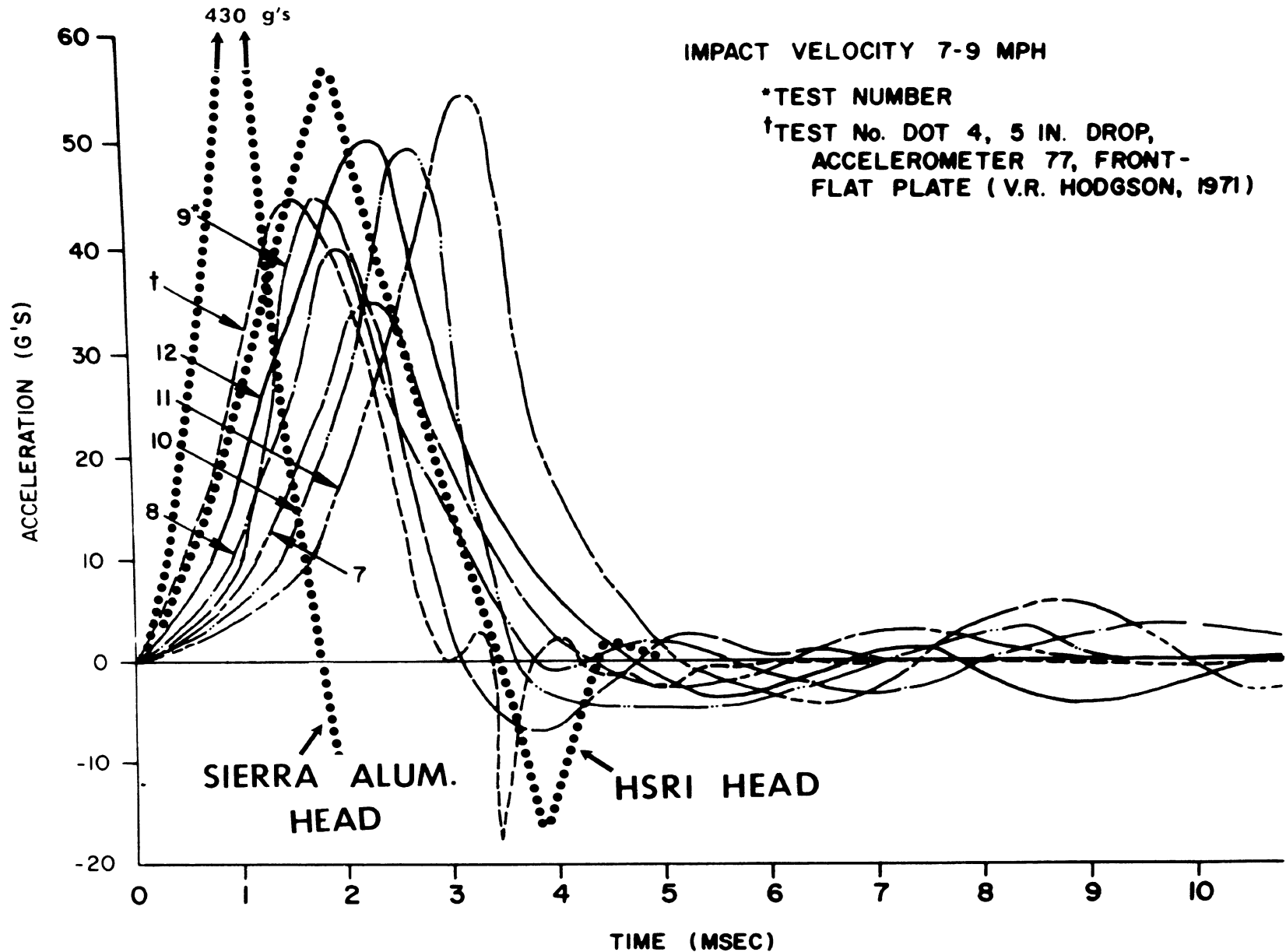


FIGURE 12 COMPOSITE ACCELERATION-TIME CURVES FROM S-1 ACCELEROMETER FOR CADAVER FRONT HEAD IMPACTS WITH RIGID IMPACTOR.

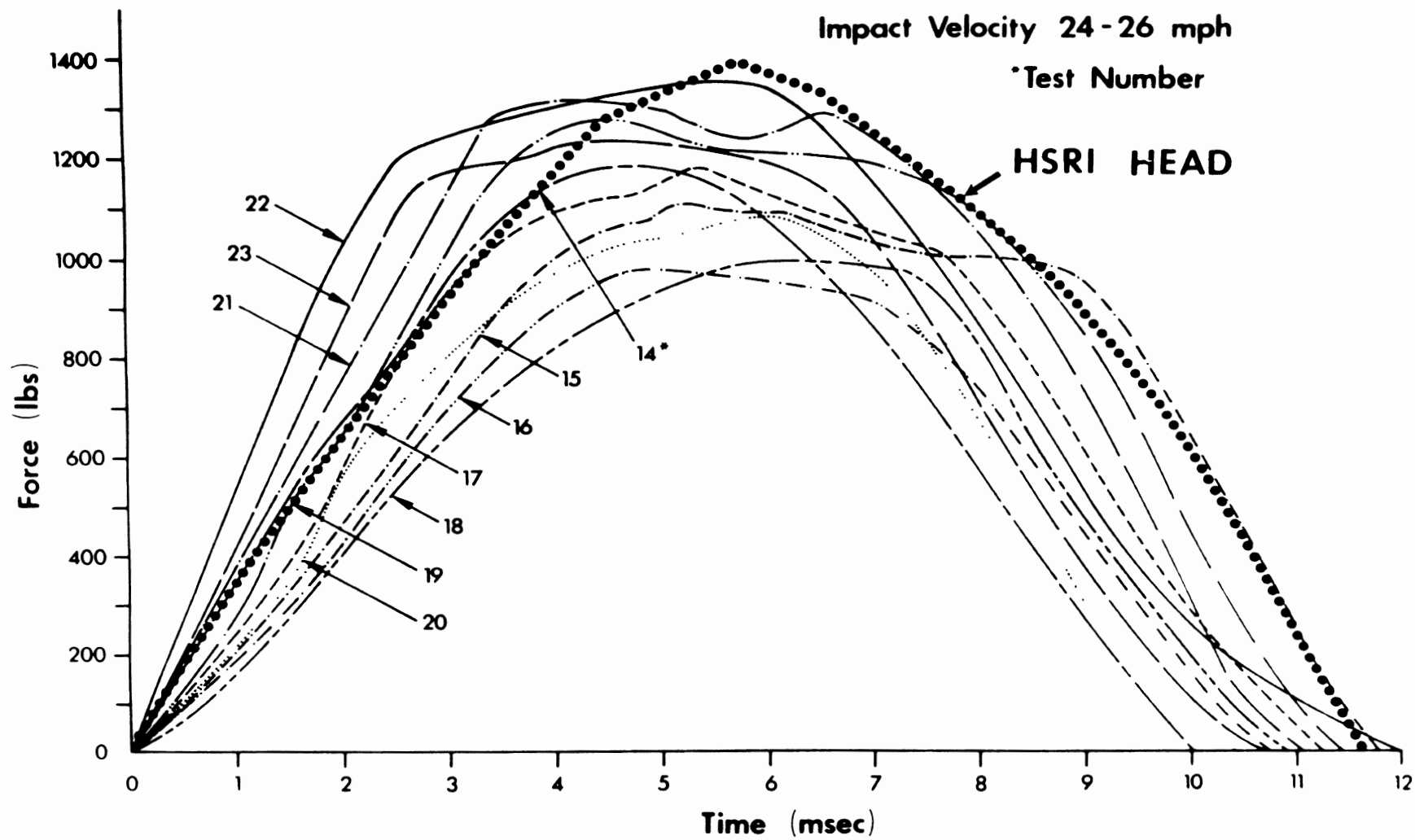


FIGURE 13 COMPOSITE FORCE-TIME CURVES FOR CADAVER FRONT HEAD IMPACTS WITH PADDED IMPACTOR.

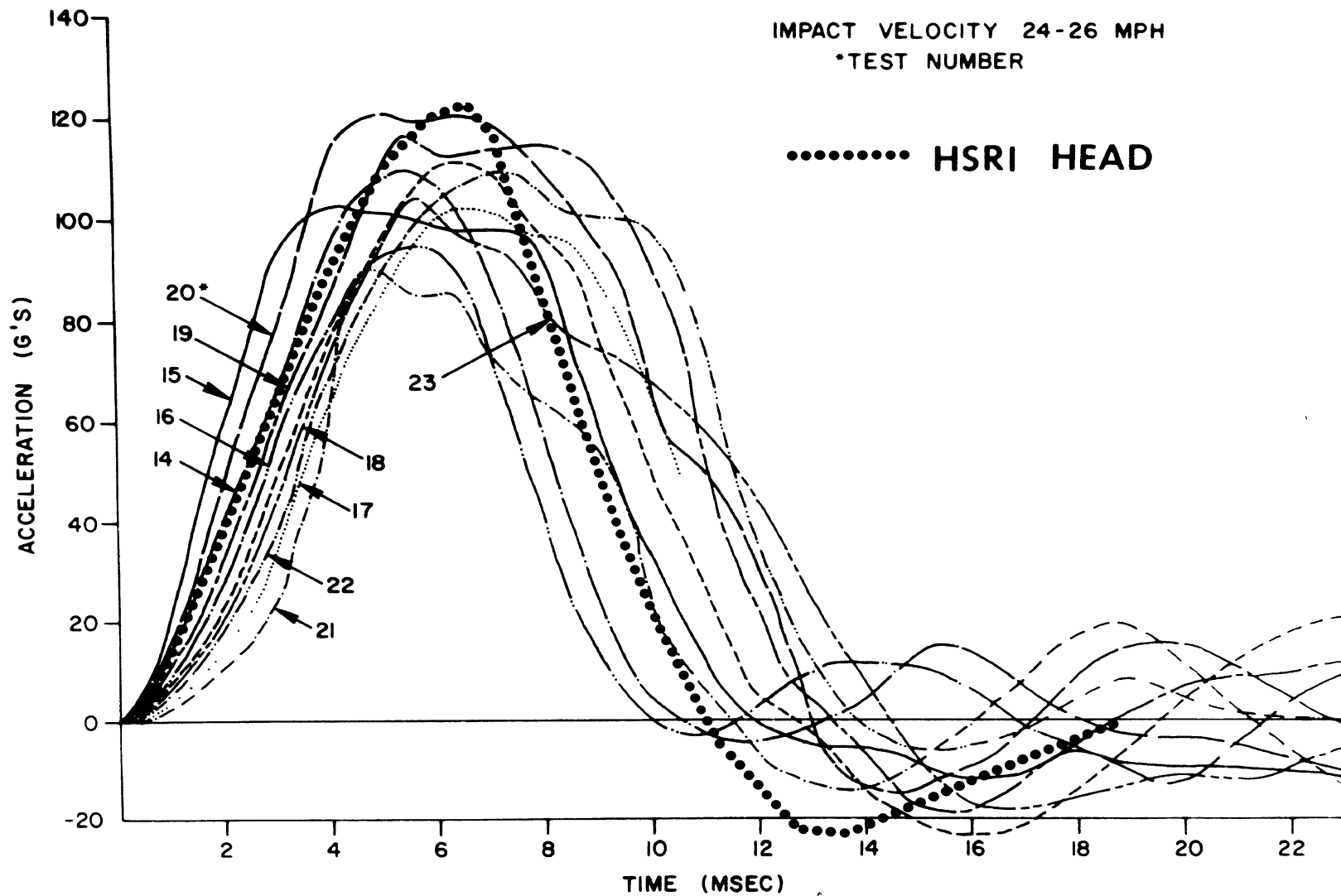


FIGURE 14 COMPOSITE ACCELERATION-TIME CURVES FROM A-P ACCELEROMETER FOR CADAVER FRONT HEAD IMPACTS WITH PADDED IMPACTOR.

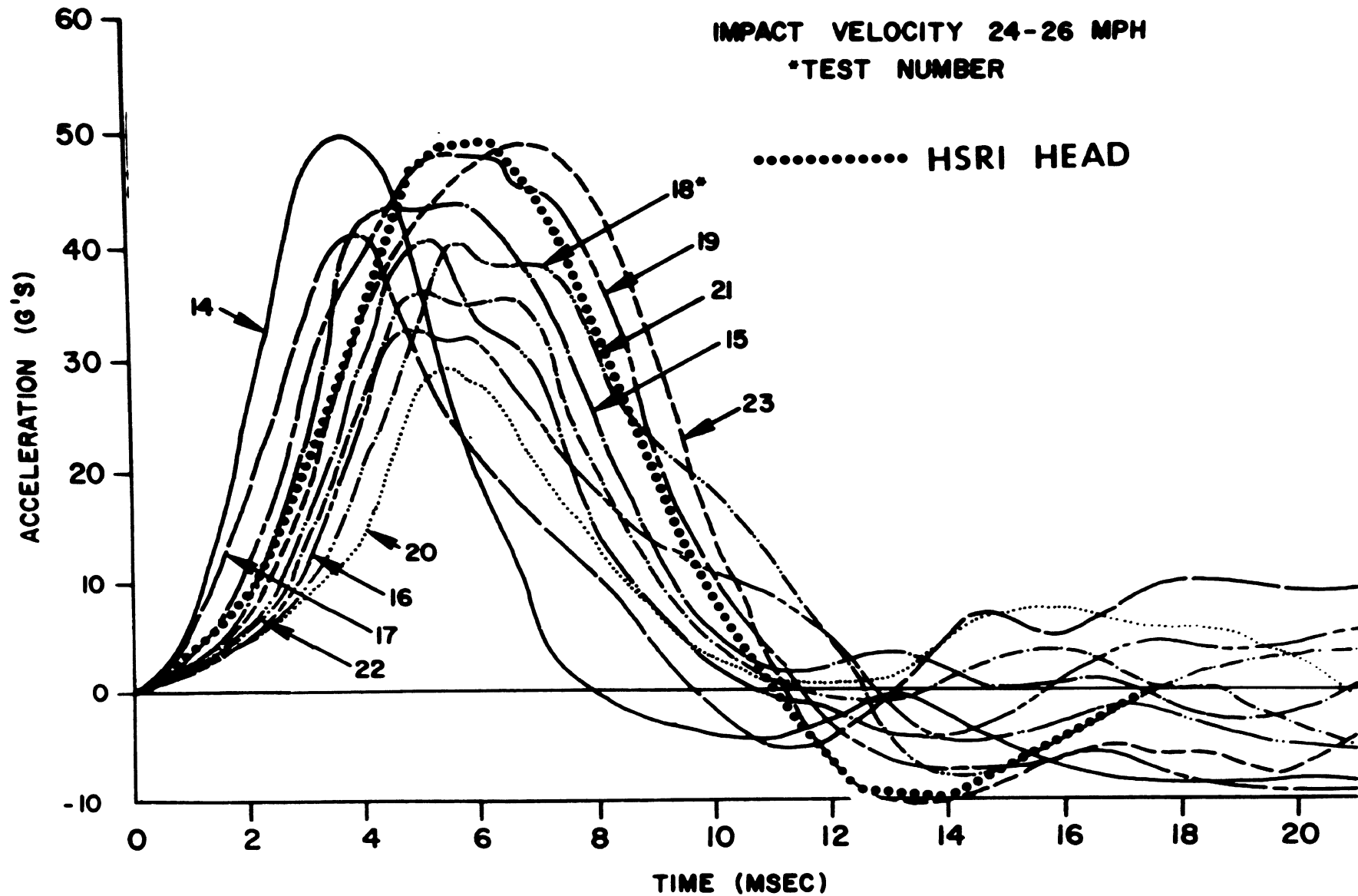


FIGURE 15 COMPOSITE ACCELERATION-TIME CURVES FROM S-1 ACCELEROMETER FOR CADAVER FRONT HEAD IMPACTS WITH PADDED IMPACTOR.

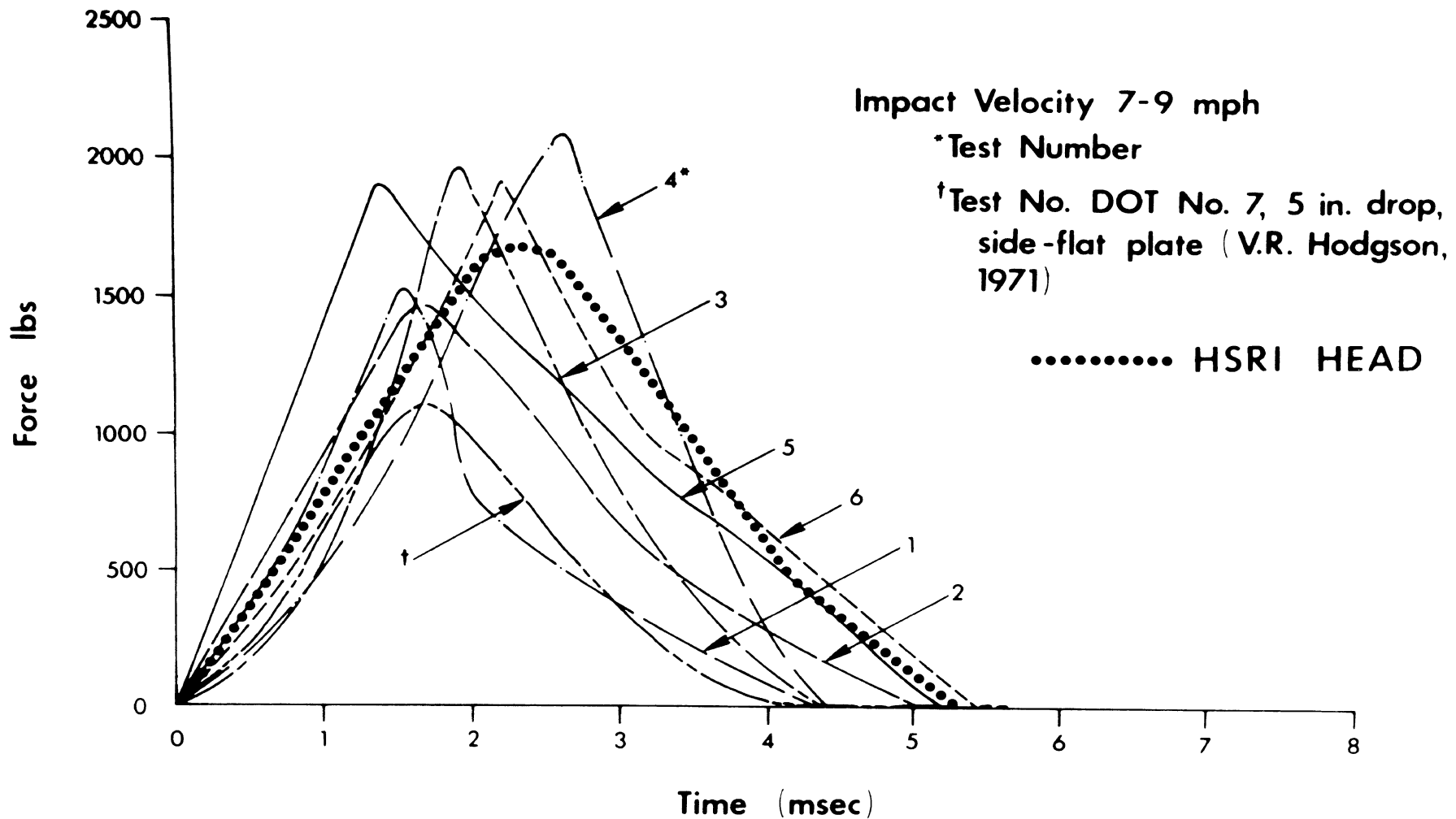


FIGURE 16 COMPOSITE FORCE-TIME CURVES FOR CADAVER SIDE HEAD IMPACTS WITH RIGID IMPACTORS.

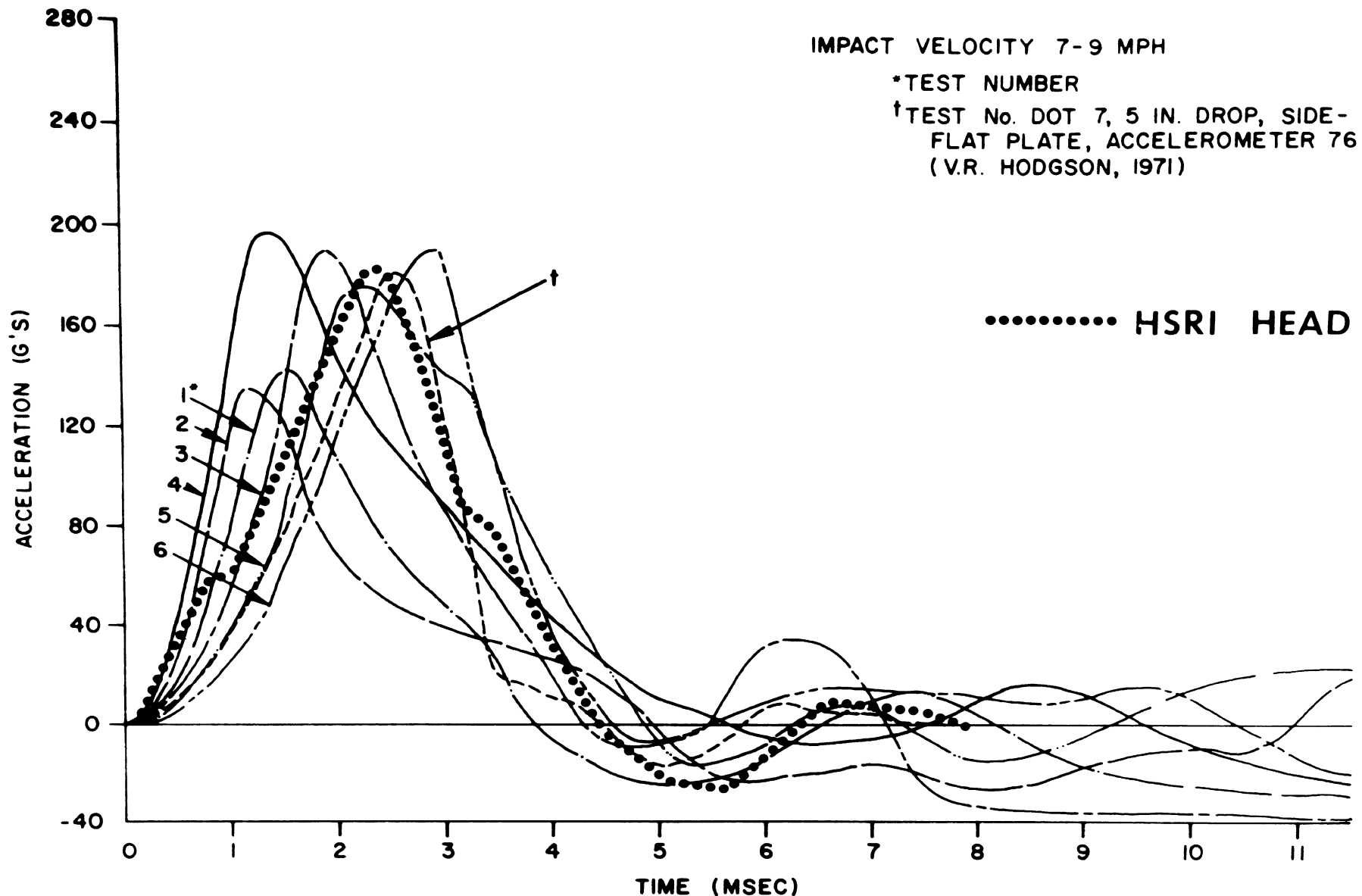


FIGURE 17 COMPOSITE ACCELERATION-TIME CURVES FROM L-R ACCELEROMETER FOR CADAVER SIDE HEAD IMPACTS WITH RIGID IMPACTOR.

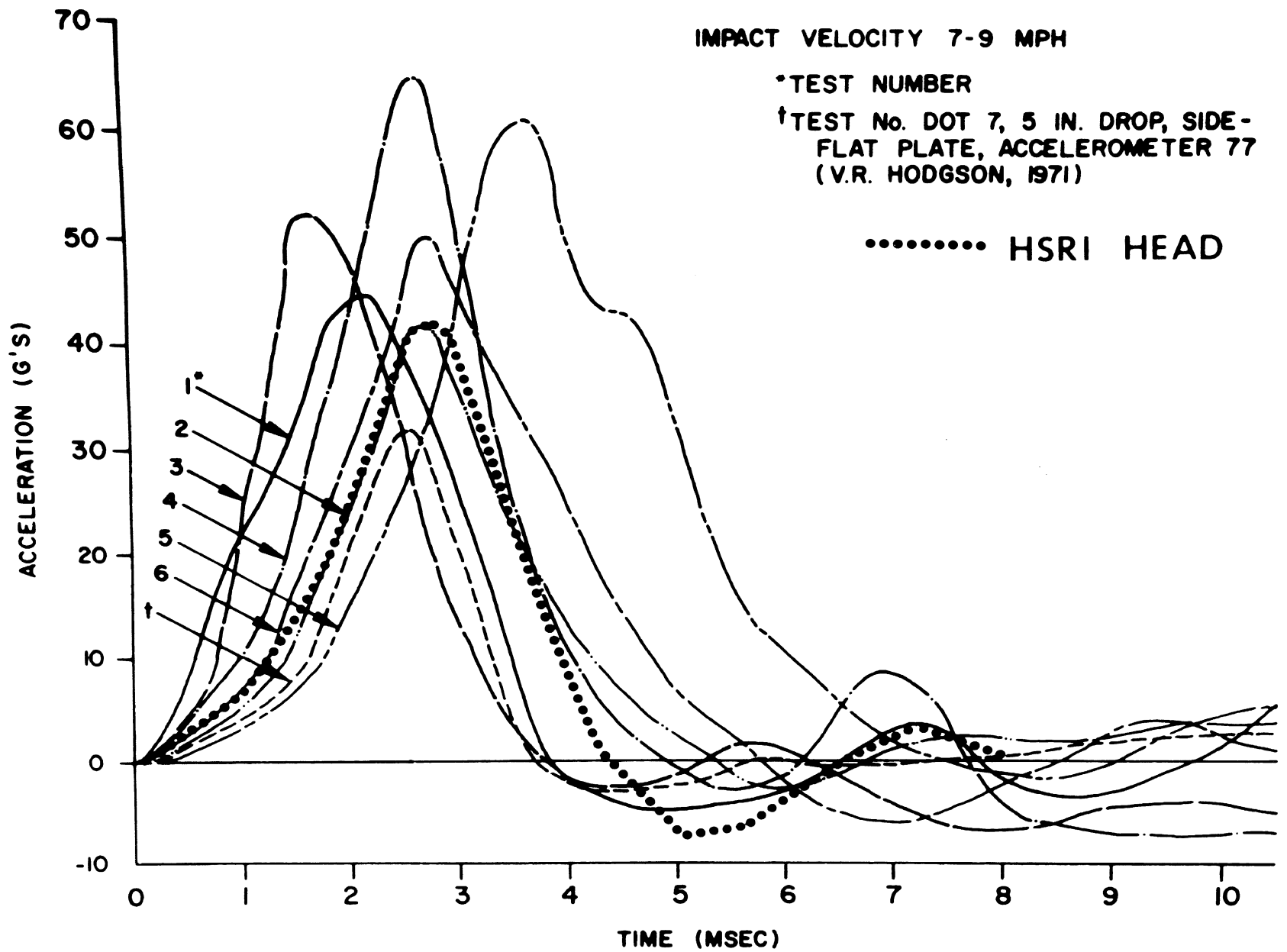


FIGURE 18 COMPOSITE ACCELERATION-TIME CURVES FROM S-1 ACCELEROMETER FOR CADAVER SIDE HEAD IMPACTS WITH RIGID IMPACTOR.

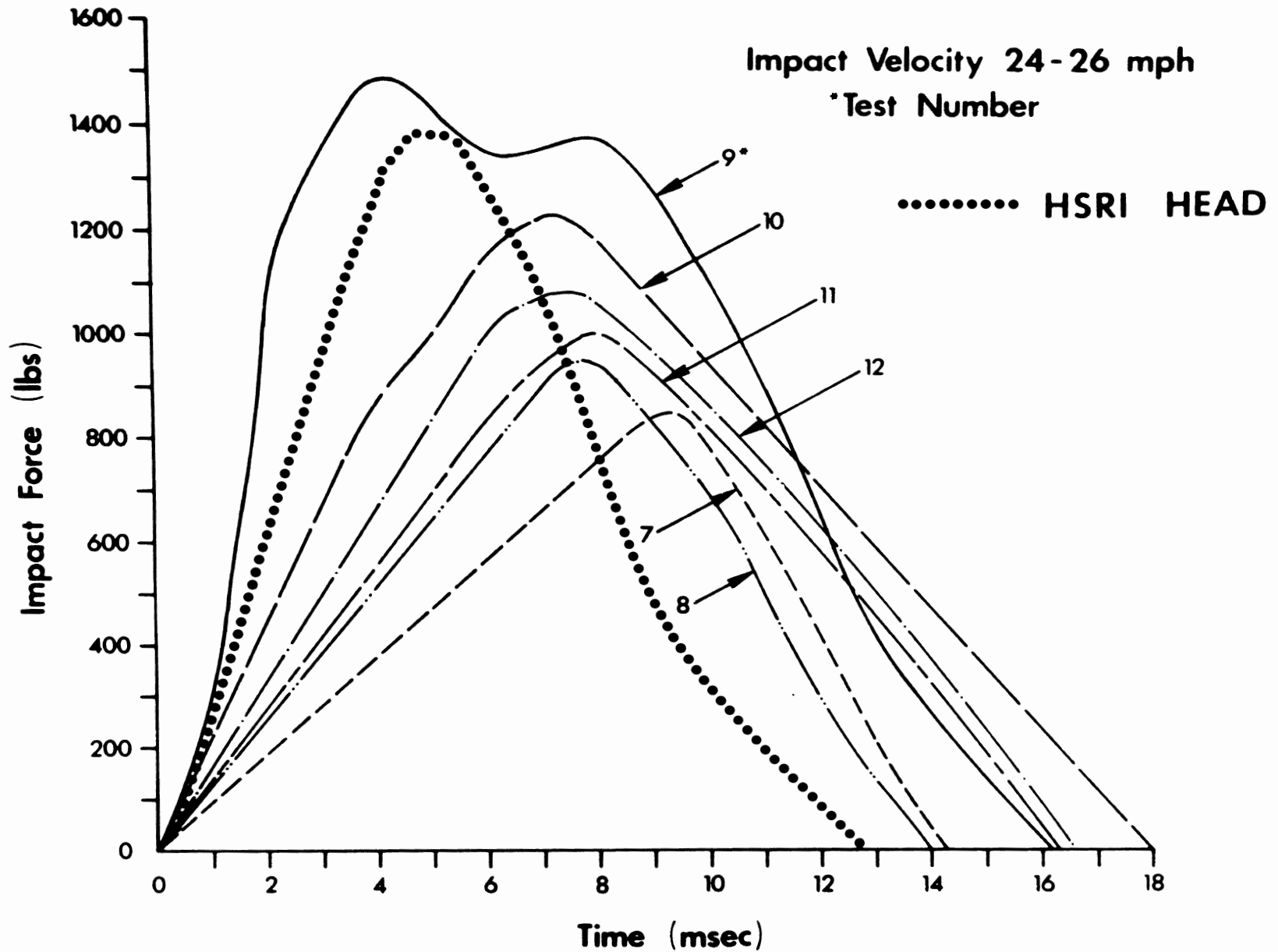


FIGURE 19 COMPOSITE FORCE-TIME CURVES FOR CADAVER SIDE HEAD IMPACTS WITH PADDED IMPACTOR.

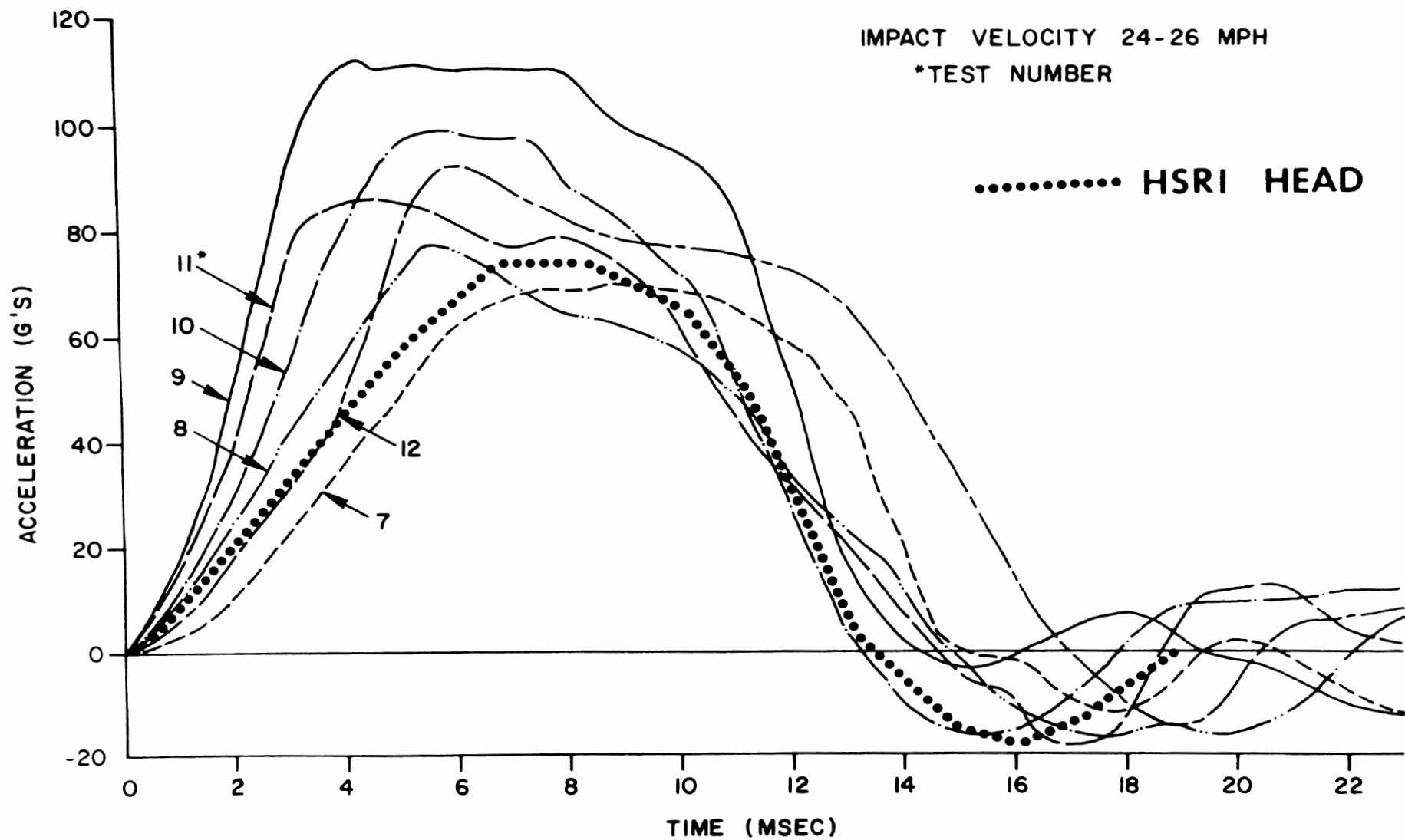


FIGURE 20 COMPOSITE ACCELERATION-TIME CURVES FROM L-R ACCELEROMETER FOR CADAVER SIDE HEAD IMPACTS WITH PADDED IMPACTOR.

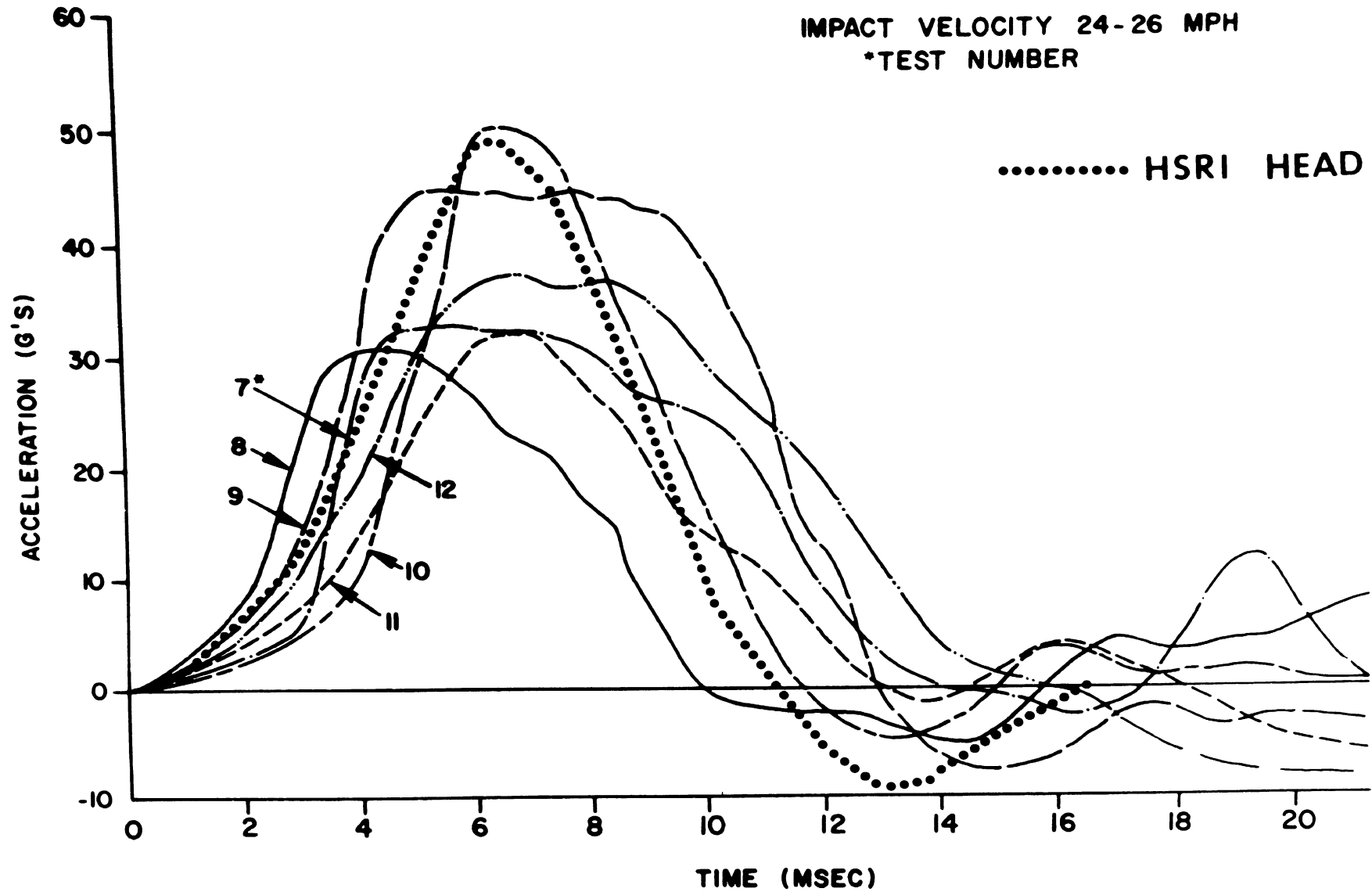


FIGURE 21 COMPOSITE ACCELERATION-TIME CURVES FROM S-1 ACCELEROMETER FOR CADAVER SIDE HEAD IMPACTS WITH PADDED IMPACTOR.

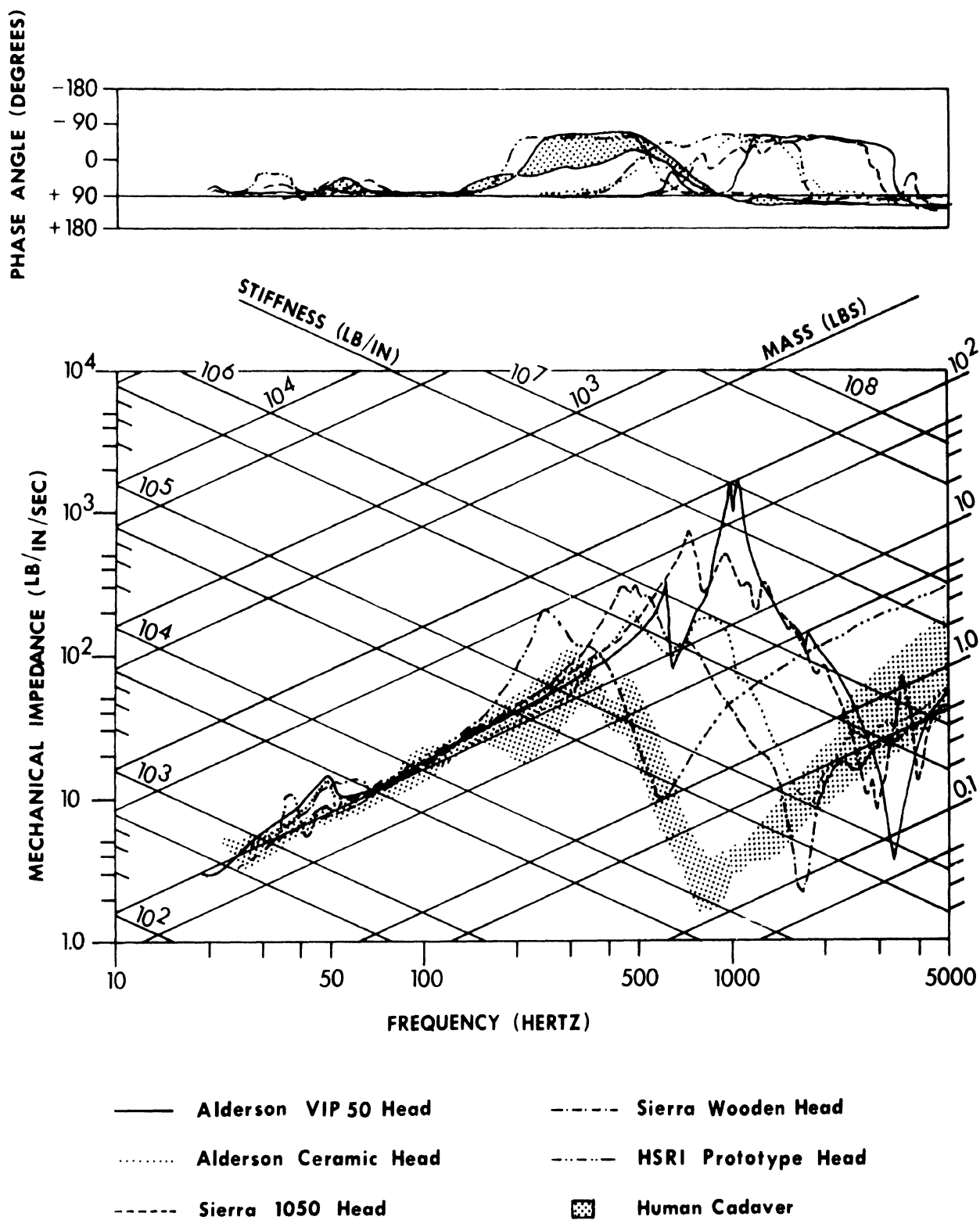


Figure 22 Mechanical Impedance of Heads (Frontal).

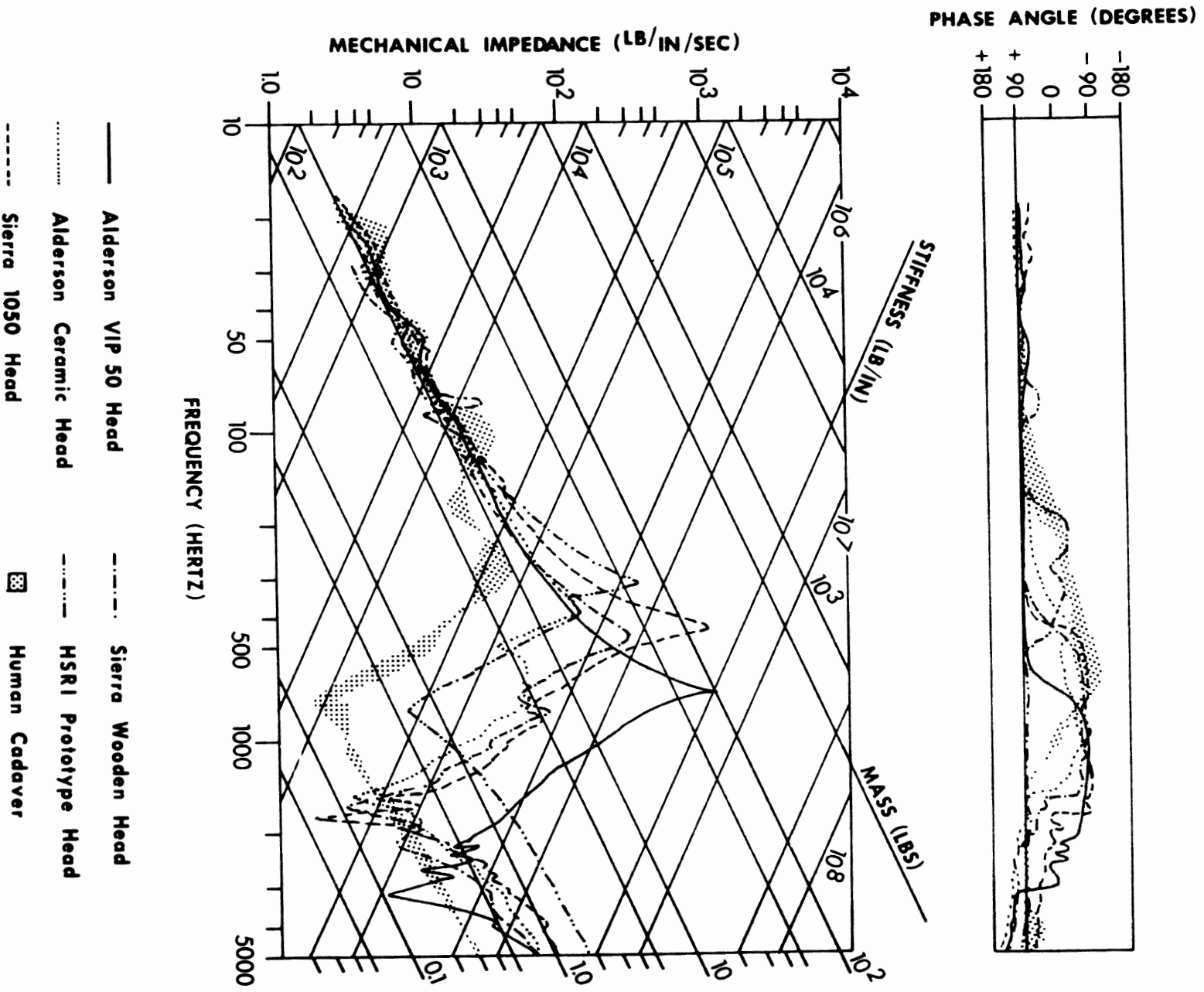


Figure 23 Mechanical Impedance of Heads (Parietal).

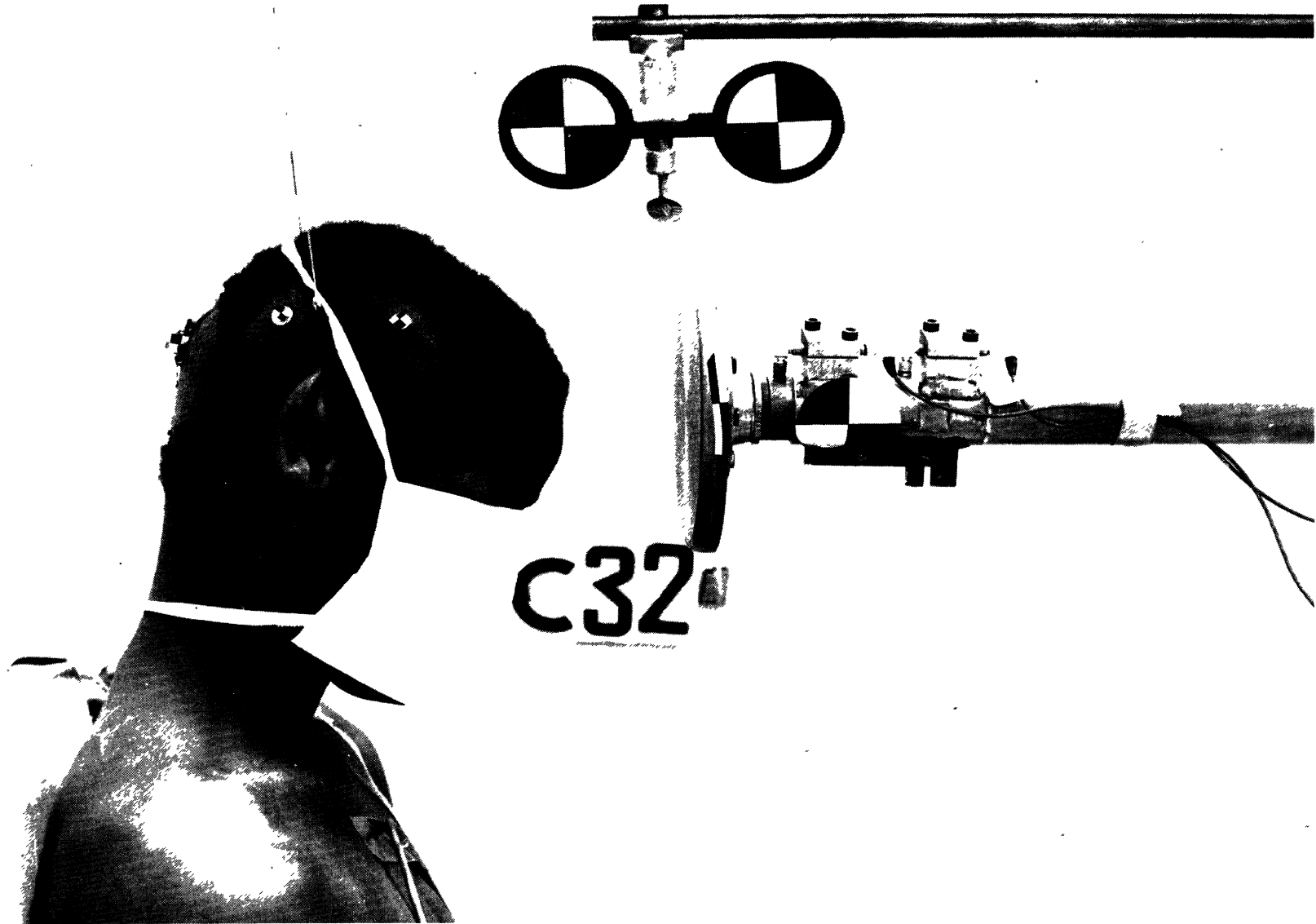


Figure 24 Typical Setup for Front Head Impact with Rigid Impactor.



Figure 25 Typical Setup for Front Head Impact with Rigid Impactor.

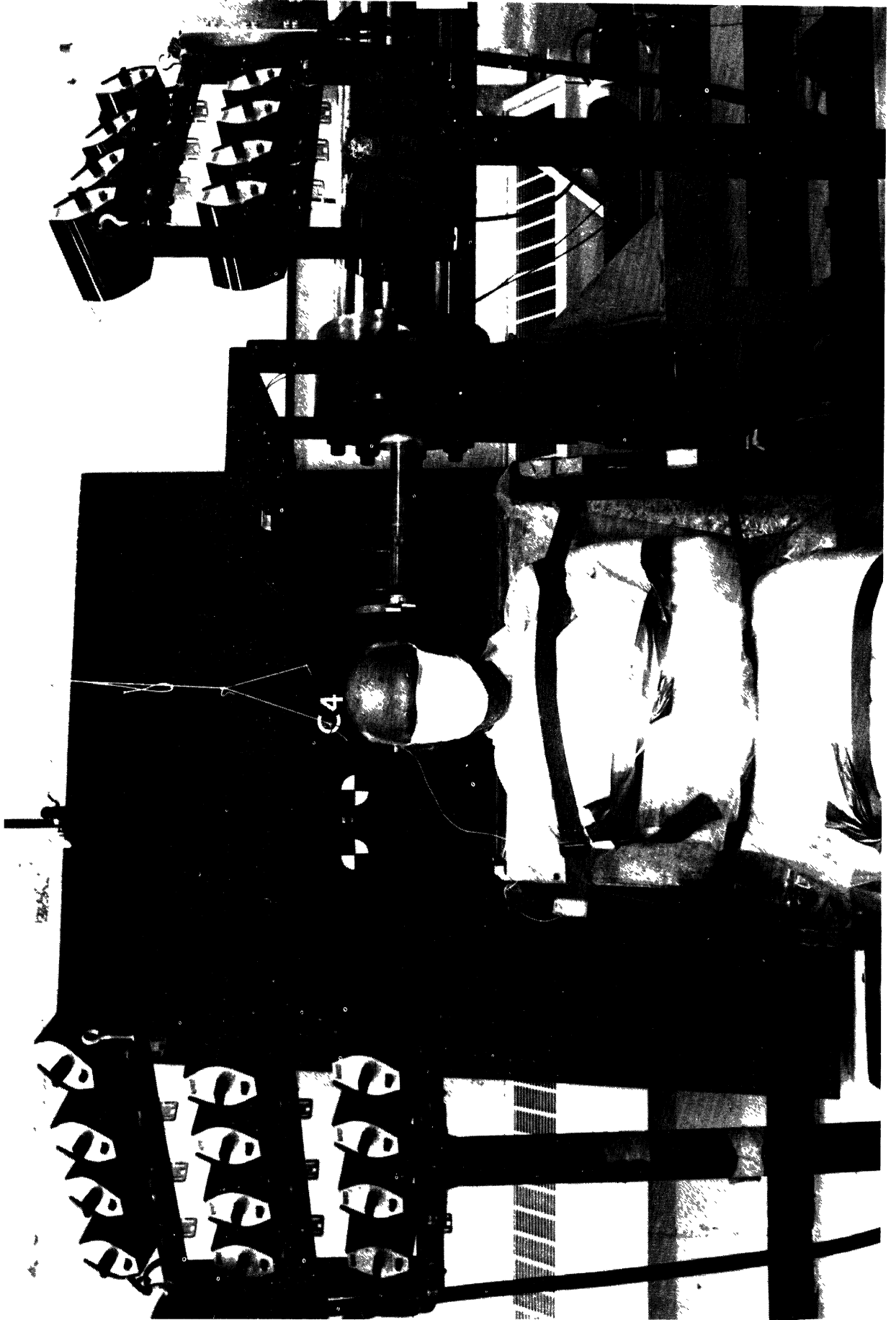


Figure 26 Typical Setup for Side Head Impact with Rigid Impactor.



Figure 27 Typical Setup for Side Head Impact with Rigid Impactor.



Figure 28 Typical Setup for Padded Impact.



Figure 29 Typical Setup for Padded Impact.



Figure 30 Static Head Compression Test.

Figure 31 Driving Point Impedance Test.



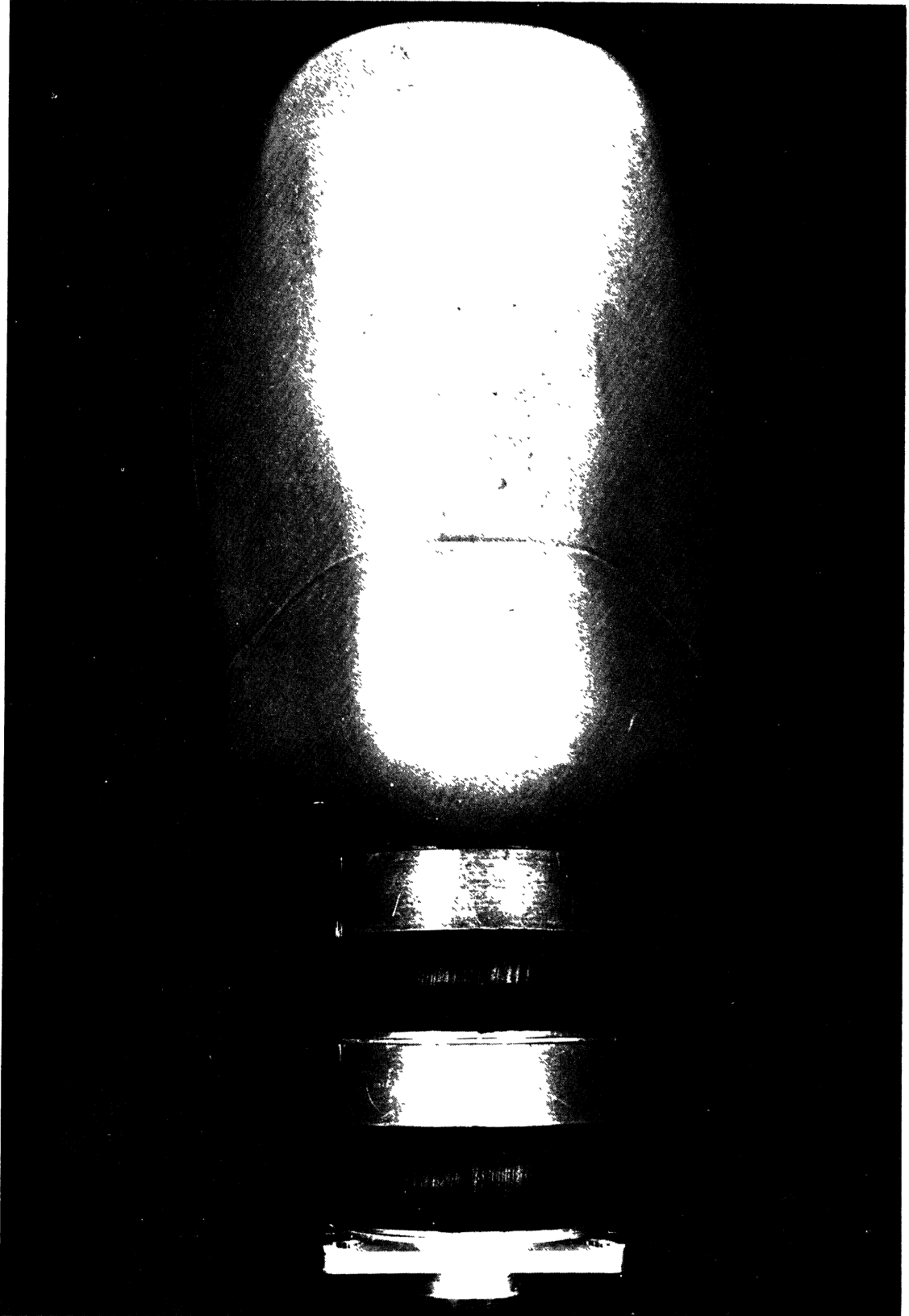


Figure 32 Front View HSRI Head and Neck.

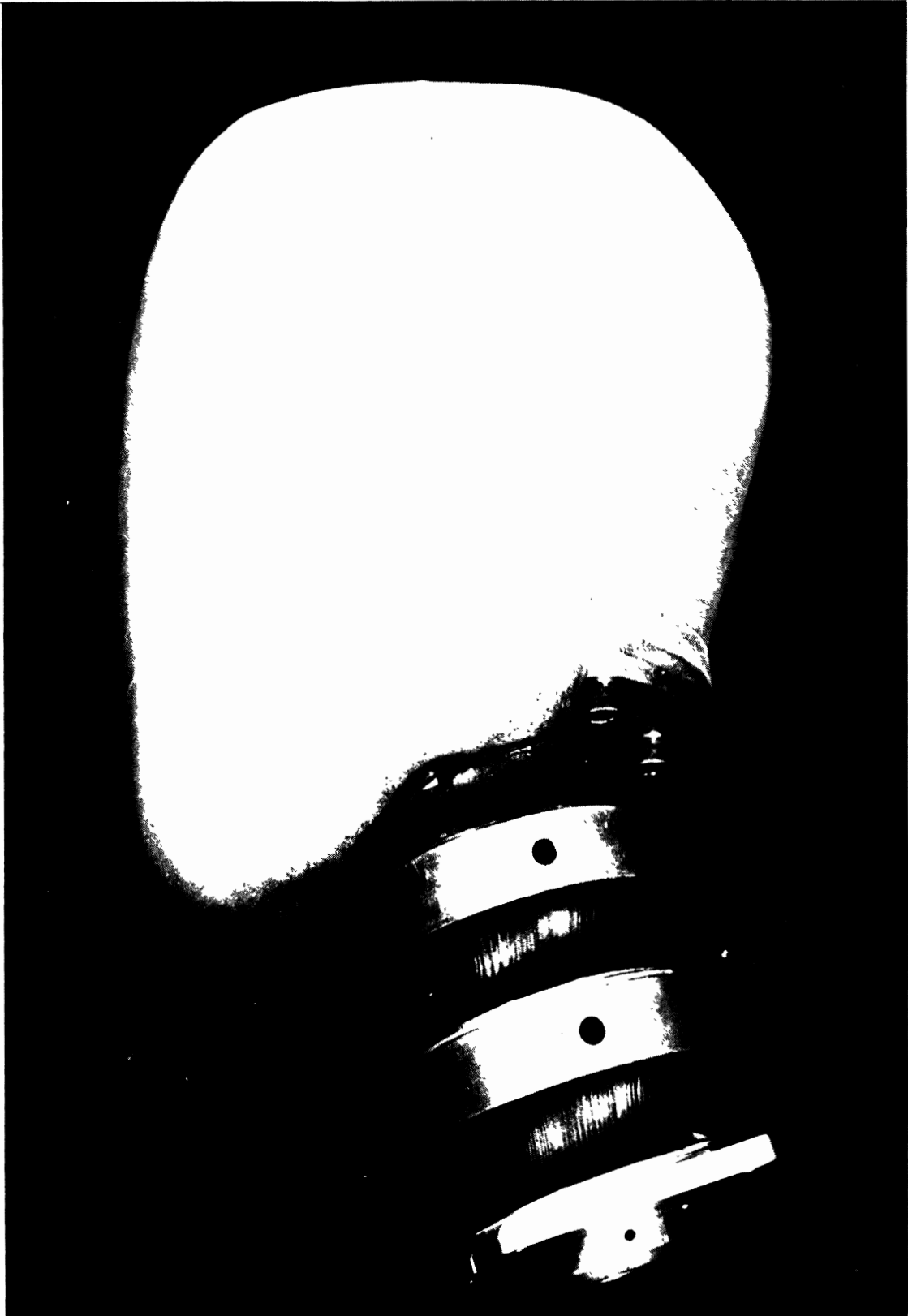


Figure 33 Side View HSRI Head and Neck.

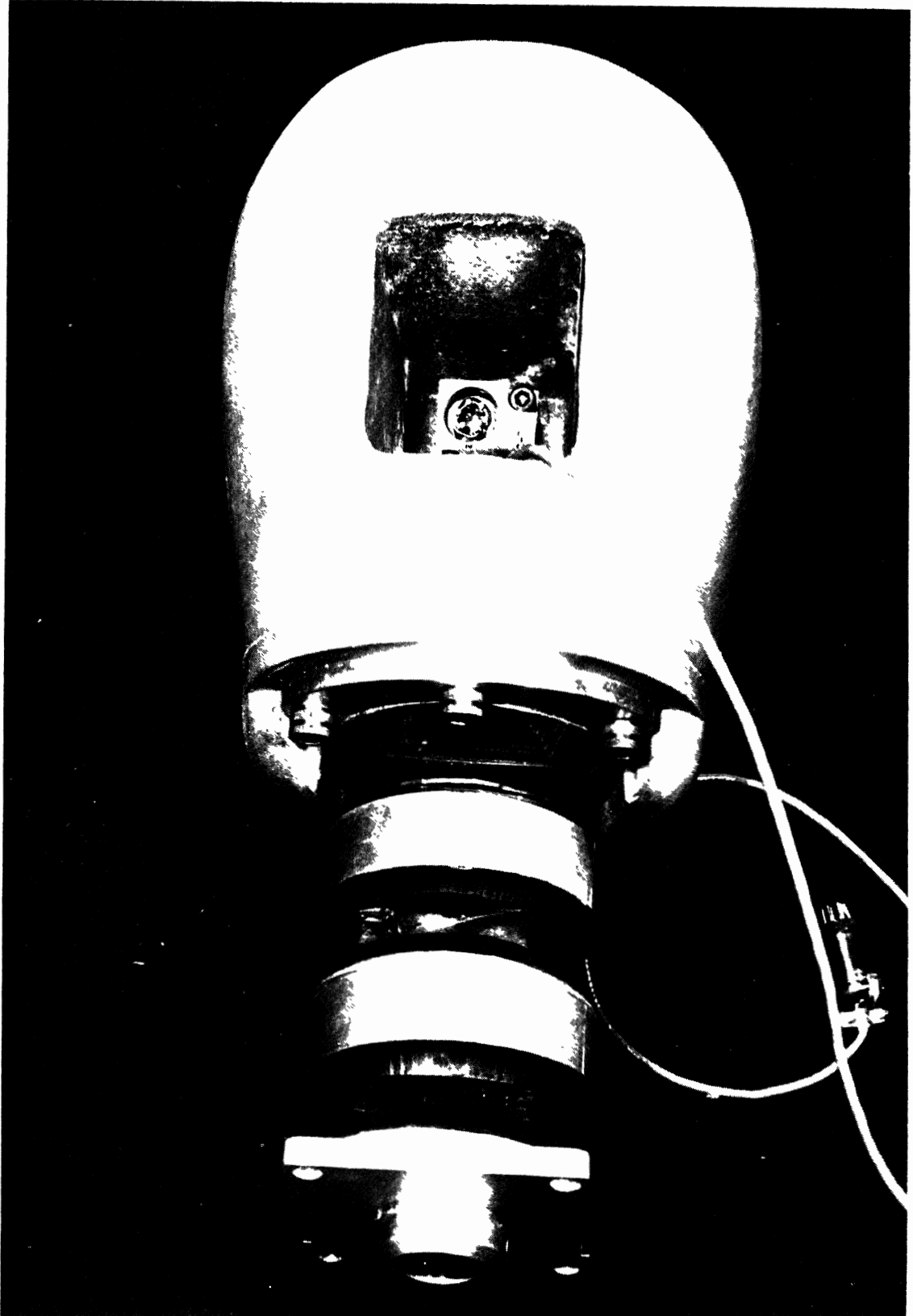


Figure 34 Rear View HSRI Head and Neck.

1. "Tolerance and Properties of Superficial Soft Tissues in Situ" by Charles W. Gadd, Alan N. Nahum, Dennis C. Schneider and Richard G. Madeira, SAE Paper No. 700910, 14th Stapp Car Crash Conference; and,

2. "Dynamic Characteristics of the Tissues of the Head," by James H. McElhaney, John W. Melvin, Verne L. Roberts and Harold D. Portnoy, 1972 Proceedings Symposium on Biomedical Engineering; is considered representative.

Scalp-like materials have been selected to match as nearly as possible the responses presented in Figure 5 of Reference 1 and the four parameter models for human scalp presented in Reference 2. The final material selected was a soft urethane available from Hexcel Corporation as Uralite #3110. Figures 32, 33 and 34 show the final head design.

3.6 Instrumentation

Standard instrumentation for the head consists of a triax accelerometer mounted at the C.G. of the head and part of the neck as required by MVSS 208. The accelerometer mounting will be designed to accept an Endevco triax accelerometer model 2267C-750. Accelerometers of similar size will also be accommodated with slight modification.

The mounting and head design have been developed to prevent spurious vibrations and shocks from influencing the transducer signals. Acceptable performance have been established by determining the resonant frequencies of the head-accelerator mount combination and comparing these with accelerometers mounted at the A-P and L-R impact sites. The accelerometers mount resonance frequencies are lower than the head impact site resonance frequencies. Transfer impedance techniques have been used to establish these criteria through the three internal accelerometer axes.

4.0 TORSO

The crash test device torso has been designed and constructed to match the following mechanical properties of fresh cadaver torsos. These properties have been measured in our laboratory and by C. K. Kroell and A. M. Nahmn.

Two papers describing this work are:

1. "Deflection of the Human Thorax Under Sternal Impact," SAE Paper No. 700400 by Alan M. Nahum, Charles W. Gadd, Dennis C. Schneider and Charles K. Kroell.

2. "Impact Tolerance and Response of the Human Thorax," SAE Paper No. 710851 by Charles K. Kroell, Dennis C. Schneider and Alan M. Nahum.

4.1 Static Stiffness

The static load-deformation characteristics of a significant number of fresh cadaver torsos is presented in Figure 5 of Reference 1 above.

The crash test device torso has been designed and constructed so that its static stiffness falls within the band of this data. The method of testing the static crash test device torso performance was as described in the reference.

4.2 Dynamic Stiffness and Damping

Dynamic stiffness and damping properties for fresh cadaver torsos have been determined by HSRI using the methods of Kroell and Nahum. Figure 38 shows the results from 10 different cadaver tests. The impact velocity varied between 12 and 14 miles per hour and a 22-pound 6-inch diameter impactor centered on the space between the fourth and fifth ribs was used. No ribs were fractured in these impacts. The crash test device torso has been designed and constructed so that its dynamic stiffness and damping fall within this band.

The HSRI results have been taken as the crash test device torso performance criteria because:

1. Ten tests at a standardized velocity and piston weight are available without broken ribs.

2. The identical equipment and instrumentation is available for evaluation of dummy torsos.

3. An inertia compensated load cell was used.

4.3 Repeatability

A major design consideration for this crash test device torso is repeatability and reproducibility of test results. To verify repeatability at the component level, all final qualifying impact tests have been performed six times. Not more than 5% variation between the mean value of the peak load and deformation for the six tests and the outlier was observed.

4.4 Chest Design

The final chest design incorporated six flexible steel ribs moulded in a solid soft urethane shell. The urethane used was Uralite 3111. Figure 35 shows the final configuration. The steel ribs are attached to the spine by screws and maintain relative alignment of the chest and spine.

4.5 Instrumentation

4.5.1 Accelerometers

Standard instrumentation consists of a triax accelerometer centrally mounted in the chest on a simulated spinal base so that the intersection of the seismic mass centers of the tria-axial cluster is in the midsagittal plane 5.7 inches below the neck-to-thorax attachment surface and 4.3 inches forward of the dummy's back line, and the X-Y-Z axes of the accelerometer cluster are parallel with the X-Y-Z axes of the dummy with maximum permissible offset and orientation misalignment not exceeding 1/2 inch and 5° respectively.

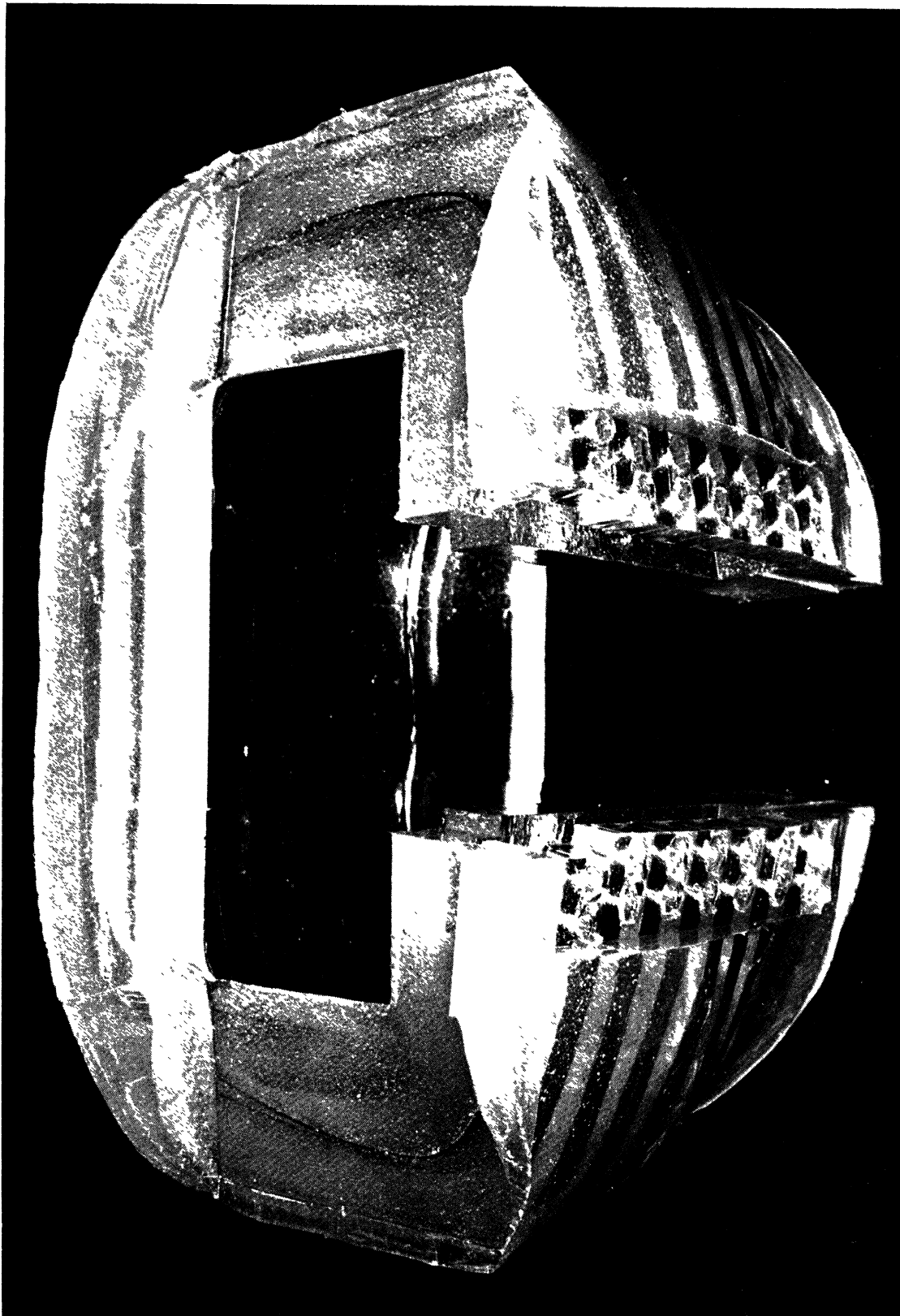


Figure 35 HSRI One Piece Chest.

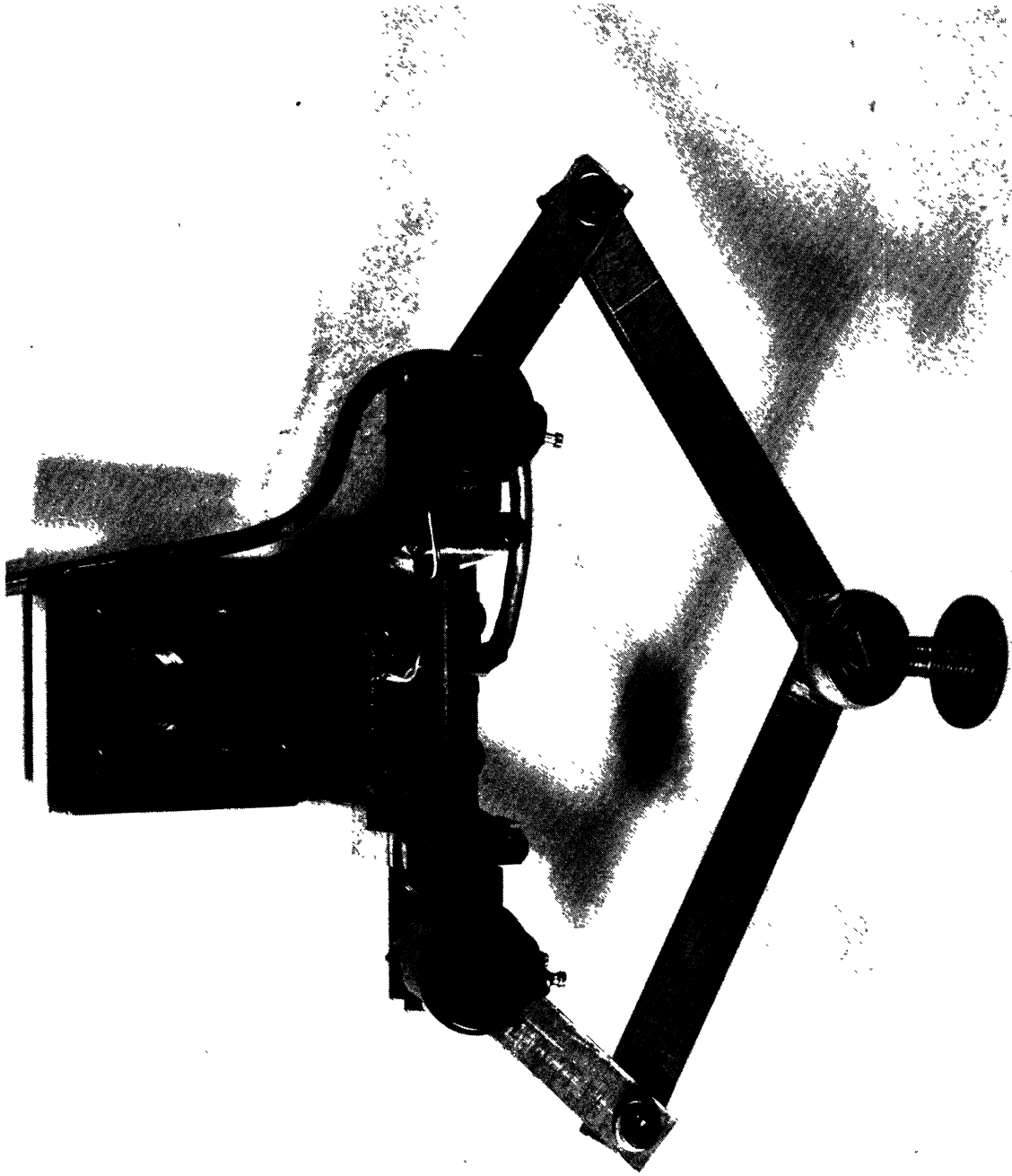


Figure 36 Chest Displacement Transducer.

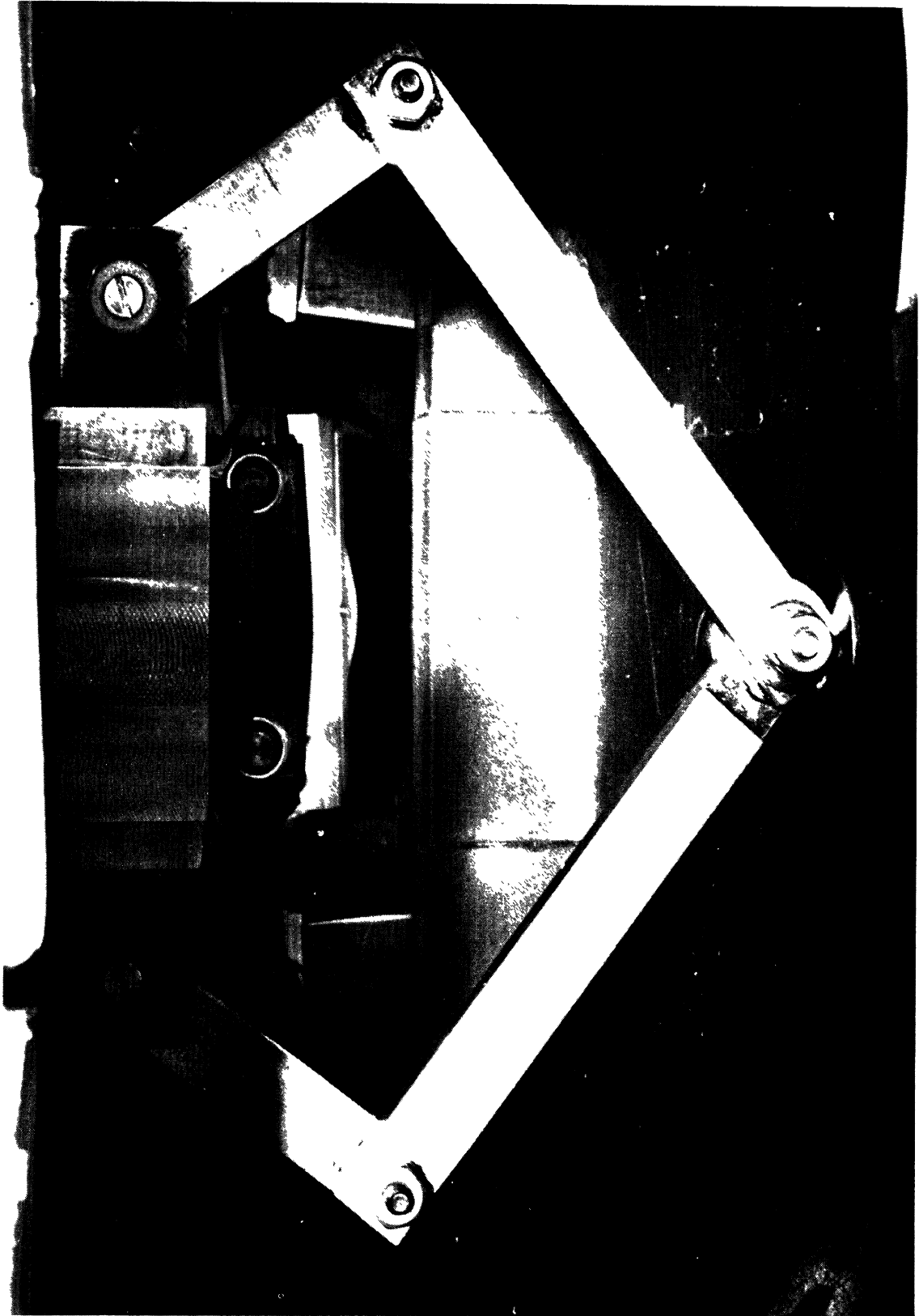


Figure 37 Chest Displacement Transducer Installed in Chest.

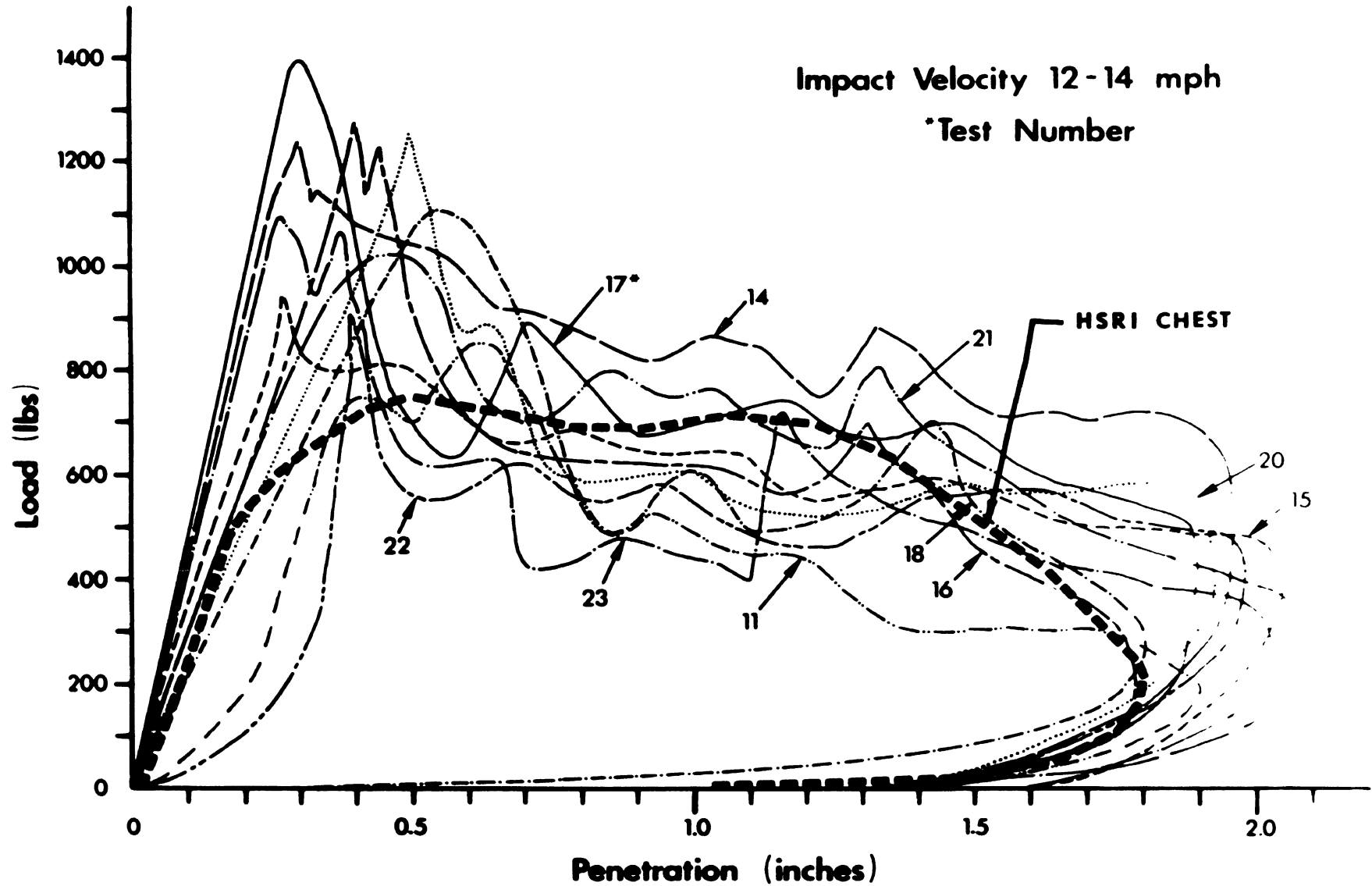


FIGURE 38 COMPOSITE LOAD-DEFLECTION CURVES FOR CADAVER FRONT CHEST IMPACTS.

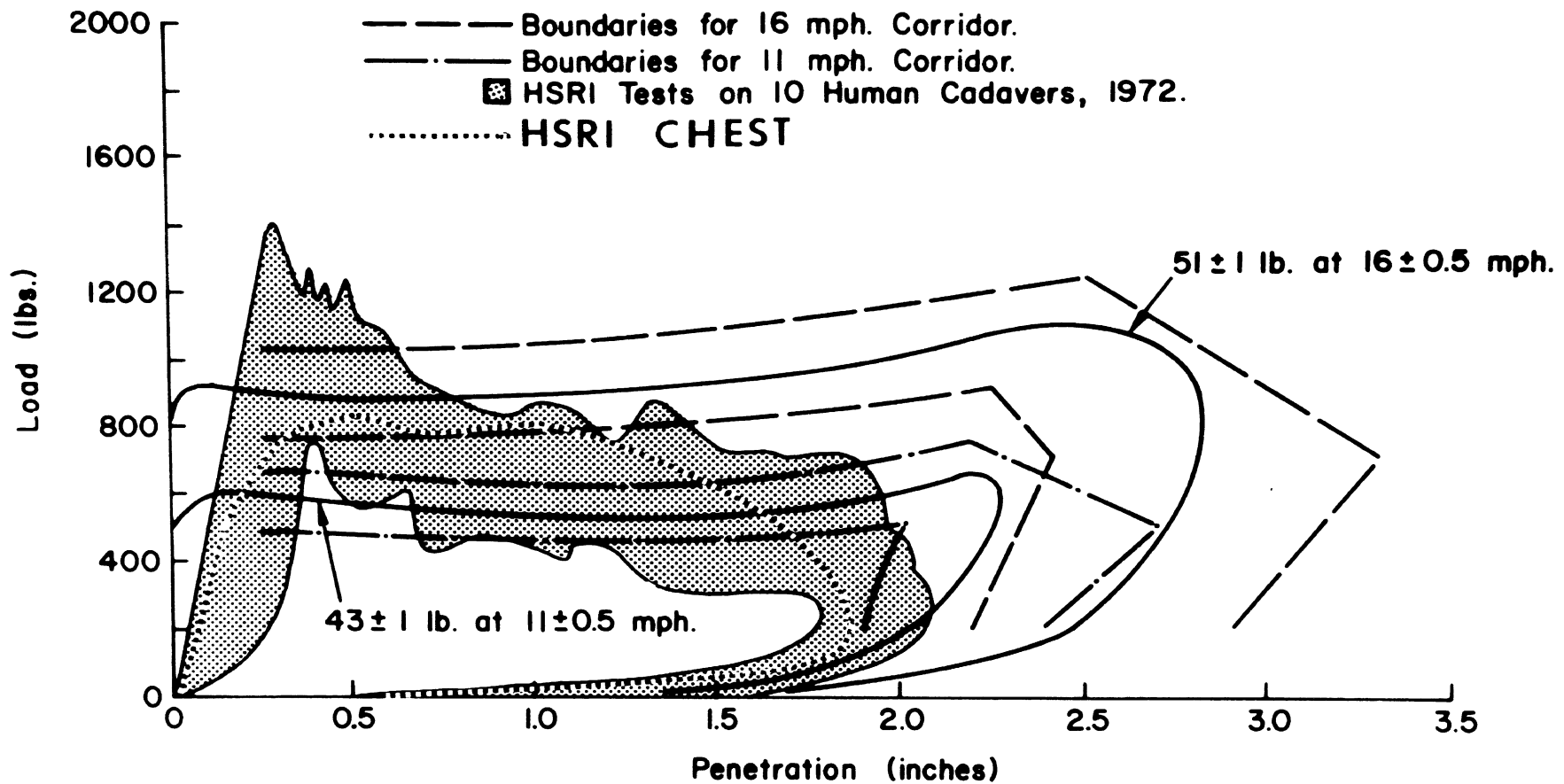


FIGURE 39
 GM BLUNT IMPACT PERFORMANCE CORRIDORS AND HSRI DATA ON CHEST IMPACTS.

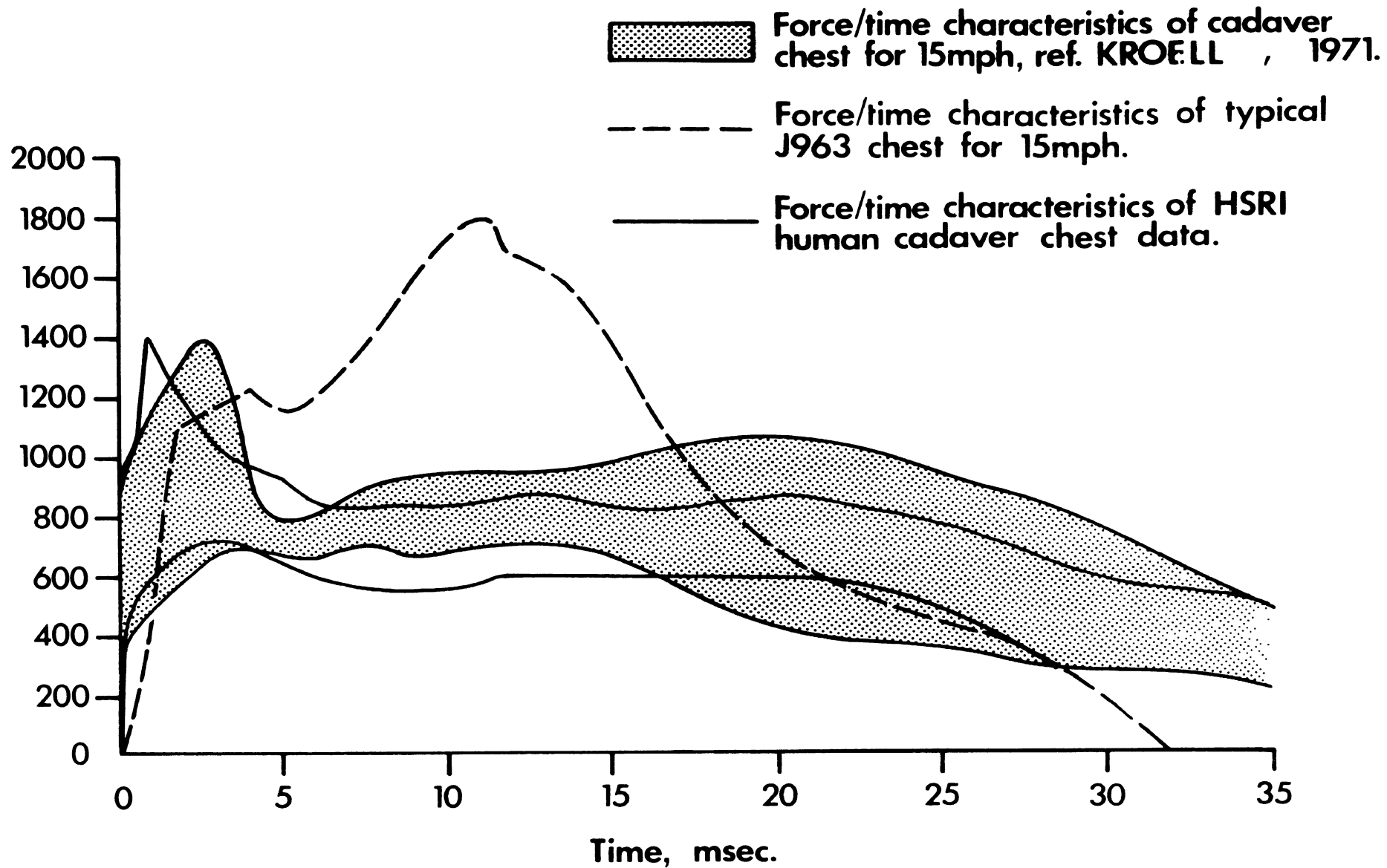


FIGURE 40 . HUMAN CHEST IMPACTS.

4.5.2 Chest Displacement Transducer

Provision has also been made for mounting internally a displacement transducer to measure relative motion between the sternum and the spine. Any of the various displacement transducers used for this purpose can be mounted in the HSRI chest with a few simple modifications. Because an adequate chest displacement transducer was unavailable at the time of the chest component testing, a unique and highly acceptable device was designed and constructed. The device consists of a space linkage that can be moved in three directions, thus allowing the chest to deform naturally. The space linkage drives two rotary film pots, whose output is added differentially. The linkage arms are such that the output is proportional to the horizontal motion of the chest attachment point and independent of the other components of this motion. Figure 36 shows the chest displacement transducers and Figure 37 shows it installed in the dummy chest.

5.0 NECK

This crash test device utilizes the HSRI neck simulation developed separately and reported in detail in the final report, "AMA Neck Study Project," June 1972.

The HSRI neck was developed to produce realistic motions of the head in the sagittal plane during indirect impact at acceleration levels similar to the inputs experienced by human volunteers. The performance criteria by which the head-neck response was judged included the dynamic neck response envelope of Mertz and Patrick and also considered:

1. The range of angular motion of the head relative to the torso.
2. The trajectory of the center of gravity of the head with respect to the torso.

3. The angular and linear accelerations of the head produced during the head motion.

The criteria and performance of the prototype neck is shown in Figures 42, 43 and 44 in flexion and in Figures 45, 46 and 47 for extension. The details of the neck design and the test program used to develop the neck can be found in the AMA report.

The HSRI neck design has been adapted to the crash test device and its characteristics tuned to produce optimal head-neck performance based on the above criteria. Figure 41 shows the final neck design.

6.0 PELVIS

The crash test device utilized a modified Sierra brass pelvis meeting the following requirements:

6.1 Geometry

The general configuration of the pelvis conforms to the human-like shape of the master pelvis, now in possession of the SAE J963 Crash Test Device Subcommittee. In addition, the pelvis meets the dimensional requirements, with the tolerances shown in Figure 48, that were submitted to the SAE J963 Crash Test Device Subcommittee and subsequently have been incorporated into MVSS 208.

6.2 Ranges of Motion

The hip joint is of such design that it meets the full ranges of motion specified for the thigh at the hip in Table 3 (See Section 8, joints).

Since the primary usage of this crash test device is in seated position, the human-like skin covering will be cast in seat form so as to provide a better fit and easier positioning in the test vehicle. The effect of the skin and padding will be designed to be small in comparison with the controlled resistance to the motion at the hip joint.

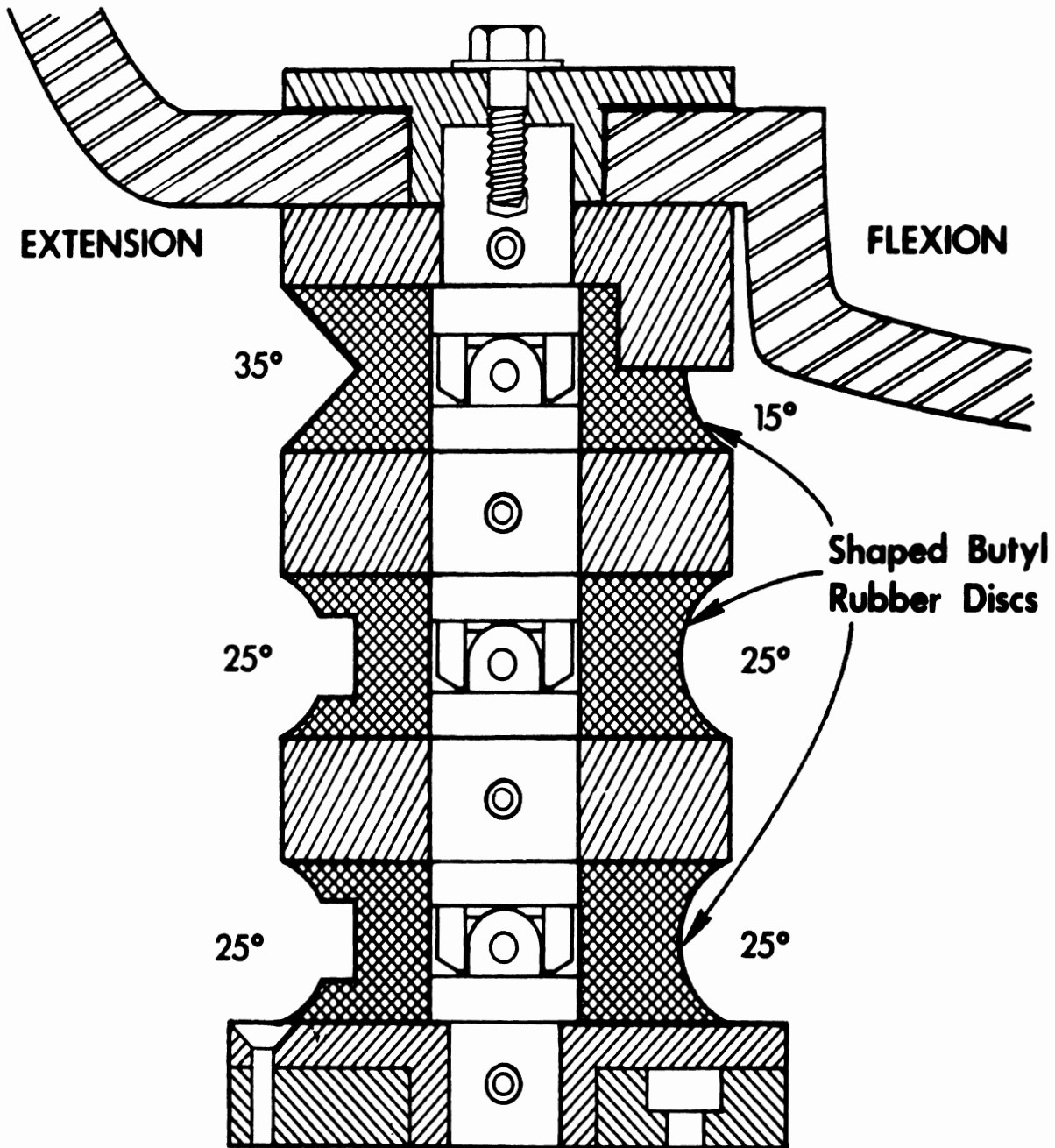


FIGURE 41 HSRI DUMMY NECK.

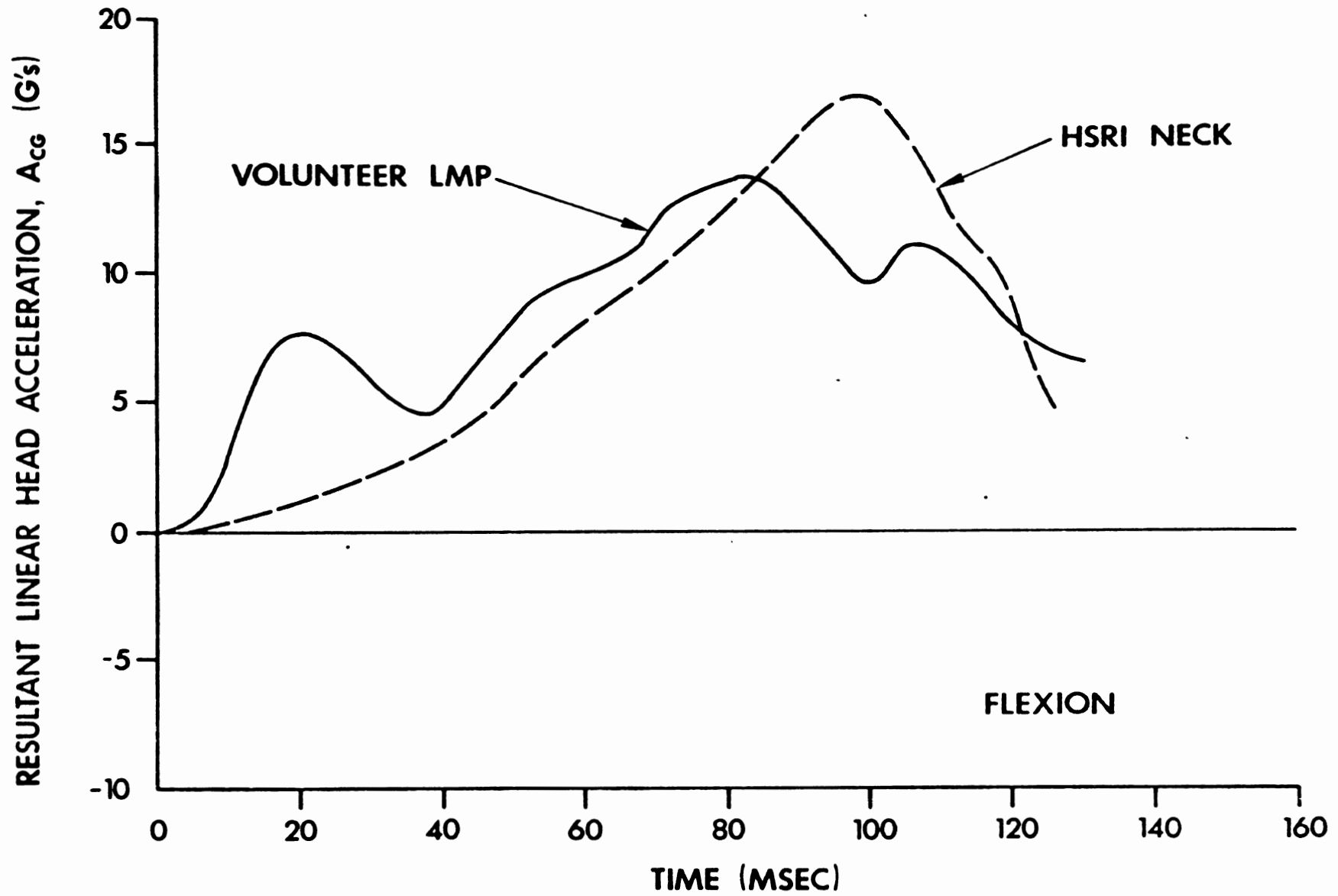


FIGURE 42 COMPARISON OF RESULTANT LINEAR HEAD ACCELERATIONS FOR THE HSRI NECK AND HUMAN VOLUNTEERS IN FLEXION.

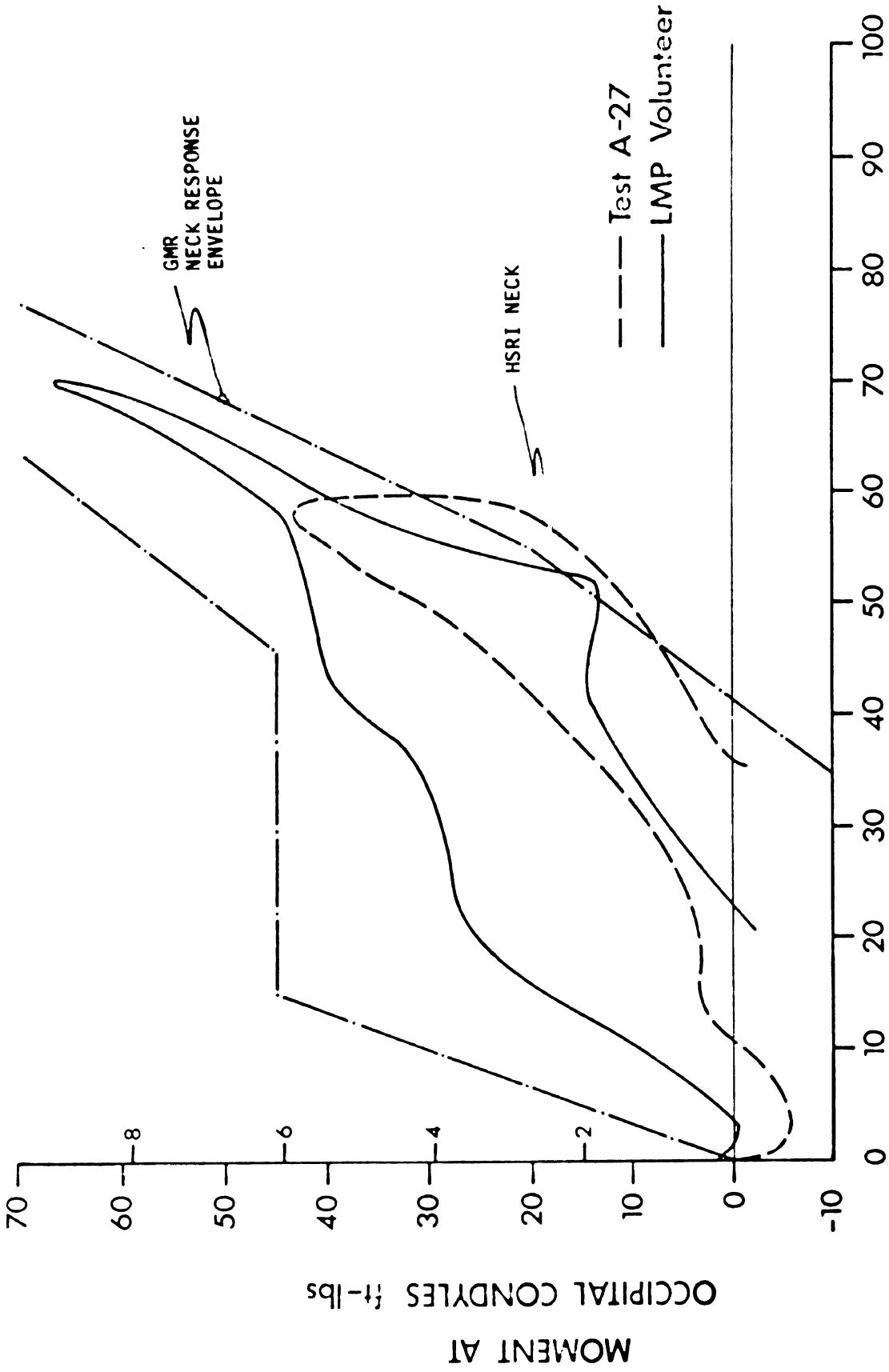


FIGURE 43 COMPARISON OF NECK MOMENT FOR THE HSRI NECK AND HUMAN VOLUNTEERS IN FLEXION.

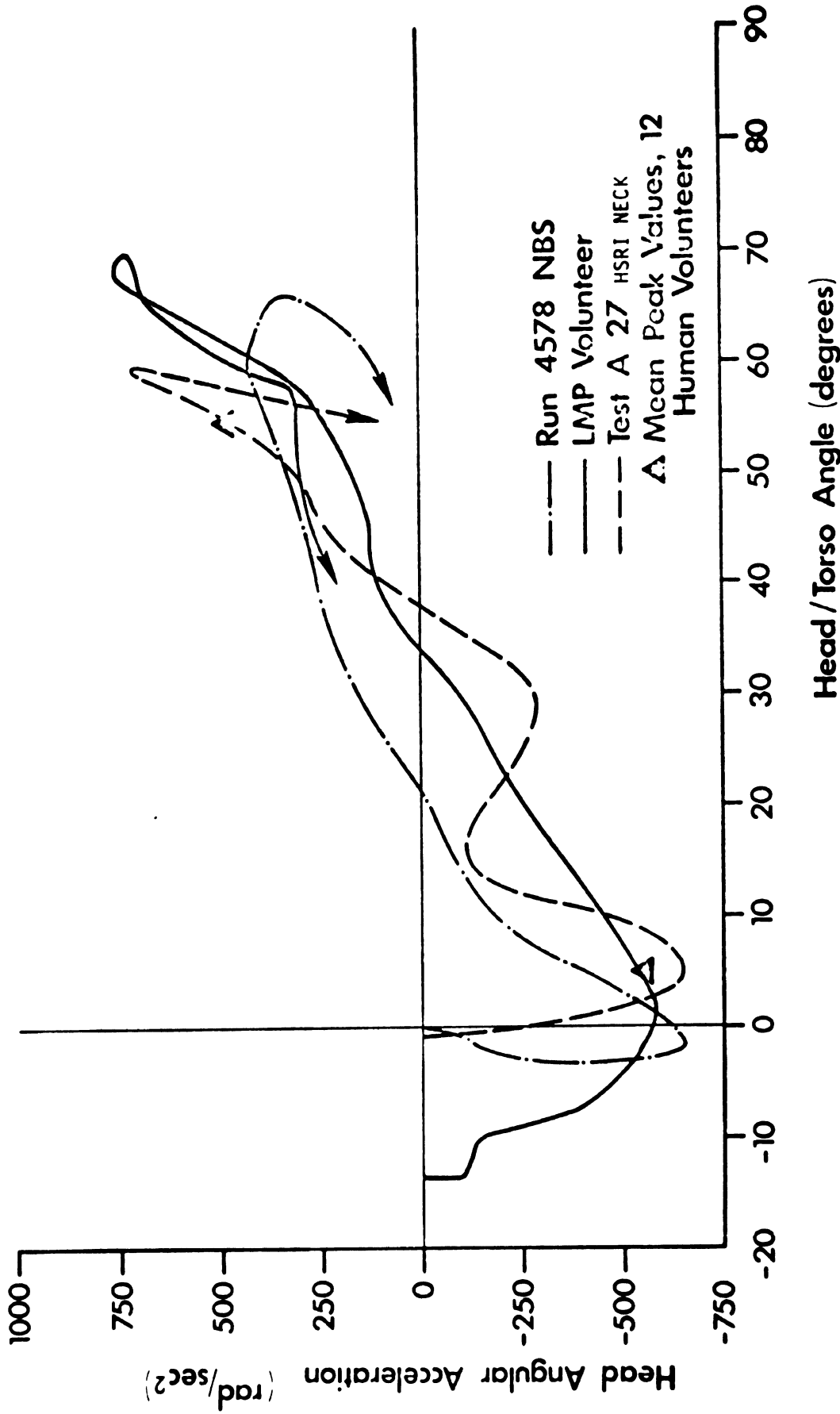


FIGURE 44 COMPARISON OF HEAD ANGULAR ACCELERATIONS AND RANGE OF ANGULAR MOTION FOR THE HSRI NECK AND HUMAN VOLUNTEERS IN FLEXION.

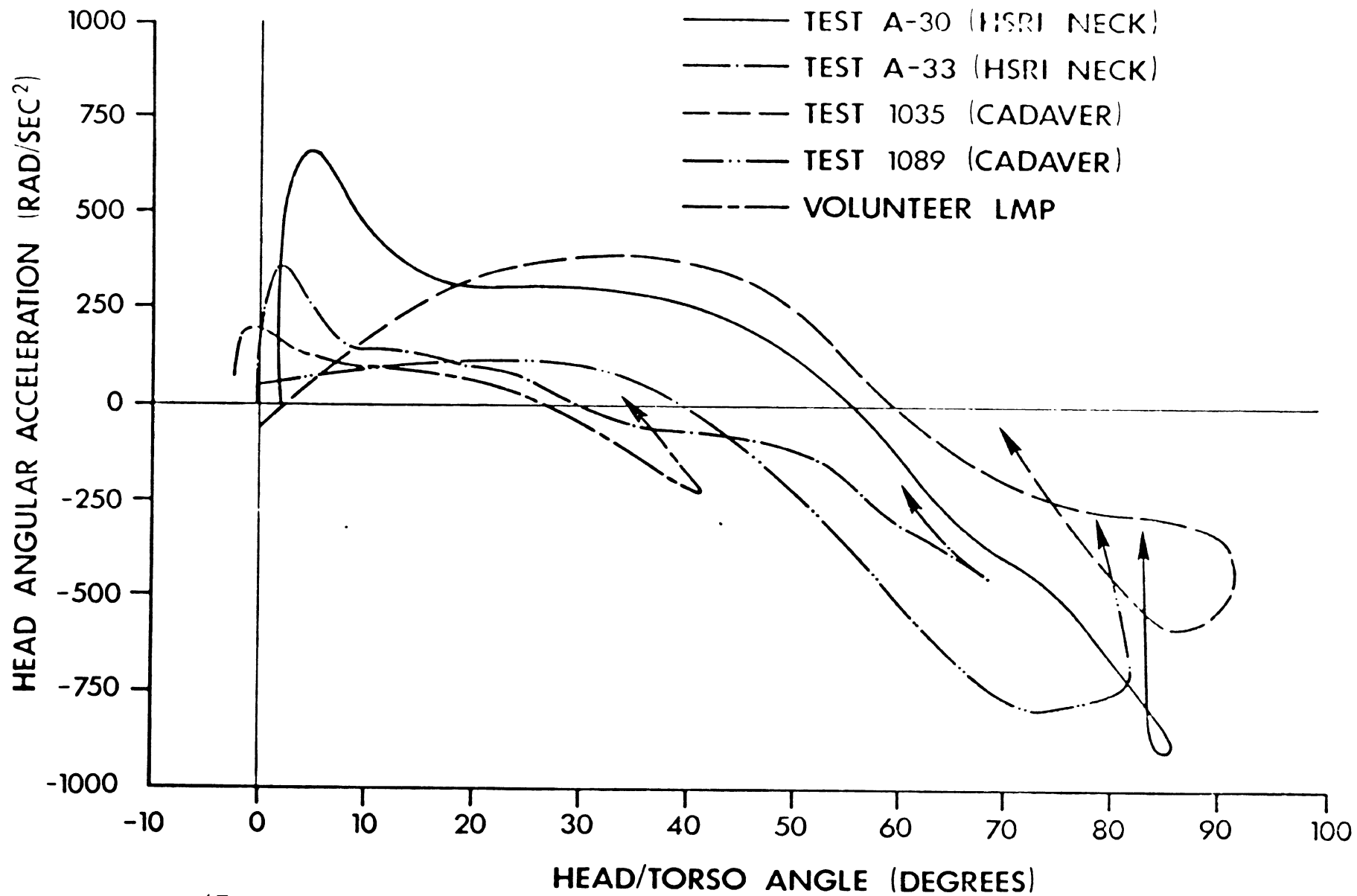


FIGURE 45 COMPARISON OF HEAD ANGULAR ACCELERATIONS AND RANGE OF ANGULAR MOTION FOR THE HSRI NECK, HUMAN VOLUNTEERS, AND CADAVERS IN EXTENSION.

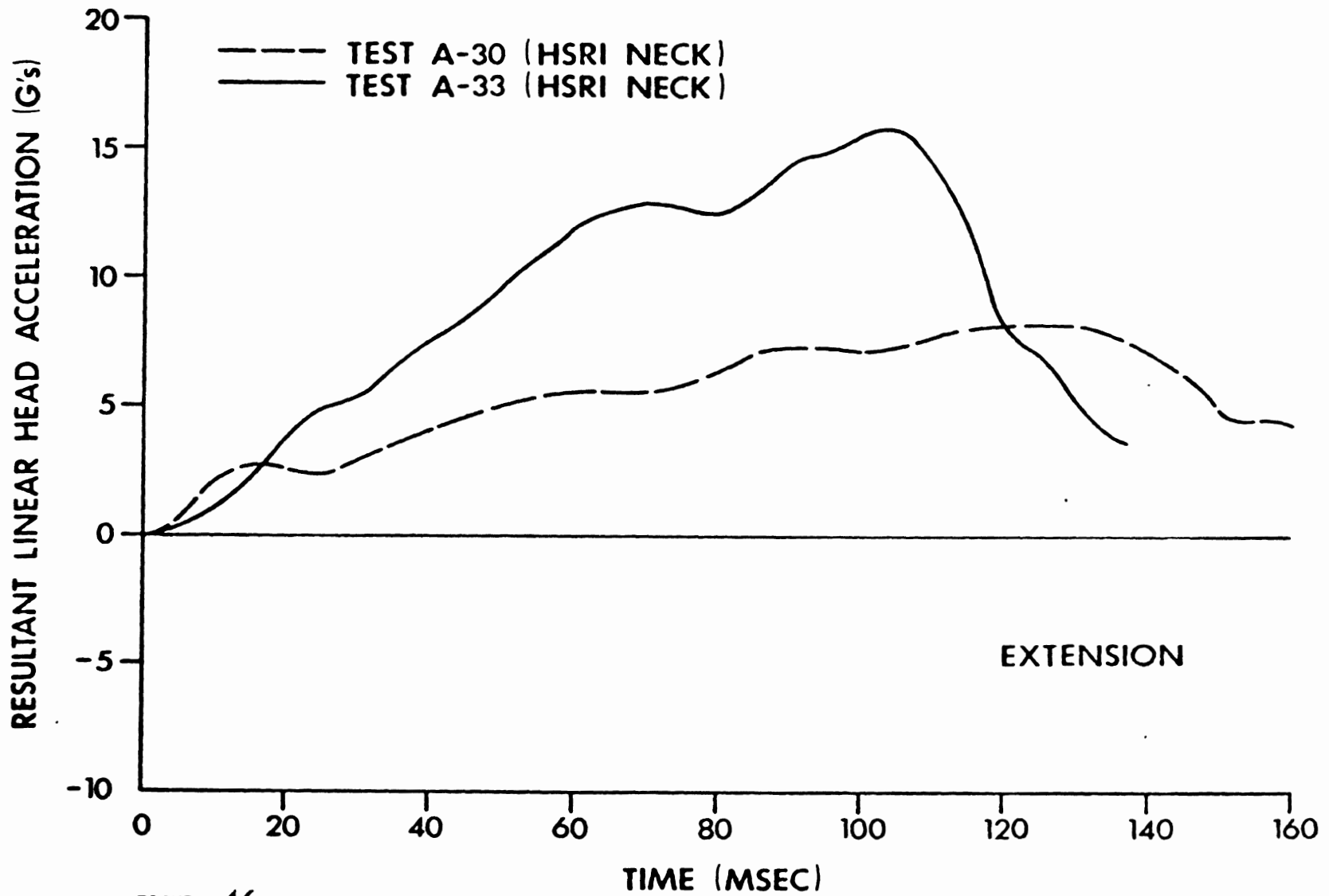


FIGURE 46 RESULTANT LINEAR HEAD ACCELERATIONS FOR THE HSRI NECK IN EXTENSION FOR 5g (A-33)
 AND 9.5g (A-30) INPUT ACCELERATIONS.

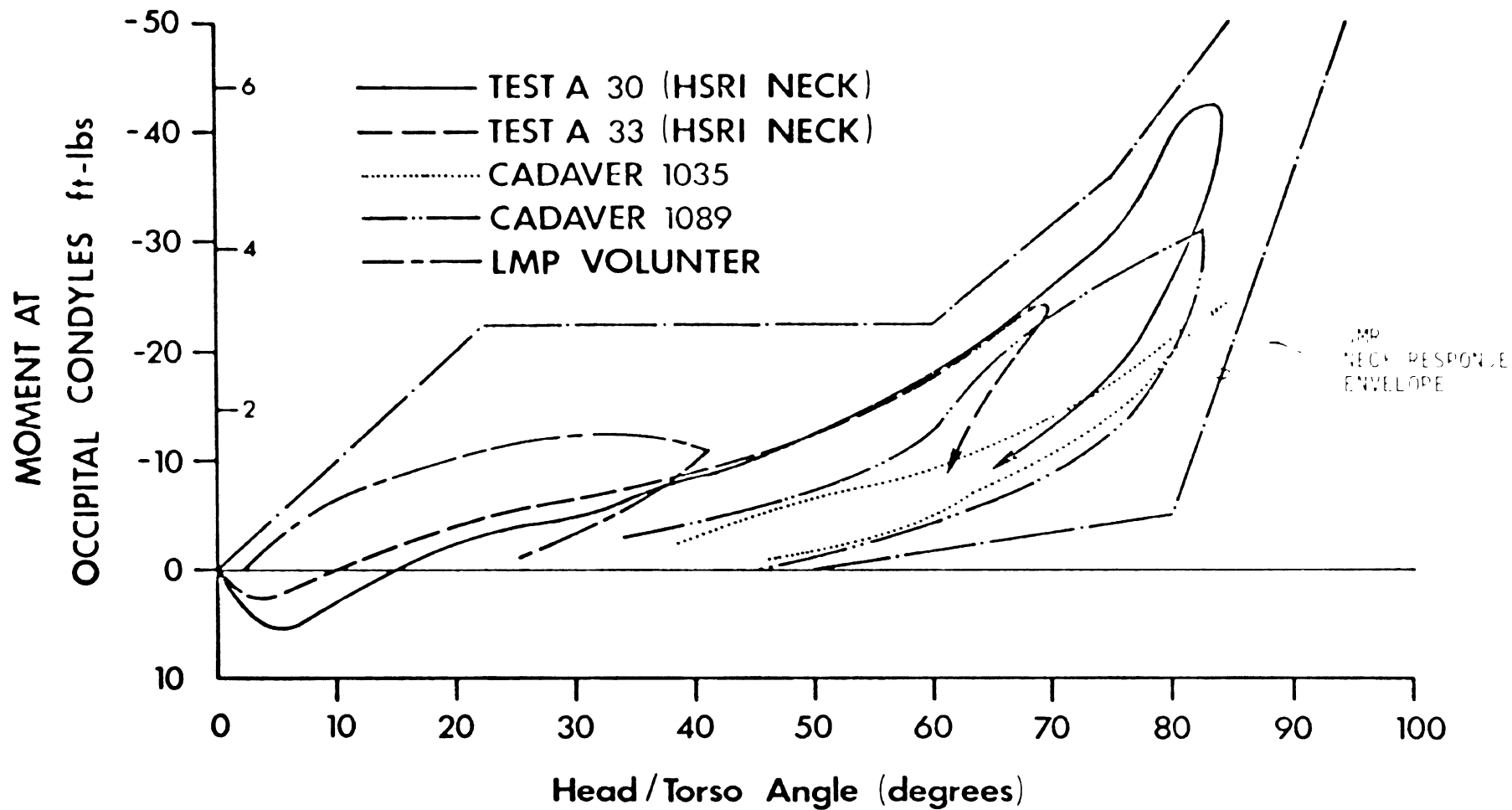
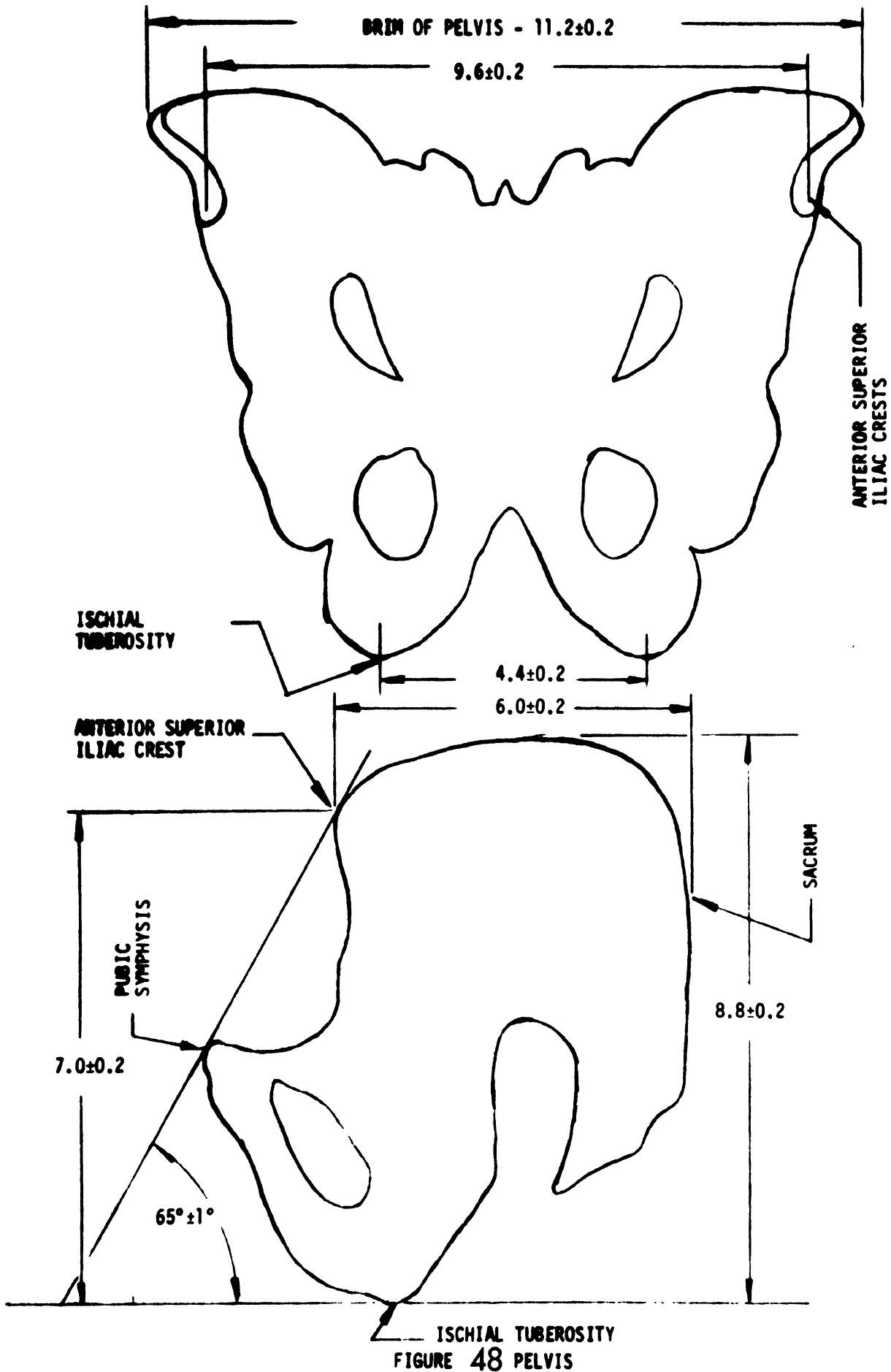


FIGURE 47 COMPARISON OF NECK MOMENT FOR THE HSRI NECK, HUMAN VOLUNTEERS, AND CADAVERS IN EXTENSION.



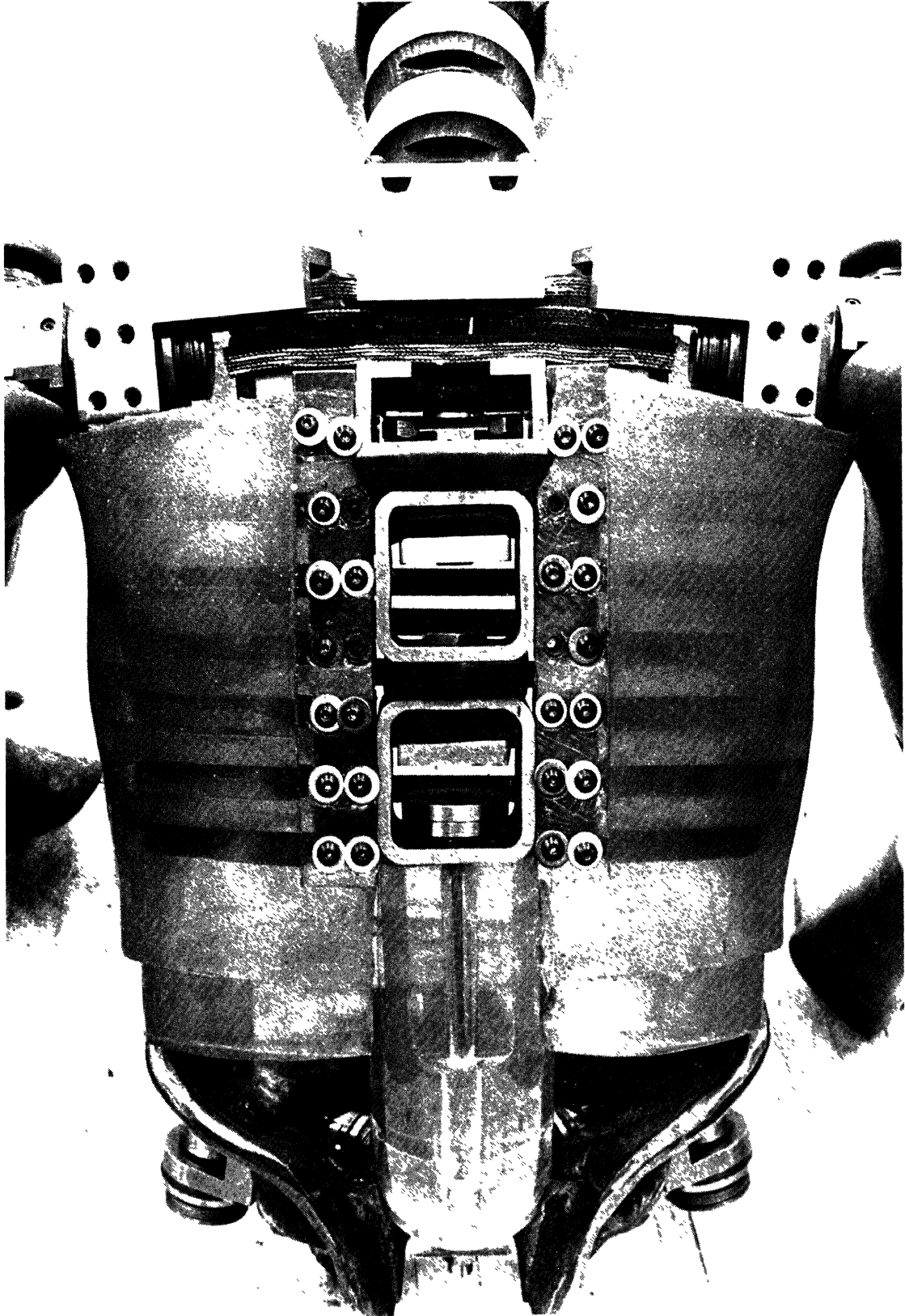


Figure 49 Rear Assembly "Repeatable Pete."

7.0 SPINE

An improved spine has been developed. The thoracic region consists of three steel boxes isolated from each other by butyl rubber pads. The chest section is attached to these steel boxes (see Figure 49). The thoracic spine is a flexible urethane bar with a through cable for tensile strength. Uralite 3111 is used. The cable is attached to the lower thoracic box at the top and the pelvis at the bottom. Human-like flexibility is obtained in all directions.

8.0 JOINTS

8.1 Design Features

A new and unique joint system has been developed. The basic features of these joints are:

1. Extreme strength and durability.
2. A single setting that does not require frequent adjustment or check out.
3. Long life without any maintenance.

Figures 50 and 51 show typical joints while Figures 52, 53 and 54 show the design details for all joints.

8.2 Life Tests

Life tests on the joints were performed by cycling the angular displacement sinusoidally for 1000 cycles. The torque did not change more than 7% over this period. Moreover, there was no significant difference between static and dynamic motions. Figure 55 shows a typical set of displacement and torque histories for these tests while Figure 56 shows the test setup.

9.0 LIMBS

The limbs are moulded of self-skinning urethane foam consisting of a resin part RX723 and isothanite IX700 available from the Poly-Chem Corp. Figure 57 shows a typical section through the forearm.

9.1 Patella

The patella is spherical in shape and large enough to protect the movable knee joint elements. It is integral with the knee clevis which is directly connected to the femur load cell. Figure 58 shows the knee joint assembly.

9.2 Femur Loads

Provision for either GSE or Endevco femur load cells has been made. The load cells must be drilled out to accept 1/2 inch diameter expandable bolts provided with the device.

9.3 Seating Position

Repeatable Pete is designed to sit upright in the usual automotive seat with his head facing forward. This is unlike current dummies whose backs are generally straight. Because of this, Repeatable Pete will be hunched over when seated erect on a horizontal flat surface (See Frontispiece).

TABLE 7

Dummy # 1

JOINT TORQUE SPECIFICATIONS

| ID # | JOINT | TORQUE SPECIFICATIONS in # | TORQUE MEASURED in # |
|------|-------------------------|-------------------------------|-------------------------|
| 1. | Ankle Right | 5.7± .57 | 6.1 |
| 2. | Ankle Left | 5.7± .57 | 6.0 |
| 3. | Knee Right | 109.1± 10.9 | 107 |
| 4. | Knee Left | 109.1± 10.9 | 105 |
| 5. | Hip Right (double) | 237.8± 23.8 | 221 |
| 6. | Hip Left (double) | 237.8± 23.8 | 231 |
| 7. | Hip Right (single) | 237.8± 23.8 | 239 |
| 8. | Hip Left (single) | 237.8± 23.8 | 233 |
| 9. | Shoulder Right (double) | 96.4± 9.6 | 93 |
| 10. | Shoulder Left (double) | 96.4± 9.6 | 98 |
| 11. | Shoulder Right (single) | 96.4± 9.6 | 95 |
| 12. | Shoulder Left (single) | 96.4± 9.6 | 94 |
| 13. | Elbow Right | 29.9± 3.0 | 27 |
| 14. | Elbow Left | 29.9± 3.0 | 28 |
| 15. | Arm Twist Right | 29.9± 3.0 | 27 |
| 16. | Arm Twist Left | 29.9± 3.0 | 29 |
| 17. | Wrist Right | 4.1± .41 | 4.3 |
| 18. | Wrist Left | 4.1± .41 | 4.2 |

TABLE 8

Dummy # 2

JOINT TORQUE SPECIFICATIONS

| ID # | JOINT | TORQUE SPECIFICATIONS | | TORQUE MEASURED |
|------|-------------------------|-----------------------|------|-----------------|
| | | in # | | in # |
| 1. | Ankle Right | 5.7± | .57 | 5.9 |
| 2. | Ankle Left | 5.7± | .57 | 6.2 |
| 3. | Knee Right | 109.1± | 10.9 | 103 |
| 4. | Knee Left | 109.1± | 10.9 | 108 |
| 5. | Hip Right (double) | 237.8± | 23.8 | 229 |
| 6. | Hip Left (double) | 237.8± | 23.8 | 222 |
| 7. | Hip Right (single) | 237.8± | 23.8 | 225 |
| 8. | Hip Left (single) | 237.8± | 23.8 | 228 |
| 9. | Shoulder Right (double) | 96.4± | 9.6 | 101 |
| 10. | Shoulder Left (double) | 96.4± | 9.6 | 104 |
| 11. | Shoulder Right (single) | 96.4± | 9.6 | 91 |
| 12. | Shoulder Left (single) | 96.4± | 9.6 | 95 |
| 13. | Elbow Right | 29.9± | 3.0 | 31 |
| 14. | Elbow Left | 29.9± | 3.0 | 29 |
| 15. | Arm Twist Right | 29.9± | 3.0 | 31 |
| 16. | Arm Twist Left | 29.9± | 3.0 | 30 |
| 17. | Wrist Right | 4.1± | .41 | 4.4 |
| 18. | Wrist Left | 4.1± | .41 | 4.3 |

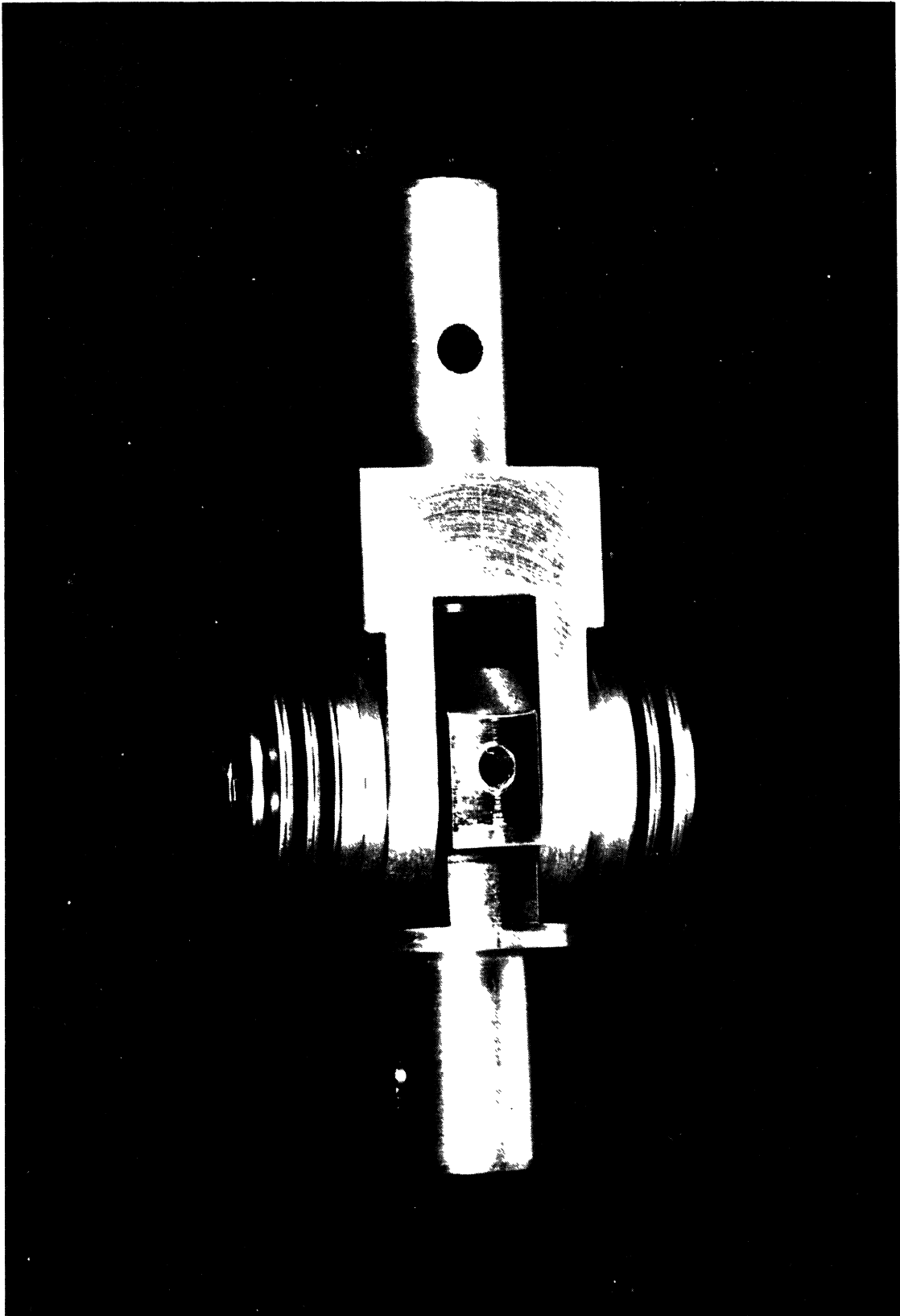


Figure 50 Typical Joint Assembly.

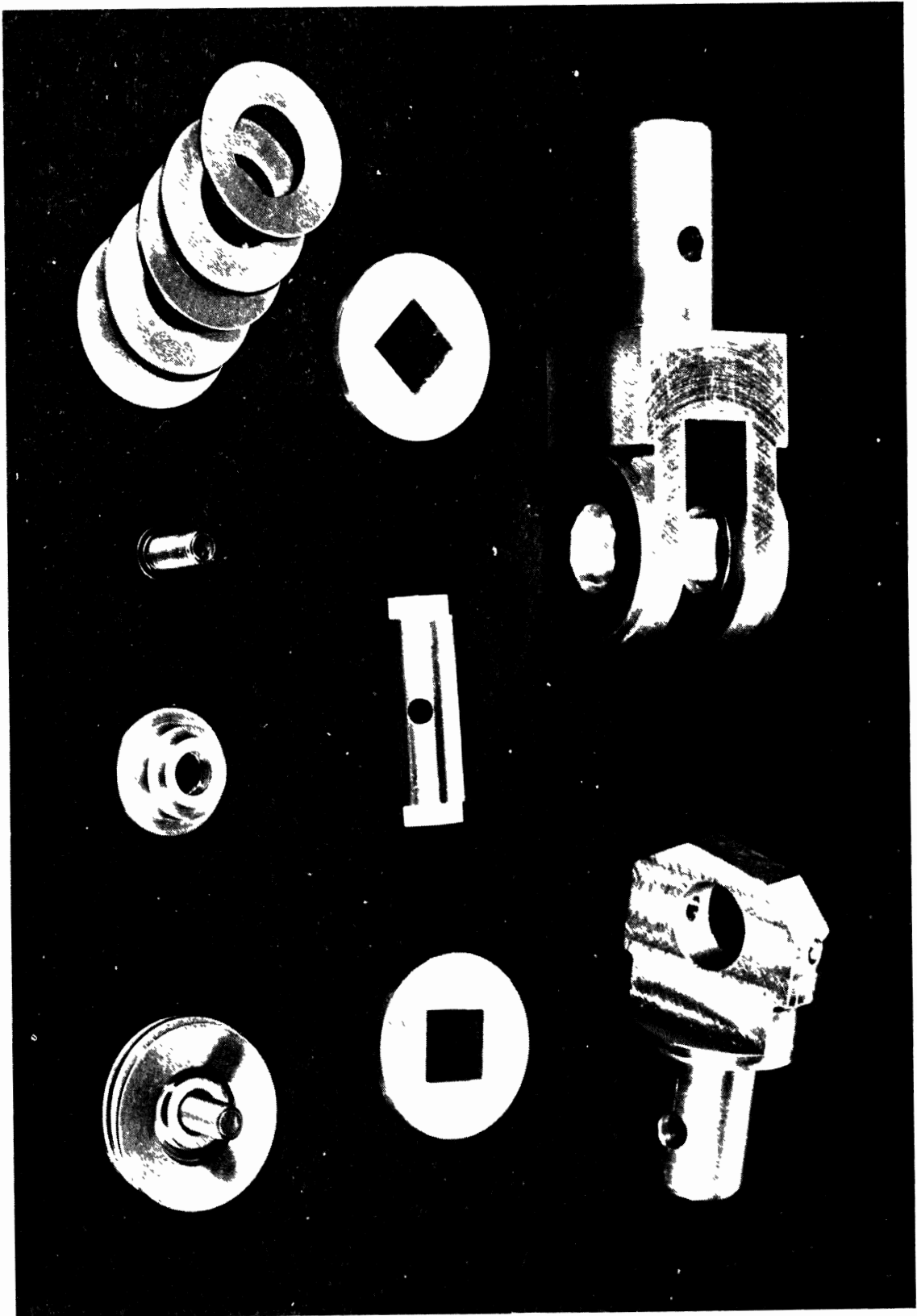


Figure 51 Typical Joint Components.

| | | |
|----|-------------------------|---------------------|
| 1 | PIVOT | PT. NO. 101-691-D |
| 2 | SPINDLE PIN | 1/2 P 5 X 1 1/2 - 4 |
| 3 | PIN | 5 - 3 - 16 - 5 - B |
| 4 | TRUCKER | |
| 5 | BUSHING | PT. NO. 100-381-A |
| 6 | 11/16 STEEL - FRICTION | PT. NO. 100-380-B |
| 7 | REASVILLE SPRING WASHER | |
| 8 | 11/16 STOP | PT. NO. 101-794-B |
| 9 | 1/2 HD. SCR. | 5 - 24 X 7 1/2 - 4 |
| 10 | CLEVIS | PT. NO. 101-600-D |
| 11 | WASHER - FIBER | PT. NO. 101-750-A |

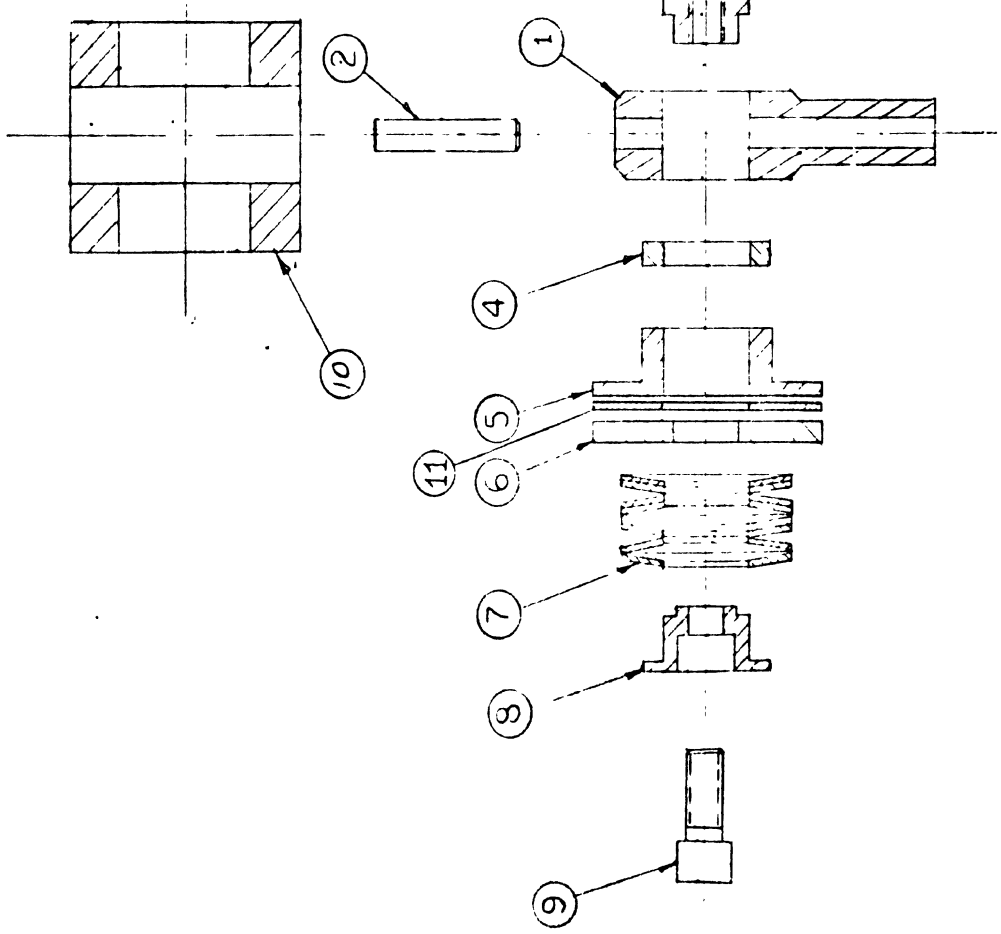
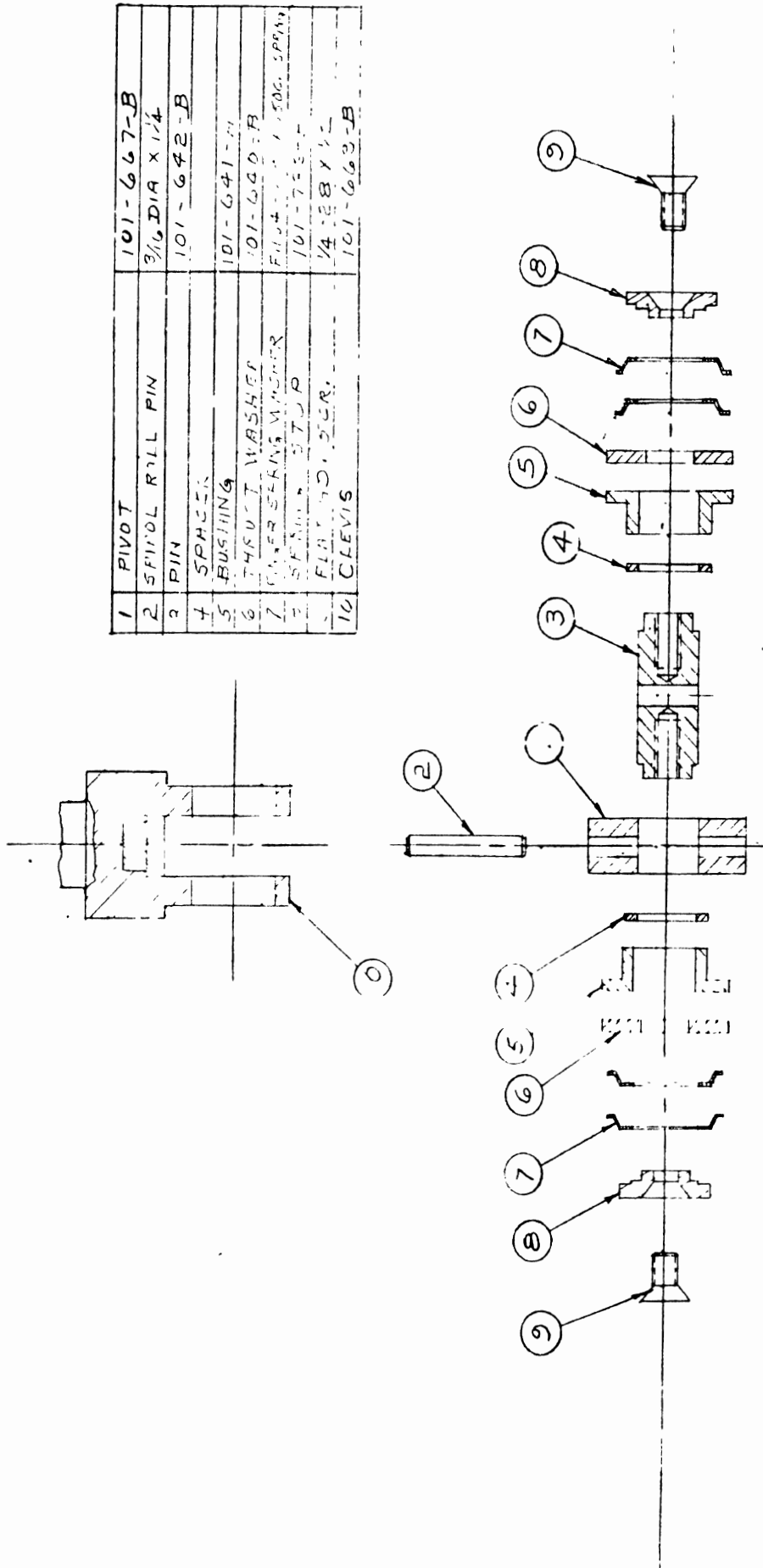


FIGURE 52 TYPICAL JOINT ASSEMBLY



| | | |
|----|-----------------------|----------------------|
| 1 | PIVOT | 101-667-B |
| 2 | SPINDLE ROLL PIN | 3/16 DIA X 1/4 |
| 3 | PIN | 101-642-B |
| 4 | SPACER | |
| 5 | BUSHING | 101-641-B |
| 6 | THRUST WASHER | 101-660-B |
| 7 | THRUST BEARING WASHER | FILED 10/1/50G. SPAN |
| 8 | SPACER | 101-753-B |
| 9 | FLAT END PIER. | 1/4 X 28 X 1/2 |
| 10 | CLEVIS | 101-663-B |

FIGURE 53 TYPICAL WRIST AND ANKLE JOINT

| STACK | PART NO. & NAME | JOINT |
|-------|-------------------------------------|-----------------|
| "A" | B1750-057 BELLEVILLE SPRING WASHER | HIP |
| "A" | B1500-0455 BELLEVILLE SPRING WASHER | KNEE & SHOULDER |
| "B" | B1250-040 BELLEVILLE SPRING WASHER | ELBOW |
| "C" | F1164-018 FINGER SPRING WASHER | ANKLE & WRIST |

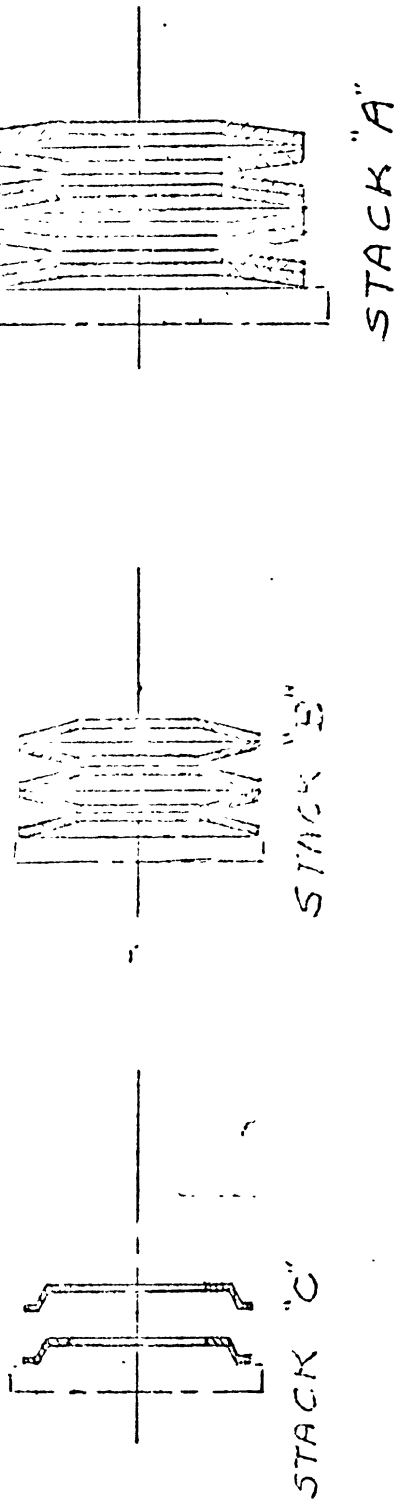


FIGURE 54 JOINT SPRINGS

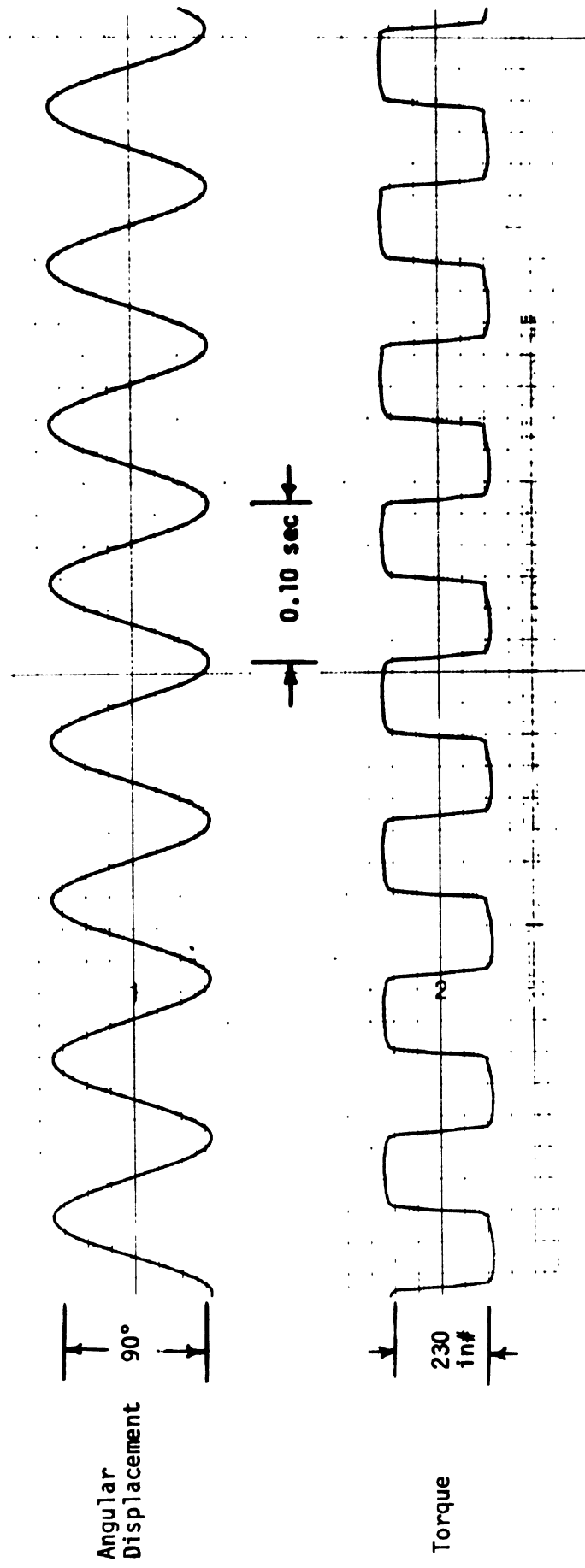


Figure 55
Life Test of Knee Joint

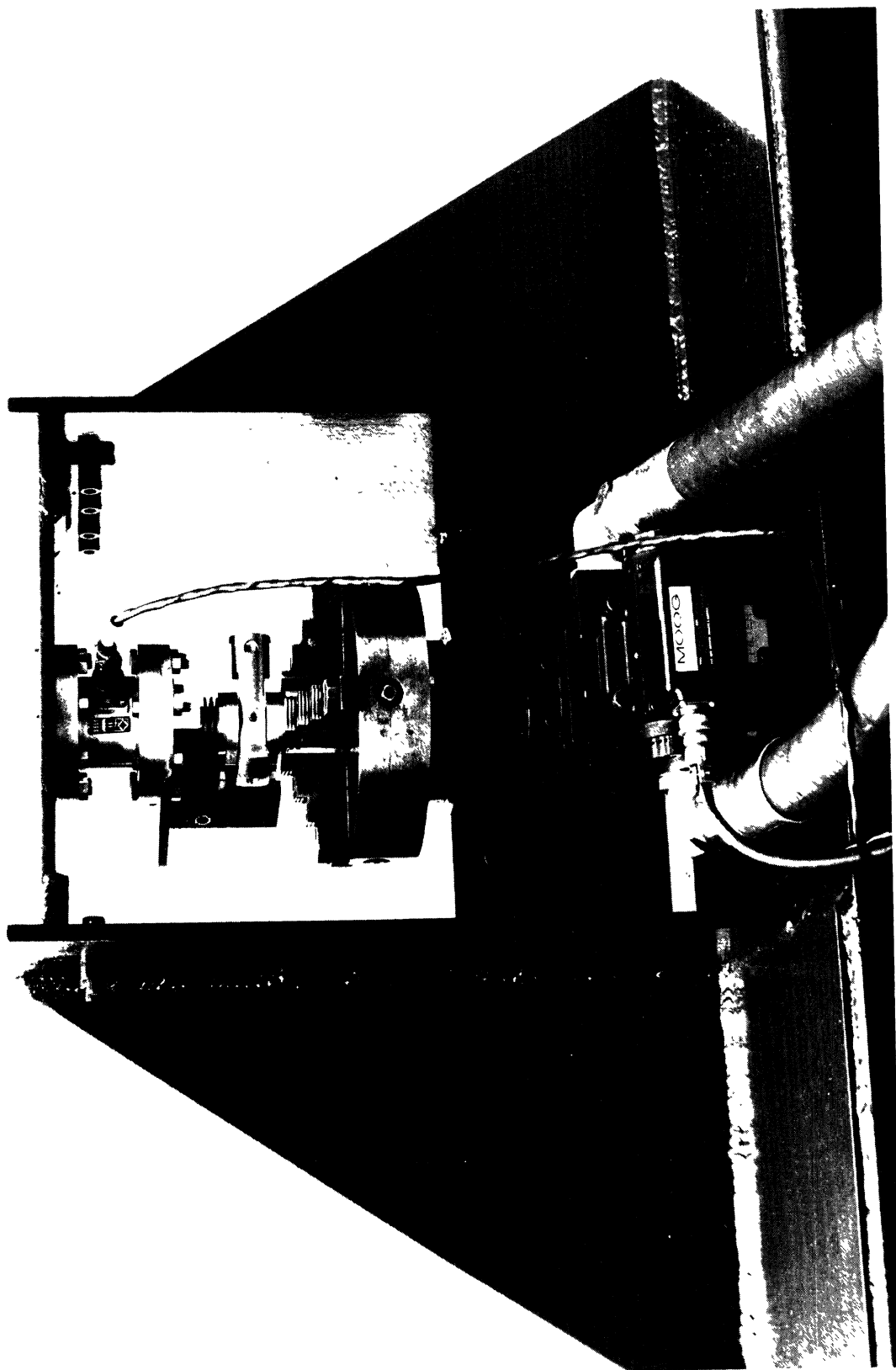


Figure 56 Typical Setup for Joint Fatigue Testing.

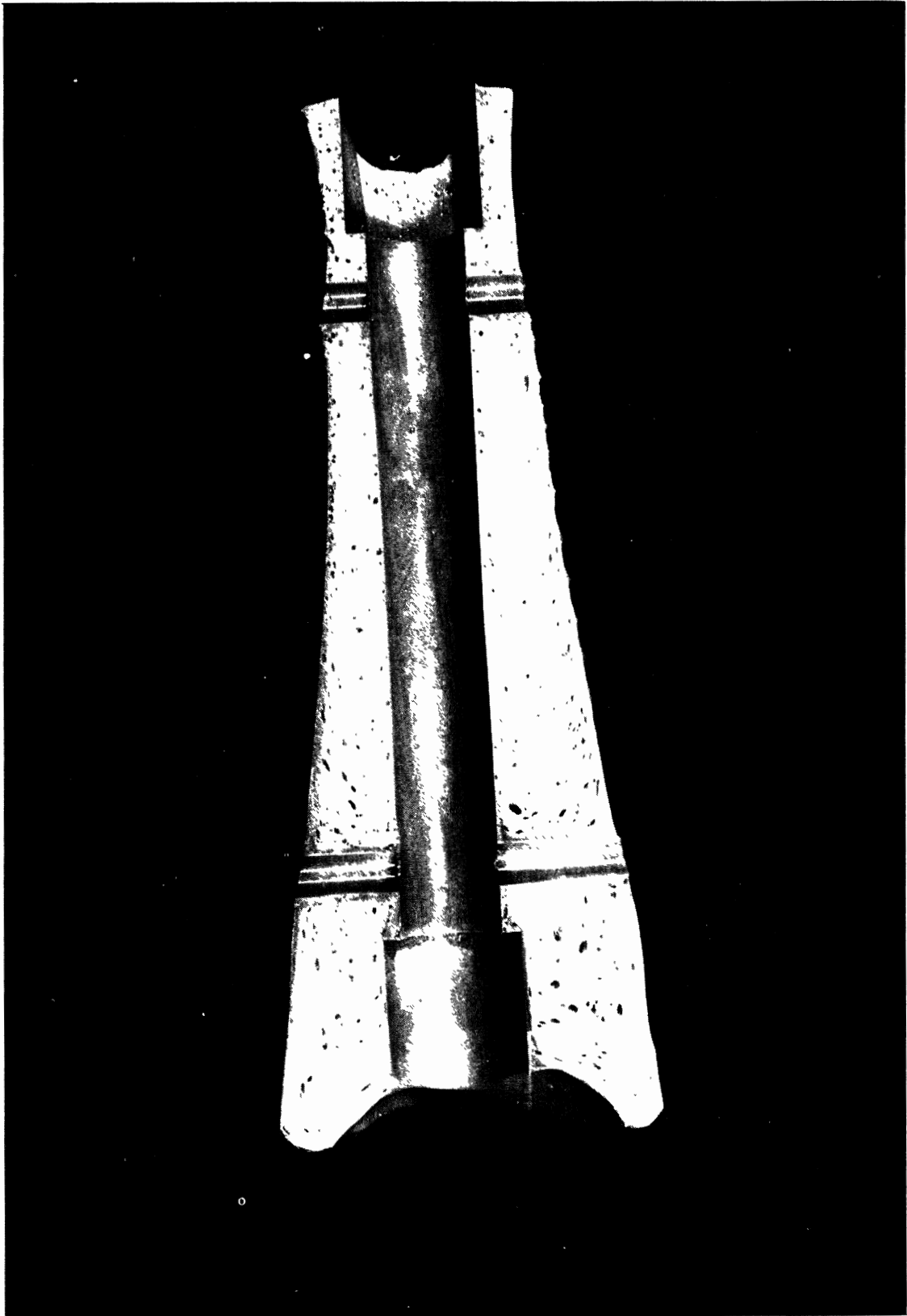


Figure 57 Section through Self-Skinning Urethane Foam Forearm.

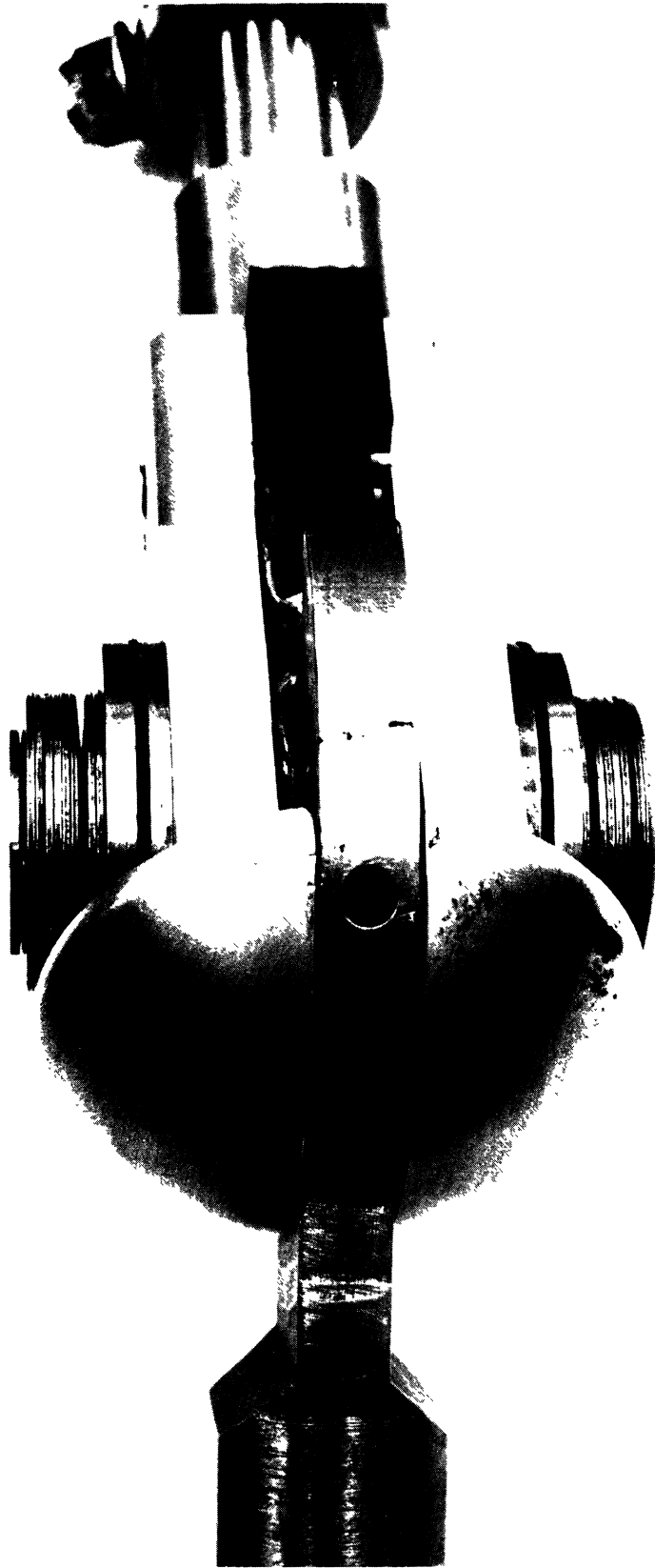


Figure 58 Knee Joint Assembly.

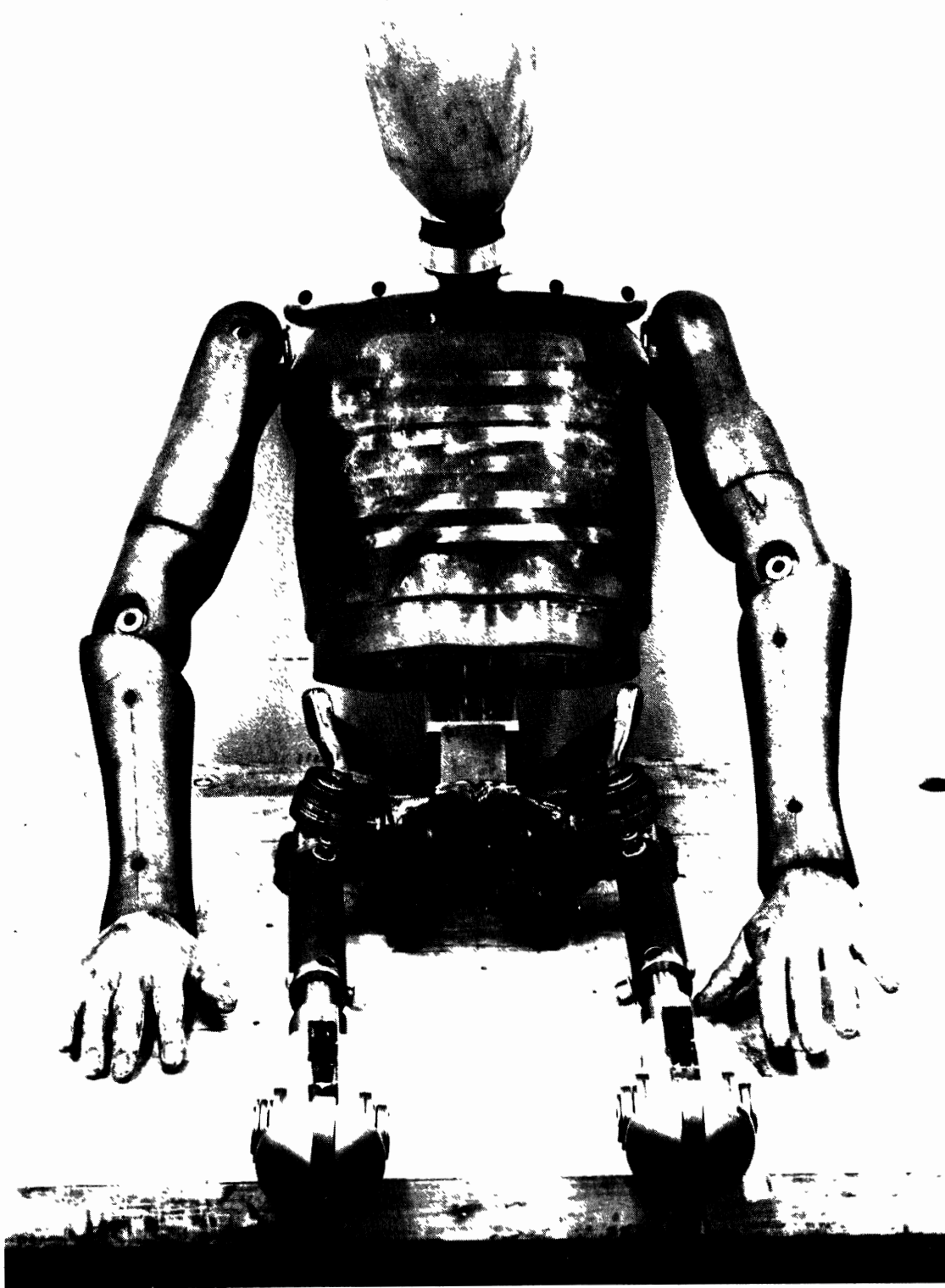


Figure 59 Front Assembly "Repeatable Pete."

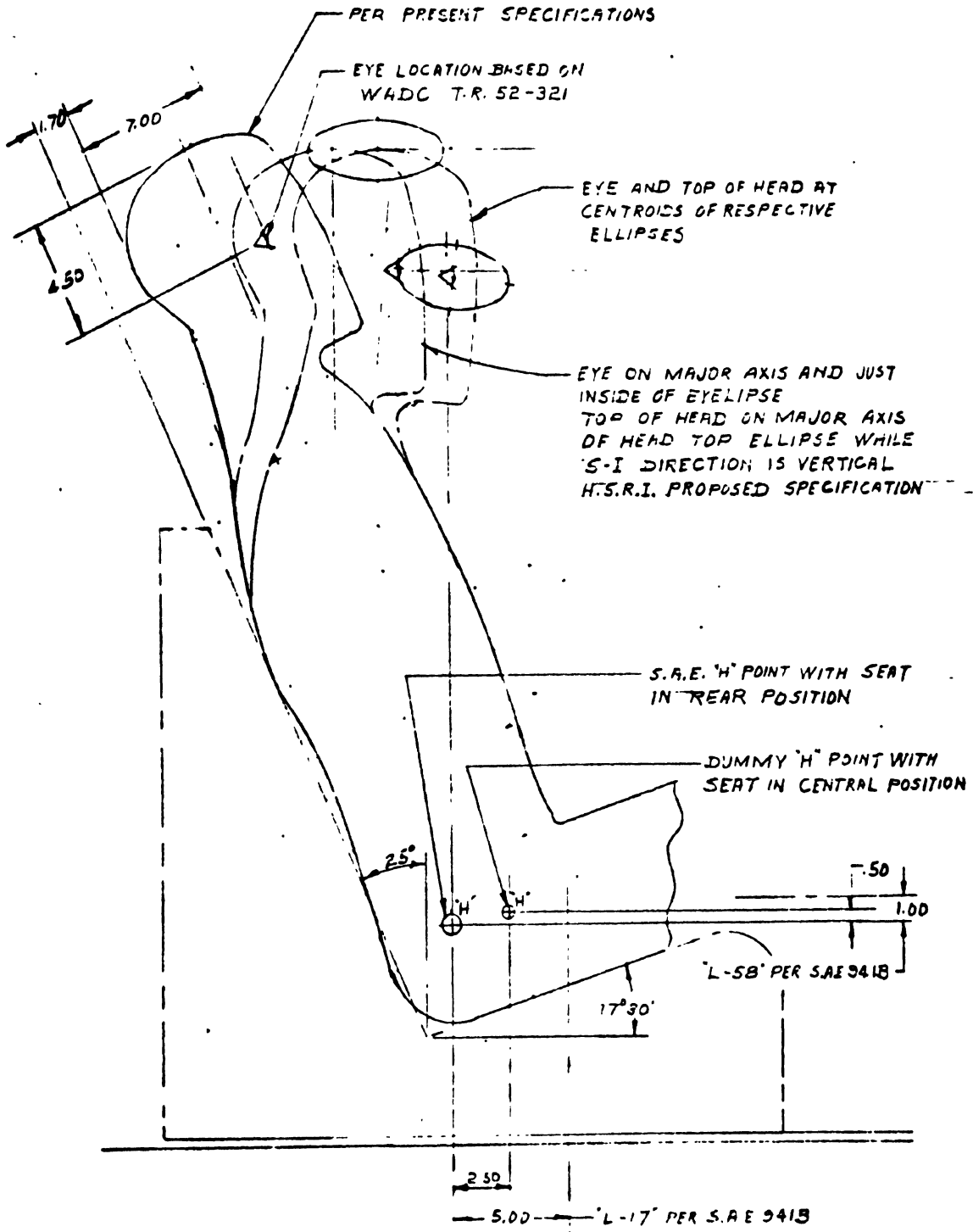


FIGURE 60. DUMMY SEATING POSITIONS

10.0 SYSTEM PERFORMANCE

10.1 Sled Test Program

10.1.1 Introduction

Forty-eight sled tests were conducted to verify the repeatability and durability of the two HSRI dummies. Each was subjected to twenty-four tests, six in each of four modes: lap- and torso-belted (Mode I); lap-belted, striking a pre-inflated airbag (Mode II); unrestrained (hip tether only), striking dash and windshield (Mode III); and lap-belted, striking steering wheel/collapsible steering column (Mode IV).

Nominal impact velocity and deceleration level for all tests was 30 mph and 20 G, respectively. More detailed descriptions of the four test modes and of the consequent test results are provided below.

10.1.2 Mode I: Lap- and Torso-Belted Tests

For this test series and for the twelve steering column impact tests (Mode IV), a strong and rigid seat structure was constructed to minimize possible variation in the dummies' pre-impact set-up position. As shown in Figure 61, a framework of welded 1" square steel tubing supported a seat-pan and seat-back that were further strengthened with 1/8" sheet steel, then padded with 1" thick Ensolite foam. Three-point belt attachments were added (in compliance with the guidelines of FMVSS 210), the torso belt running from the right shoulder to the left hip.

For use with this seat structure, a positioning fixture was designed to further reduce test-to-test variation in dummy set-up position (see Figure 62). With the dummy roughly positioned in the seat, two rigid steel plates were mounted to the sides of the seat via guide-pins. On the inboard side of each plate adjustable sliding rod assemblies picked up specific points on the



Figure 61 Mode I: Pre-Test Configuration (Foot Straps not Shown)

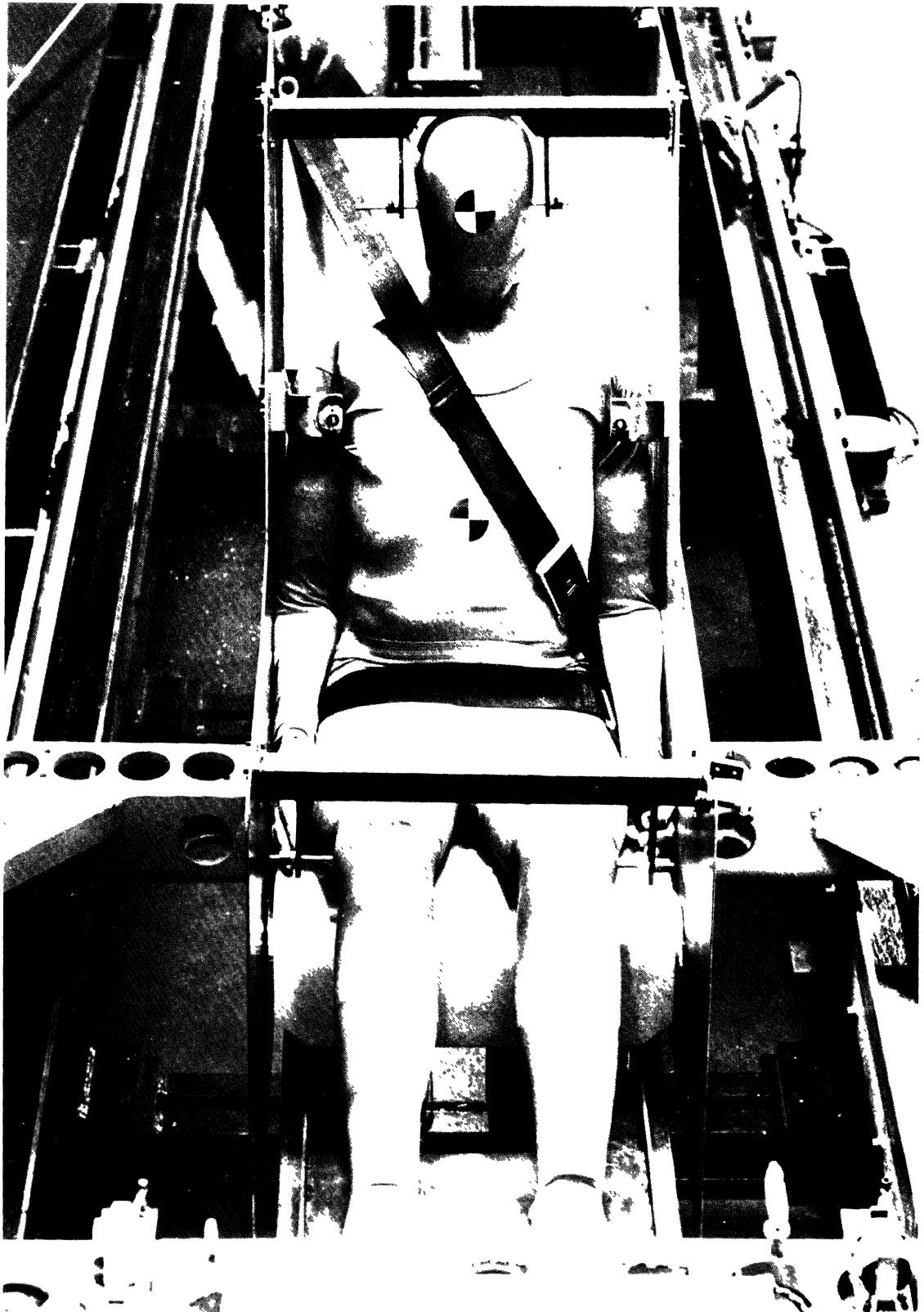


Figure 62 Mode I: Dummy Positioning Fixture

shoulders, head and knees of the dummy. Elbows/wrists and ankles/feet were located differently. The upper arm was pushed inward until flush with the torso, then rotated rearward about the shoulder until the back of the elbow contacted the seat-back surface. The lower arm was then rotated downward about the elbow until the edge of the hand rested on the seat-pan with the palm against the side of the thigh. The soles of the feet were positioned within outlines permanently drawn on the foot-rest, then belted in place with seat belt webbing.

After the dummy had been positioned in the seat, with lap and torso belts adjustable to a three finger spacing, the steel-plate fixtures were removed and the sled made ready for firing.

10.1.3 Mode II: Pre-inflated Airbag Tests

This test series was conducted with a cut-down 1971 Ford Maverick 2-door hardtop body buck mounted on the sled, and with a full-size Eaton airbag installed in the buck (Figure 63).

The doors, windows and a section of the roof were removed to facilitate high-speed photography of the impact event; the dash, parcel-shelf, steering wheel/column and all under-dash equipment were removed to permit air-bag installation. The front split-back bench seat remained in place, bolted to the floor (through its tracks) in its rearwardmost position. (The original seat was replaced about half-way through the test series when deformation affecting dummy pre-impact position became evident.)

The Eaton airbag was mounted in the center of the dash-support area (instead of in the right front passenger position), since the center of the bench seat was chosen as a position datum for the dummy (Figure 64). This position insured that the dummies' impact kinematics would not be complicated by contact with the A-pillar, the windshield header or the buck support

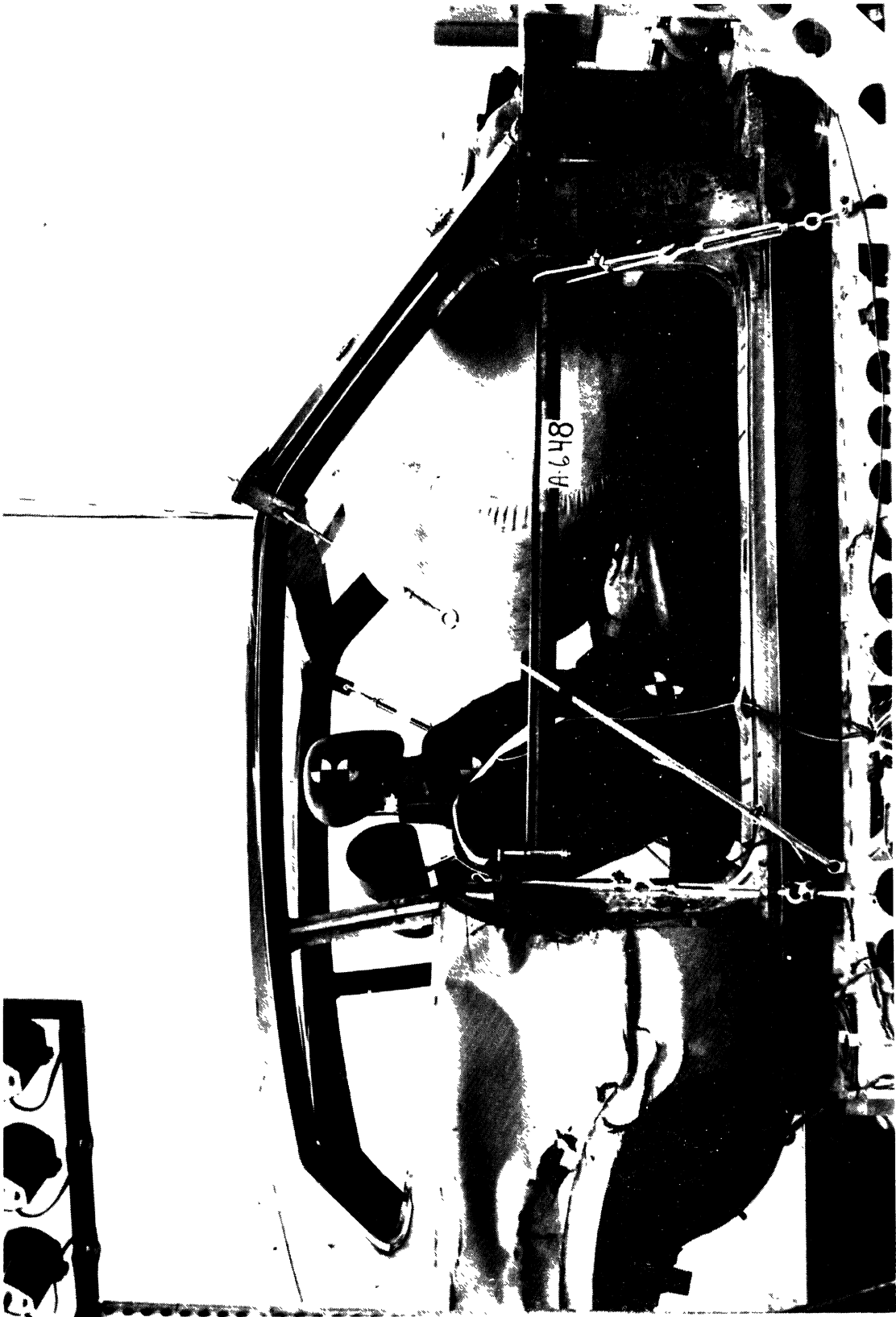


Figure 63 Mode II: Pre-Test Configuration of Body Buck with Airbag Preinflated



Figure 64 Mode II: Pre-Test Configuration

structure that spanned both door openings. A blower motor was permanently mounted inside the buck in the right front foot-well and was ducted to the airbag inlet.

Before each sled run, the dummy was positioned in the seat with a two-part fixture that located shoulders and knees. Foot position was again determined by patterns marked on the floor pan but the feet were not fixed in place. The dummy was securely lap-belted after positioning. (Since the non-rigid auto seat made it difficult to eliminate all variation in dummy position, and since the airbag itself tended to alter dummy position slightly when preinflated before a sled run, the positioning fixture used for this series was less elaborate than that used for the Mode I and Mode IV tests with the special-design rigid seat.)

To assure proper operation of the 10" diameter "blow-out" port in one end of the airbag, a special support panel was devised (Figures 65 and 66). This panel was mounted in such a way that the port was pushed flush against it, effectively sealing the open port, when the bag was positioned by hand and pre-inflated to approximately 3 psi. (Pre-inflation of the bag was the last step in preparation of the sled for each run; the bag maintained its position, shape and pressure with no difficulty for the 1 or 2 minutes that elapsed between pre-inflation and sled impact.)

At impact, the force exerted on the bag by the unrestrained dummy caused sufficient bag distortion to pull the port-end away from the panel and allow rapid blow-down, since the port was not attached to the support panel. It should also be noted that a standard windshield was installed in the buck for these tests to assure proper orientation and support of the inflated airbag.



Figure 65 Mode II: Pre-Test Configuration of Deflated Bag, Knee Catcher and Support Panel

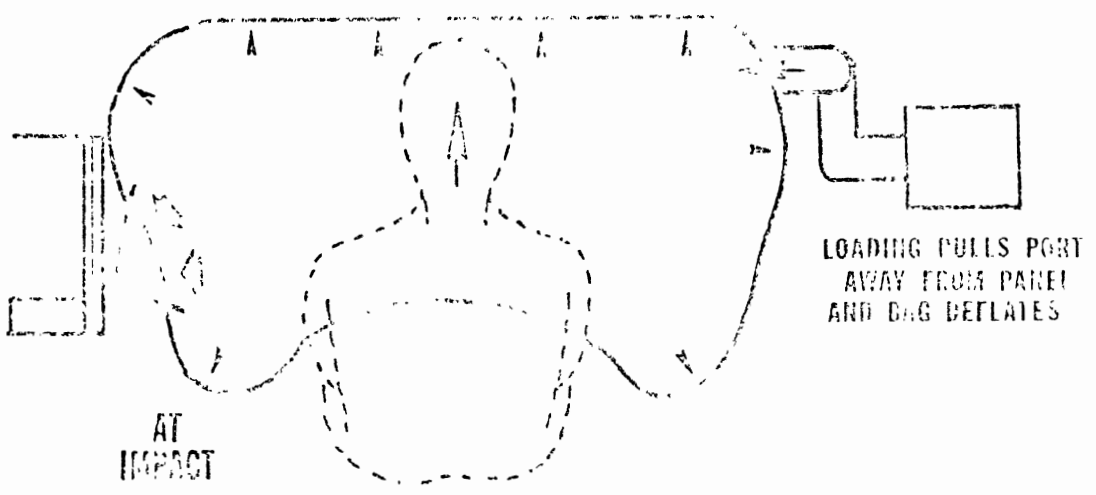
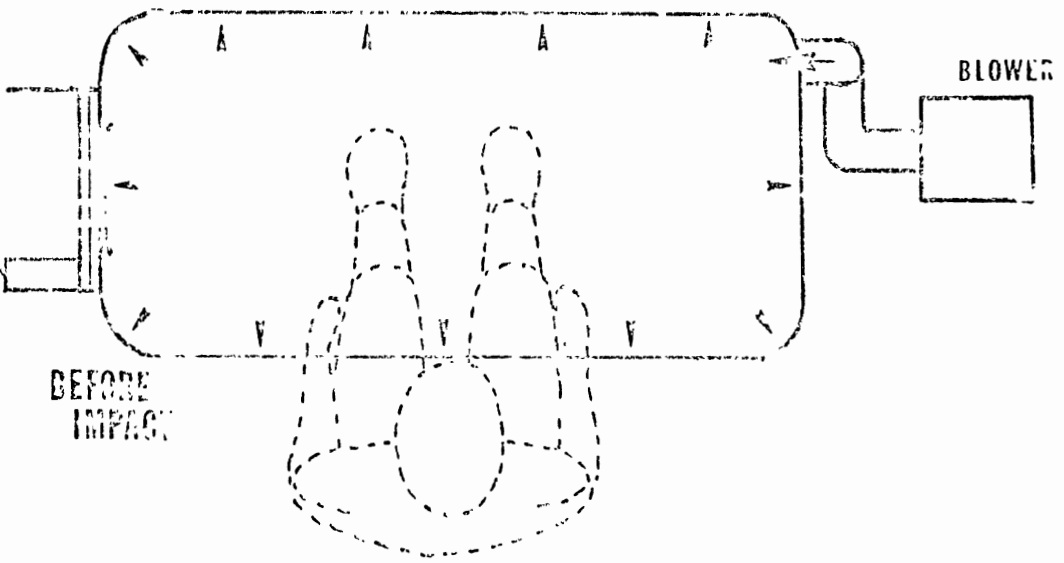
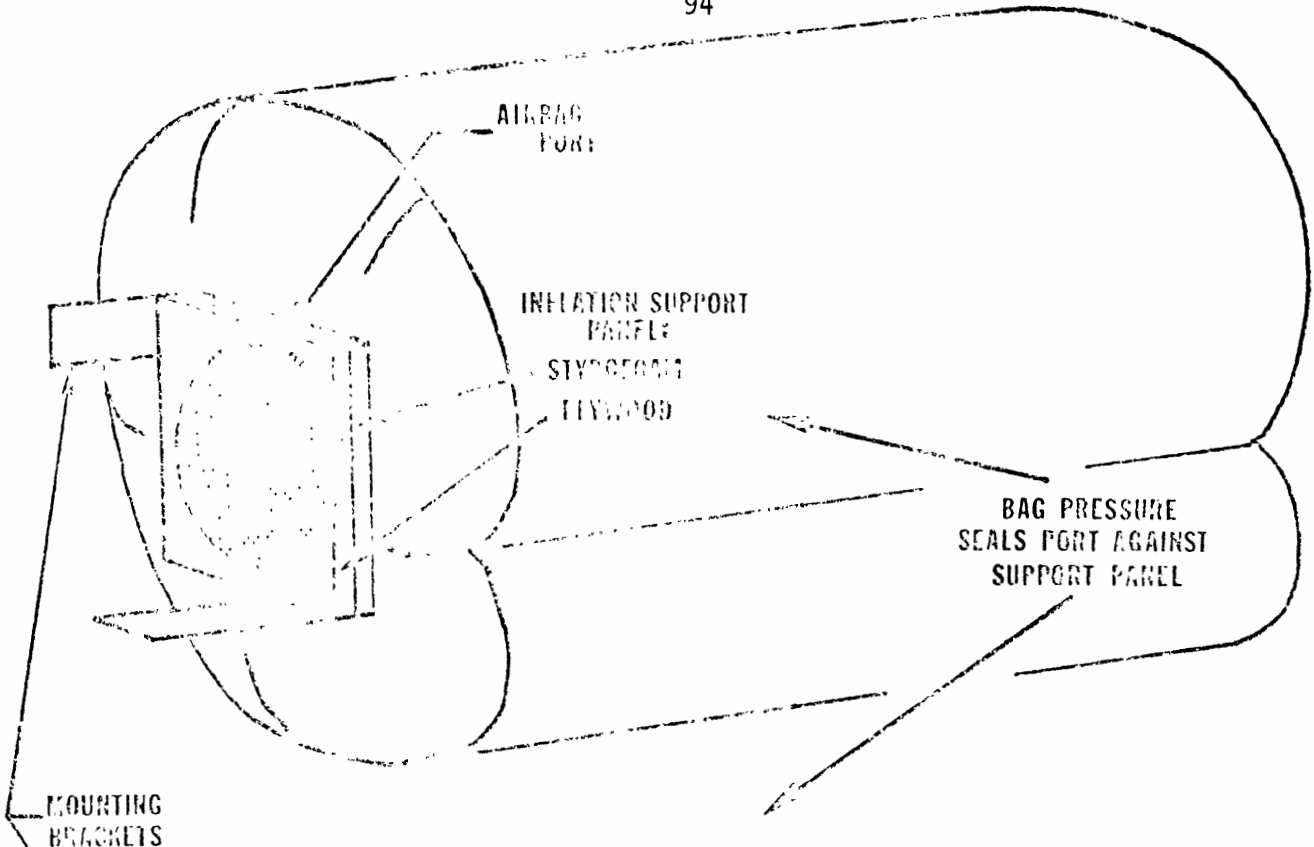


FIGURE 63: AIR BAG INFLATION AND DEFLATION

A balsa/foam knee impact panel was mounted under the center dash area to catch the dummy's knees at the same point in excursion into the bag (Figure 66).

10.1.4 Mode III: Dash/Windshield Impact Tests

Six dash/windshield impact tests were run on each dummy, using the same Maverick body buck used for the Mode II airbag tests, but with some important changes in set-up and dummy position.

As before, a split-back front bench seat was bolted to the floor in full-rearward position on its tracks. For these tests, however, the dummy was seated in the right front passenger position (Figure 67) and secured only with a loose hip tether to permit forward excursion into dash and windshield. (A positioning fixture similar to the one used for the Mode II tests was used to locate the dummy in the seat before each run.) For each test a new padded dash and windshield were installed, the latter held in place with a specially-built removable support frame (see Figure 68).

Below the dash, in front of the dummy, a balsa/styrofoam pad was built up to catch the dummy's knees and thereby pivot his upper torso and head into the windshield and dash in the same way during each test. New styrofoam slabs (four one-inch-thick panels) were installed for each sled run (see Figure 67).

10.1.5 Mode IV: Steering Wheel Impact Tests

For these tests, the same rigid seat used in the Mode I test series was modified to include a support structure for a steering wheel/collapsible steering column assembly. Although Ford Maverick steering wheels and collapsible columns were used in these tests, considerable modifications were made to construct a simple, strong, "quick-changeover" test fixture. No



Figure 67 Mode III: Pre-Test Configuration



Figure 68 Mode III: Post-Test Configuration of Windshield and Support Frame



Figure 69 Mode III: Post-Test Configuration



Figure 70 Mode III: Post Test Configuration



Figure 71 Mode III: Dummy Head after Six Windshield Impacts

attempt was made to compare steering-column performance in these tests with that of vehicle-installed steering columns in real-world impact situations, and no such comparison is implied. The intent was to use identical, reasonably realistic, and easily replaceable components in a test fixture that would provide a valid indication of dummy repeatability.

As Figure 72 shows, the base of the collapsible column was attached to the foot pan, while the upper end was supported (at a 25° angle) in a split-sleeve clamp. The column could slide within this sleeve, and a pad of Teflon was installed in the sleeve to assure that this sliding motion would be unrestricted as the tube collapsed axially under load.

Coaxial with the collapsing tube and running down through its center was the solid telescoping steering shaft, serving to support the outer tube and to guide its axial collapse. Both the steering shaft and the collapsing tube mated to the hub of the steering wheel; the wheel and the collapsible tube were replaced for each test, while the same steering shaft was used for all 12 tests.

The dummy was securely lap-belted for each run (Figure 73), after being positioned in the same way as for the Mode I tests. (The only difference was that the hands were placed on the steering wheel, instead of resting on the seat-pan.)

10.2 Instrumentation and Data Acquisition

The impact event for all tests was recorded in three forms: output signal traces (G-level versus time) of accelerometers mounted on the sled and in the dummy; high-speed (1000 frames/sec) color motion pictures taken from beside and above the impact point; and a trackside sequence photograph (Polaroid) for rapid test evaluation.

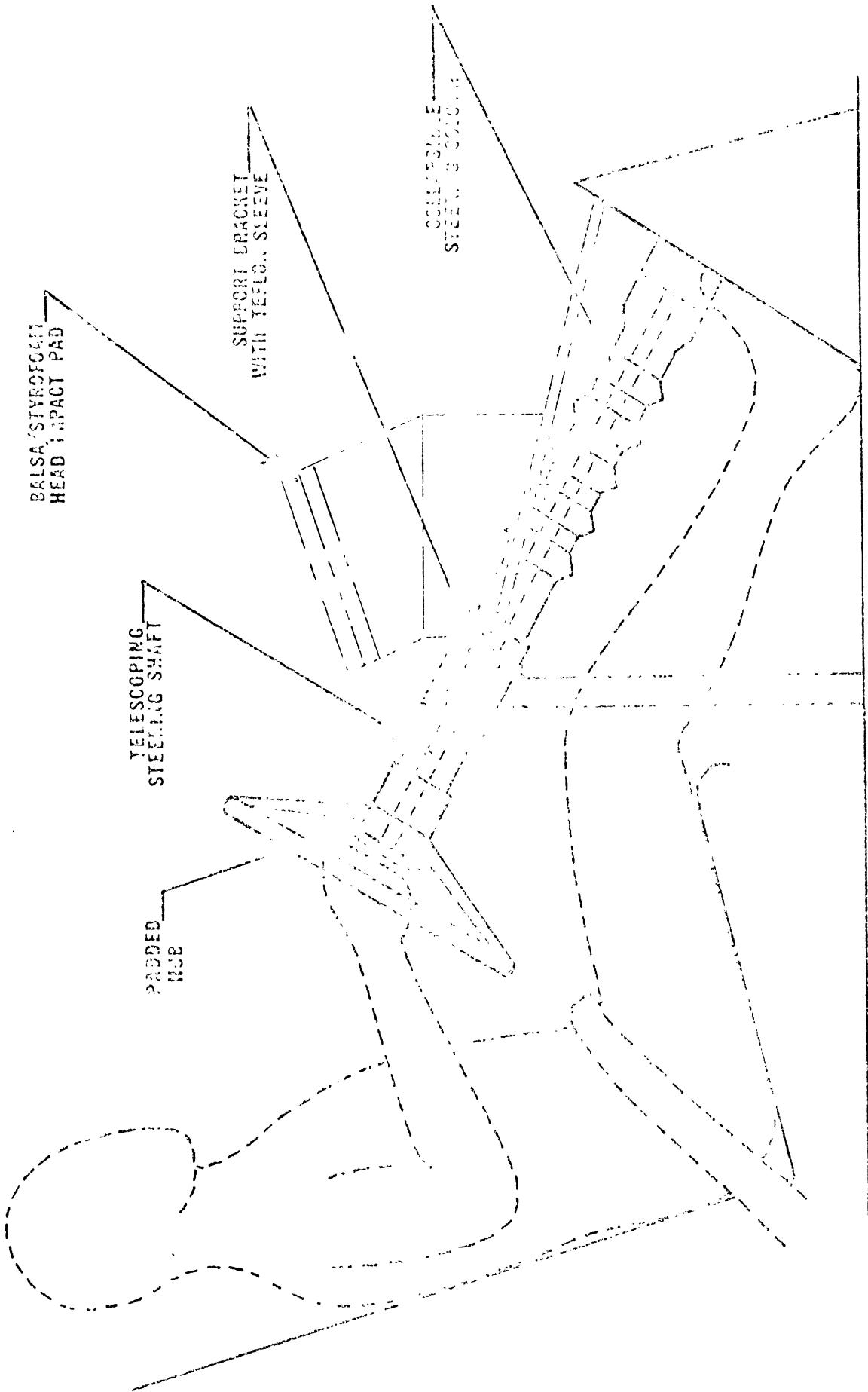


FIGURE 72 : STEERING COLUMN TEST SET-UP

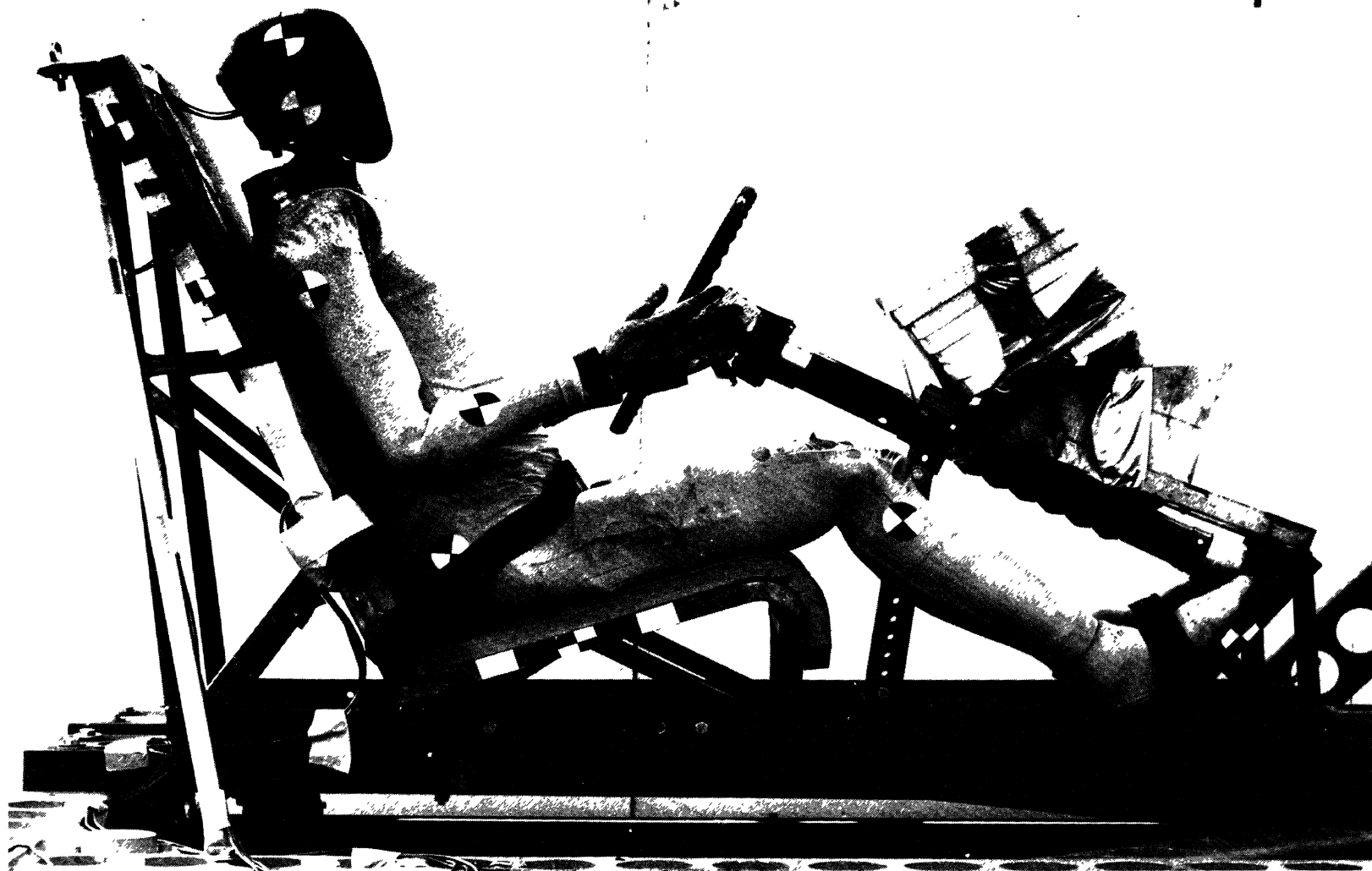


Figure 73 Mode IV: Pre-Test Configuration



Figure 74 Mode IV: Post-Test Configuration

10.2.1 Accelerometer Data

For all 48 tests, a triaxial pack of Setra Model 113 accelerometers was mounted in the head of the HSRI dummies at the center of gravity. For tests A-641 through A-654 inclusive, a second triaxial pack of Setra Model 113's was also mounted in the HSRI dummy chest at the center of gravity of the torso. Erratic chest acceleration traces during A-653 and A-654 (traced to a pinched cable) required the replacement of the Model 113 chest accelerometers with Model 111's; the replacement accelerometers remained in the dummies for tests A-655 through A-689 inclusive.

The output signals from the dummy accelerometers and from the Statham Model 93 accelerometer on the sled were recorded in unfiltered form on magnetic tape and in filtered form on a Honeywell Oscillograph during impact. The tape-recorded data was processed later for analysis and presentation while the oscillograph traces provided an immediate post-test indication of peak decelerations during impact.

10.2.2 High Speed Motion Pictures

Two Photosonics high speed motion picture cameras -- one at trackside, another overhead -- recorded dummy impact kinematics at 1000 frames/second for each test, from which comparative data on ranges of motion, linear and angular displacement were determined. Angular velocity and acceleration can also be determined from these films, although such analysis was not carried out for these tests.

10.2.3 Graph-Check Sequence Photographs

A sequence photograph -- approximately one frame every 25 msec -- recorded each test, allowing quick comparison of dummy kinematics from test to test in a series, and between similar test series on the two dummies.

Typical Graph-Check photographs from each series with each dummy are presented in a later section discussing results of the test program.

10.3 Sled Test Results

Results of the sled test program are presented in three ways on the pages that follow.

- For each 6-test series in each mode, peak head and chest accelerations as well as head severity index and HIC are tabulated. Test results for both dummies in a particular test mode are presented on the same sheet for comparison.
- Four Graph-Check photographs are presented -- one of each of the four test modes.
- Head and chest accelerometer traces for all 48 tests are included, so that test-to-test and series-to-series comparison can be made of the peaks and general shapes of the accelerometer traces.

This test program was undertaken to demonstrate the durability and repeatability of the two HSRI Repeatable Pete 50th Percentile Male anthropometric test dummies. As an indication of durability, only three instances of minor damage to the dummies were noted in the entire 48-test program:

- in test A-662, after three dash/windshield impacts, the bolts by which the clavicles attach to the shoulder assembly on dummy # 2 had to be tightened.
- a chest accelerometer cable was apparently pinched between the dummy spine and the seat-back during rebound in tests A-653 and A-654, so the chest triax accelerometer pack was replaced and the new cables re-routed for test A-665.

TABLE 9
DUMMY PERFORMANCE SUMMARY

| | Test Mode | Resultant Peak G's | Severity Index | HIC | Resultant Peak G's | Severity Index |
|-----------|------------------------------|--|------------------------------|------------------------------|--------------------------|------------------------------|
| DUMMY # 1 | Lap- and Torso-Belted Impact | Mean = 52 Range = 50 - 55 $\sigma = 1.9$ | 487 450 - 520 23.6 | 395 380 - 411 13.2 | 48 45 - 53 3.1 | 337 320-360 13.7 |
| | Preinflated Airbag Impact | Mean = 69 Range = 67 - 72 $\sigma = 2.3$ | 603 540 - 660 41.1 | 494 440 - 518 25.2 | 55 51 - 60 3.3 | 433 340 - 520 62.6 |
| | Dash/Windshield Impact | Mean = 219 Range = 208 - 232 $\sigma = 8.9$ | 3260 3000 - 3600 233.8 | 1818 1700 - 1920 77.0 | 130 104 - 146 14.0 | 1064 840 - 1220 129.8 |
| | Steering Wheel Impact | Mean = 115 Range = 100 - 130 $\sigma = 9.9$ | 1807 1540 - 2020 175.9 | 1439 1320 - 1561 86.8 | 44 38 - 48 2.8 | 257 240 - 280 13.8 |
| DUMMY # 2 | Lap- and Torso-Belted Impact | Mean = 50 Range = 47 - 53 $\sigma = 2.2$ | 507 470 - 530 22.9 | 410 398 - 418 6.4 | 49 43 - 57 4.2 | 310 290 - 320 13.8 |
| | Preinflated Airbag Impact | Mean = 72 Range = 70 - 75 $\sigma = 1.9$ | 665 590 - 710 41.2 | 517 484 - 540 18.3 | 54 47 - 66 6.3 | 422 380 - 550 58.7 |
| | Dash/Windshield Impact | Mean = 241 Range = 200 - 264 $\sigma = 22.9$ | 3367 2700 - 3800 349.9 | 1875 1650 - 2030 117.1 | 127 112 - 148 13.7 | 1113 1000 - 1400 132.9 |
| | Steering Wheel Impact | Mean = 115 Range = 96 - 130 $\sigma = 11.4$ | 1773 1640 - 2000 139.3 | 1456 1396 - 1580 63.4 | 45 38 - 56 6.2 | 280 220 - 340 43.4 |

- the left hand of dummy # 1 was torn and battered during Mode III testing (dash/windshield impact), but since the wrist joint was not damaged, the hand was not replaced.

Dummy repeatability -- test-to-test and series-to-series -- is treated in more detailed quantitative terms in the sections that follow.

10.3.1 Mode I Test Results

10.3.1.1 Dummy # 1 Performance: Lap- and Torso-Belted Impact Tests A-641-A-646.

- Resultant Peak Head Acceleration:
Mean = 52 G Range = 50 - 55 G σ = 1.9
- Head Severity Index:
Mean = 487 Range = 450 - 520 σ = 23.6
- HIC:
Mean = 395 Range = 380 - 411 σ = 13.2
- Resultant Peak Chest Acceleration:
Mean = 48 G Range = 45 - 53 G σ = 3.1
- Chest Severity Index:
Mean = 337 Range = 320 - 360 σ = 13.7

See Figure 61 for typical pre-test dummy geometry.

This series established basic procedures, particularly the use of the positioning device (see Figure 62) to locate the dummy before each run. The only problem noted was an artifact in the head AP acceleration trace about 73 msec after impact in test A-645 (see Appendix B). Pinching of the head AP accelerometer cable apparently caused the artifact; a minor change in cable routing solved the problem. (The artifact was not counted in the evaluation of HIC and severity index.)

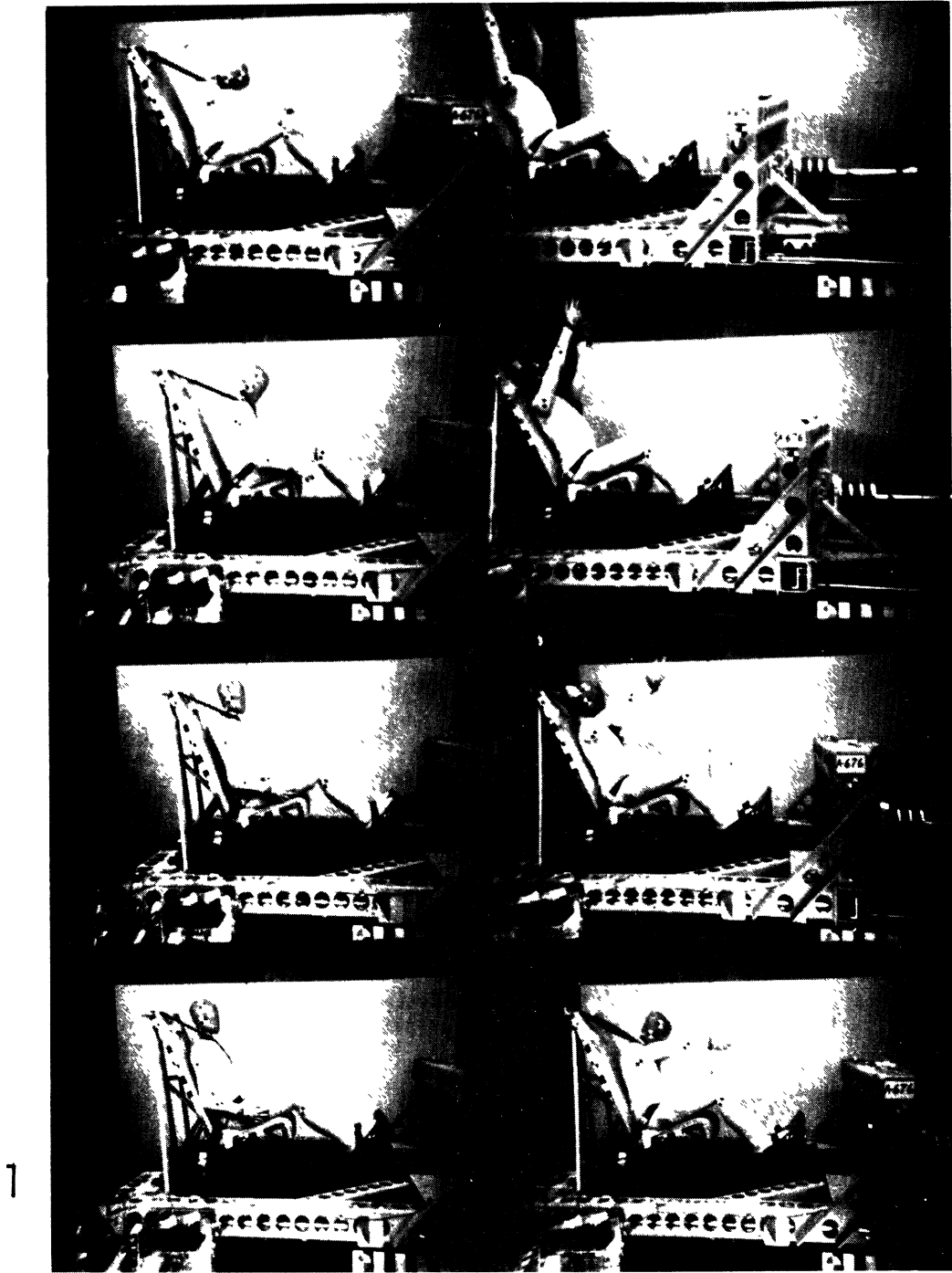


Figure 75 Mode I: Sequence Photo of Impact

TABLE 10
DATA SUMMARY: LAP- AND TORSO-BELTED TESTS

| Test No. | Dummy No. | Head | | | Chest | |
|--------------------|-----------|--------------------|----------------|------|--------------------|----------------|
| | | Resultant Peak G's | Severity Index | HIC | Resultant Peak G's | Severity Index |
| A-641 | 1 | 55 | 490 | 411 | 50 | 340 |
| 642 | 1 | 50 | 450 | 375 | 53 | 360 |
| 643 | 1 | 52 | 470 | 405 | 45 | 320 |
| 644 | 1 | 50 | 520 | 398 | 45 | 340 |
| 645 | 1 | 53 | 510 | 402 | 47 | 340 |
| 646 | 1 | 50 | 480 | 380 | 45 | 320 |
| Average | | 52 | 487 | 395 | 48 | 337 |
| Standard Deviation | | 1.9 | 23.6 | 13.2 | 3.1 | 13.7 |
| A-672 | 2 | 53 | 480 | 406 | 57 | 320 |
| 673 | 2 | 52 | 530 | 418 | 48 | 290 |
| 674 | 2 | 51 | 520 | 412 | 52 | 310 |
| 675 | 2 | 49 | 520 | 414 | 53 | 320 |
| 676 | 2 | 47 | 470 | 398 | 46 | 320 |
| 677 | 2 | 48 | 520 | 409 | 33 | 290 |
| Average | | 50 | 507 | 410 | 49 | 310 |
| Standard Deviation | | 2.2 | 22.9 | 6.4 | 4.2 | 11.1 |

Note: Test A-647 was an attempt to evaluate an Ogle/MIRA 50th percentile male dummy in the lap/torso belted configuration. The head of the dummy came loose at impact, however, and no useful head data was obtained, although head and chest accelerometer traces are included in the report. No attempt was made to re-run the test.

Refer to Tables 9 and 10 and to Appendix B for data summaries and accelerometer traces, respectively, for tests A-641 through A-647.

10.3.1.2 Dummy # 2 Performance: Lap- and Torso Belted Impact Tests A-672-A-677.

- Resultant Peak Head Acceleration:

Mean = 50 G Range = 47 - 53 G σ = 2.2

- Head Severity Index:

Mean = 507 Range = 470 - 530 σ = 22.9

- HIC:

Mean = 410 Range = 398 - 418 σ = 6.4

- Resultant Peak Chest Acceleration:

Mean = 50 G Range = 33 - 69 G σ = 10.7

- Chest Severity Index:

Mean = 297 Range 220 - 320 σ = 53.1

See Figure 61 for typical pre-test dummy geometry.

Except for minor refinements in procedure based on the experience gained from tests A-641 - A-646, this series was conducted in the same manner as the first lap/torso belted tests. Chest accelerometers for this series were Setra Model 111's (changed after test A-654 as noted in the next section). A new torso belt (buckle end only) was installed for test A-673; the tightness to which the new belt was cinched down, and possible variation

in belt path across the dummy's chest, may explain the slightly lower chest accelerations noted for tests A-673 through A-677. No malfunctions or damage to sled, dummy or data acquisition system occurred.

Refer to Tables 9 and 10 and to Appendix B, for data summaries and accelerometer traces, respectively, for tests A-672 through A-677.

10.3.2 Mode II Test Results

10.3.2.1 Dummy # 1 Performance: Pre-inflated Airbag Impact Tests A-648-A-653.

- Resultant Peak Head Acceleration:
Mean = 69 G Range = 67 - 72 G σ = 2.3
- Head Severity Index:
Mean = 603 Range = 540 - 660 σ = 41.1
- HIC:
Mean = 494 Range = 440 - 518 σ = 25.2
- Resultant Peak Chest Acceleration:
Mean = 55 G Range = 51 - 60 G σ = 3.3
- Chest Severity Index:
Mean = 433 Range = 340 - 520 σ = 62.6

See Figure 63-65 for typical pre-test dummy geometry.

This was the first test series with the Maverick body buck installed on the sled, and due to the somewhat "trial - and - error" nature of sled accelerator adjustments required when sled payload changes, sled velocity on the first two runs was about 13% lower than desired (26.5 and 26.2 mph instead of the desired 30 mph).

Chest accelerometer performance was erratic in tests A-653 and A-654; chest LR acceleration was not recorded. When chest accelerometers were installed in dummy # 2 for tests A-655 - 659 (see below), the erratic Setra

Model 113's were replaced with Model 111's. The problem in tests A-653 and A-654 was traced to a cable(s) pinched between dummy spine and torso skin during rebound into the seat. The cables of the replacement accelerometers were rerouted for tests A-655 and all that followed.

Some forward shifting of the seat on its tracks was noted in tests A-648 - A-653, but the seat shift did not affect dummy kinematics or acceleration significantly.

The airbag blowout-port support panel functioned without incident for all tests (A-648 through A-659), maintaining bag pressure before impact but allowing bag blow-down as the dummy loaded the bag. Movies and Graph-Check photos show consistent dummy kinematics for all twelve airbag tests.

Refer to Tables 9 and 11, and to Appendix B, for data summaries and accelerometer traces, respectively, for tests A-648 through A-653.

10.3.2.2 Dummy # 2 Performance: Preinflated Airbag Impact Tests A-654-A-659.

- Resultant Peak Head Acceleration:

Mean = 72 G Range = 70 - 75 G $\sigma = 1.9$

- Head Severity Index:

Mean = 665 Range = 590 - 710 $\sigma = 41.2$

- HIC:

Mean = 517 Range = 484 - 540 $\sigma = 18.3$

- Resultant Peak Chest Acceleration:

Mean 54 G Range 47 - 66 G $\sigma = 6.3$

- Chest Severity Index:

Mean = 422 Range = 380 - 550 $\sigma = 58.7$

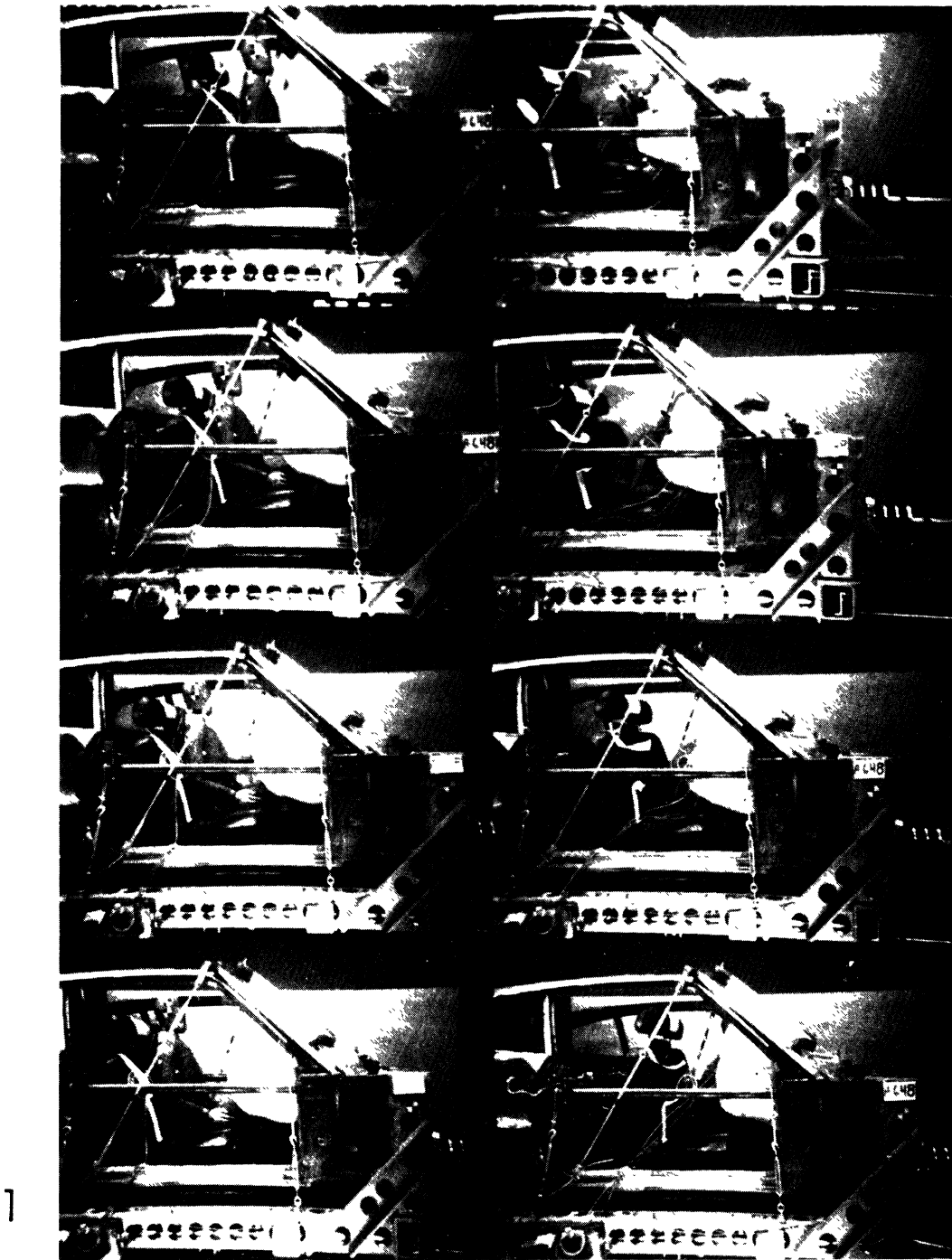


Figure 76 Mode II: Sequence Photo of Impact

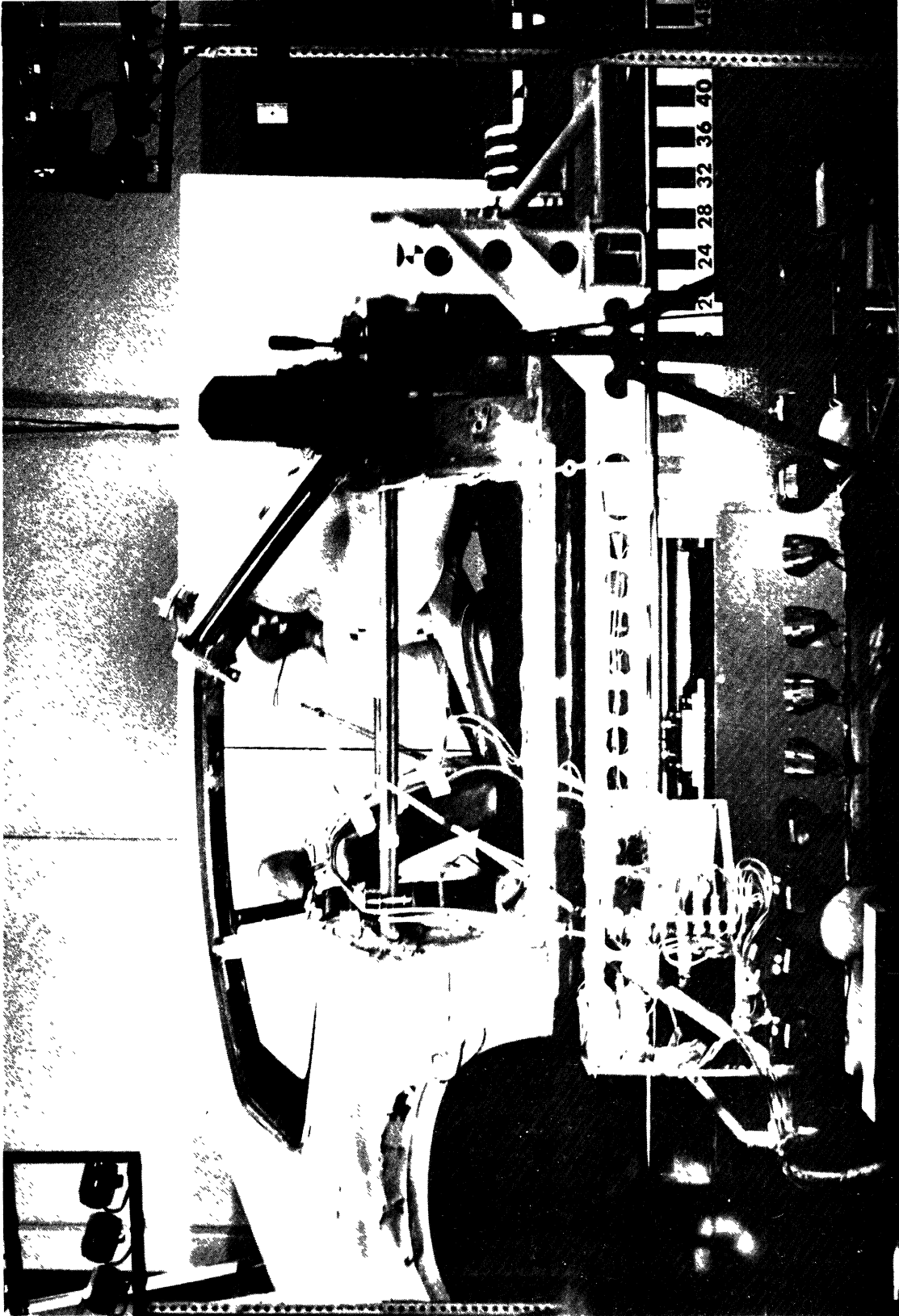


Figure 77 Mode II: Moment of Impact

TABLE 11

DATA SUMMARY: PRE-INFLATED AIRBAG TESTS

| Test No. | Dummy No. | Head | | | Chest | |
|--------------------|-----------|--------------------|----------------|------|--------------------|----------------|
| | | Resultant Peak G's | Severity Index | HIC | Resultant Peak G's | Severity Index |
| A-648 | 1 | 72 | 660 | 518 | 51 | 370 |
| 649 | 1 | 68 | 600 | 501 | 51 | 340 |
| 650 | 1 | 66 | 540 | 440 | 53 | 440 |
| 651 | 1 | 67 | 580 | 493 | 60 | 520 |
| 652 | 1 | 72 | 650 | 510 | 55 | 490 |
| 653 | 1 | 69 | 590 | 499 | 57 | 440 |
| Average | | 69 | 603 | 494 | 55 | 433 |
| Standard Deviation | | 2.3 | 41.1 | 25.2 | 3.3 | 62.6 |
| A-654 | 2 | 70 | 590 | 484 | 56 | 400 |
| 655 | 2 | 72 | 660 | 515 | 55 | 420 |
| 656 | 2 | 72 | 700 | 540 | 64 | 550 |
| 657 | 2 | 74 | 690 | 527 | 48 | 390 |
| 658 | 2 | 75 | 710 | 533 | 49 | 380 |
| 659 | 2 | 70 | 640 | 502 | 52 | 390 |
| Average | | 72 | 665 | 517 | 54 | 422 |
| Standard Deviation | | 1.9 | 41.2 | 18.3 | 5.3 | 58.7 |

See Figures 63-65 for typical pre-test dummy geometry.

Continuation of the airbag test series with dummy # 2 was uneventful, with the exception of the chest accelerometer problem in test A-654 (and the subsequent solution for A-655 - A-659) that was noted earlier. It should be noted that the loss of the chest LR acceleration trace for A-656 was due to an amplifier hook-up error following calibration, not to accelerometer malfunction or cable pinching.

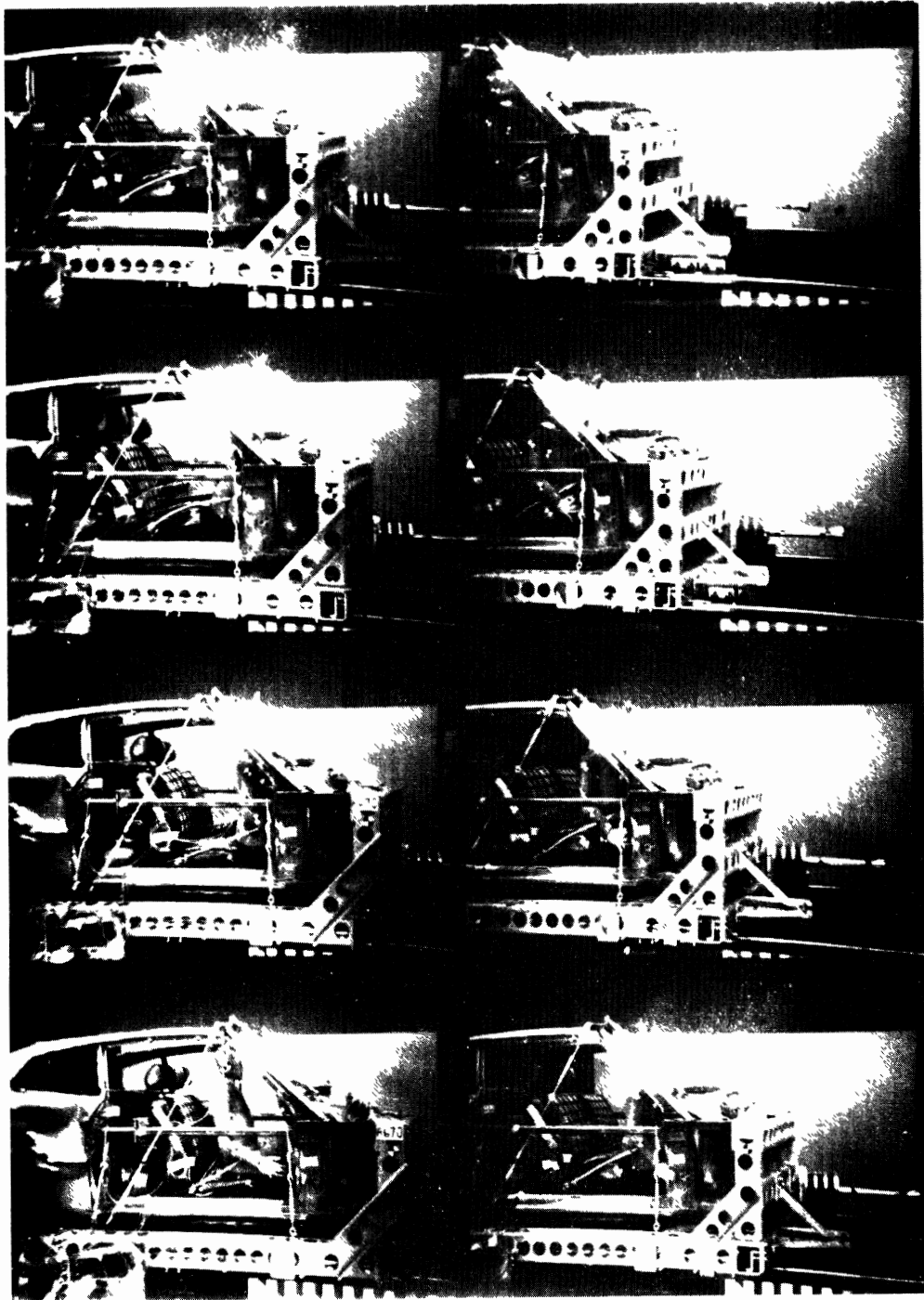
Problems with sled velocity and seat shift during tests A-648 - A-653 were corrected for this series. Again, dummy kinematics were very repeatable as indicated by movie analysis, and head/chest acceleration data for the two airbag series compare quite favorably in terms of repeatability.

Refer to Tables 9 and 11, and to Appendix B, for data summaries and accelerometer traces, respectively, for tests A-654 - A-659.

10.3.3 Mode III Test Results

10.3.3.1 Dummy # 1 Performance: Dash/Windshield Impact Tests A-667-A-671.

- Resultant Peak Head Acceleration:
Mean = 219 G Range = 208 - 232 G σ = 8.9
- Head Severity Index:
Mean = 3260 Range = 3000 - 3600 σ = 233.8
- HIC:
Mean = 1818 Range = 1700 - 1920 σ = 77.0
- Resultant Peak Chest Acceleration:
Mean = 130 G Range = 104 - 146 G σ = 14.0
- Chest Severity Index:
Mean = 1064 Range = 840 - 1220 σ = 129.8



8

Figure 78 Mode III: Sequence Photo of Impact

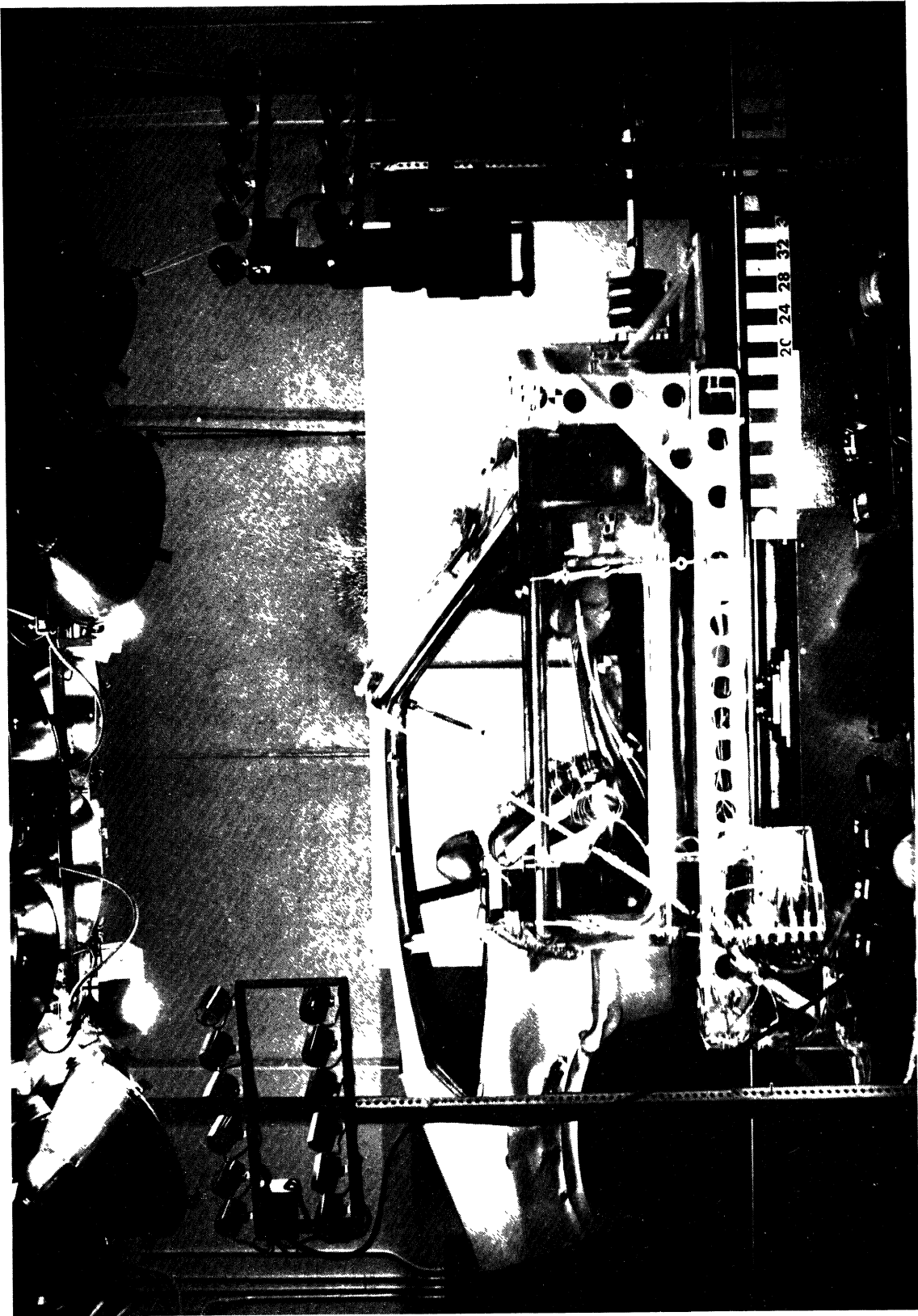


Figure 79 Mode III: Moment of Impact

TABLE 12

DATA SUMMARY: DASH/WINDSHIELD IMPACT TESTS

| Test No. | Dummy No. | Head | | | Chest | |
|--------------------|-----------|--------------------|----------------|-------|--------------------|----------------|
| | | Resultant Peak G's | Severity Index | HIC | Resultant Peak G's | Severity Index |
| A-667 | 1 | 224 | 3400 | 1880 | 134 | 1060 |
| 668 | 1 | 220 | 3300 | 1810 | 136 | 1220 |
| 669 | 1 | 208 | 3000 | 1700 | 130 | 1040 |
| 670 | 1 | 212 | 3000 | 1780 | 104 | 840 |
| 671 | 1 | 232 | 3600 | 1920 | 146 | 1160 |
| Average | | 219 | 3260 | 1818 | 130 | 1064 |
| Standard Deviation | | 8.9 | 233.8 | 77.0 | 14.0 | 129.8 |
| A-661 | 2 | 264 | 3200 | 1830 | 122 | 1116 |
| 662 | 2 | 256 | 3800 | 2030 | 122 | 1000 |
| 663 | 2 | 200 | 2700 | 1650 | 142 | 1040 |
| 664 | 2 | 264 | 3500 | 1910 | 148 | 1400 |
| 665 | 2 | 228 | 3400 | 1890 | 112 | 1060 |
| 666 | 2 | 236 | 3600 | 1940 | 116 | 1060 |
| Average | | 241 | 3367 | 1875 | 127 | 1113 |
| Standard Deviation | | 22.9 | 349.9 | 117.1 | 13.7 | 132.9 |

See Figures 68-71 for typical pre-test and post-test dummy geometry.

Dash/windshield impact tests were the most physically punishing tests of the HSRI dummies, and yet damage was virtually insignificant. Figure 71 shows the extent of damage to the head of dummy # 2 after six such impacts. The only other damage was to the left hand of dummy # 1, which was badly torn and twisted due to dashboard impact; the wrist joint suffered no damage, only the "flesh" of the hand.

Head and chest accelerations were higher in these dash/windshield tests than in any of the other three test modes. (Note the scale factors on the applicable accelerometer traces in Appendix B.) Although it was expected that the destructive nature of these tests -- windshield fracture, dash collapse -- would complicate attempts to achieve repeatability, comparison of test-to-test (A-667-671) and series-to-series (A-667-671 to A-661-666) shows good agreement of acceleration data and kinematics. The specially-designed quick-changeover windshield frame, plus careful attention to dash and knee-catcher installation (see Figures 67 and 68) helped reduce test set-up variation.

An instrumentation problem that was not apparent during the tests explains the loss of chest LR acceleration data for A-669 through A-672 inclusive. One channel of the FM magnetic tape recorder that records all accelerometer data at impact was not functioning for these tests; it was not until the tape was later played out for analysis that the malfunction was discovered. (An oscillograph trace of chest LR acceleration was recorded for these tests, but no permanent tape record was made.)

Pre-test damage to one windshield caused cancellation of one of the six scheduled tests. A replacement could not be obtained in time to re-run the test.

Refer to Tables 9 and 12, and to Appendix B, for data summaries and accelerometer traces, respectively, for tests A-667-A-671.

10.3.3.2 Dummy # 2 Performance: Dash/Windshield Impact Tests A-661-A-666.

- Resultant Peak Head Acceleration:

Mean = 241 G Range = 200 - 264 G σ = 22.9

- Head Severity Index:

Mean = 3367 Range = 2700 - 3800 σ = 349.9

- HIC:

Mean = 1875 Range = 1650 - 2030 σ = 117.1

- Resultant Peak Chest Acceleration:

Mean = 127 G Range = 112 - 148 G σ = 13.7

- Chest Severity Index:

Mean = 1113 Range = 1000 - 1400 σ = 132.9

See Figures 68-71 for typical pre-test and post-test dummy geometry.

Note: Test A-660 was the first sled run in this twelve-test dash/windshield series, but misjudgment of dummy kinematics made the test invalid. The dummy was lap-belted in position and during impact struck the dash but not the windshield. For tests A-662-A-671 inclusive, a non-restraining hip tether was used instead of a seat belt; dash/windshield contact was acceptable and quite repeatable.

Following test A-662, both left and right clavicles (aluminum "collar-bones") were found to be loose. Each is mounted on the front of its respective shoulder assembly with two bolts, and on both sides, both bolts had loosened 1 1/2 to 2 turns, allowing the clavicles to rattle. All bolts were tightened, and did not loosen in any later tests with dummy # 2. It is suspected that the bolts were installed but not tightened during dummy

preparation for test A-654. The "softer" airbag impacts of A-654 - A-659 did not loosen the bolts, but the first three dash/windshield impacts of A-660 - A-662 did. There was no significant differences between the test with the loosened clavicles and the tests with the clavicles tightened.

For A-663 an attempt was made to produce a more "repeatable" seat surface, by placing a 22" wide by 50" long sheet of Teflon over seat-back and seat-pan cushions. The slippery surface created problems in maintaining dummy pre-impact position, and modified dummy motion during rebound into the seat. For these reasons, it was not used in any other tests.

Although oscillograph traces of chest LR acceleration were recorded for tests A-662, A-665 and A-666, a malfunction of one input record channel on the magnetic tape recorder resulted in loss of this data on the permanent tape record. The failure is not apparent during a test, but only when the tape is played back later for data analysis. (See the applicable data sheets in Appendix B.)

Refer to Tables 9 and 12, and to Appendix B, for data summaries and accelerometer traces, respectively, for tests A-661 - A-666.

10.3.4 Mode IV Test Results

10.3.4.1 Dummy # 1 Performance: Steering Wheel Impact Tests A-684 - A-689.

- Resultant Peak Head Acceleration:

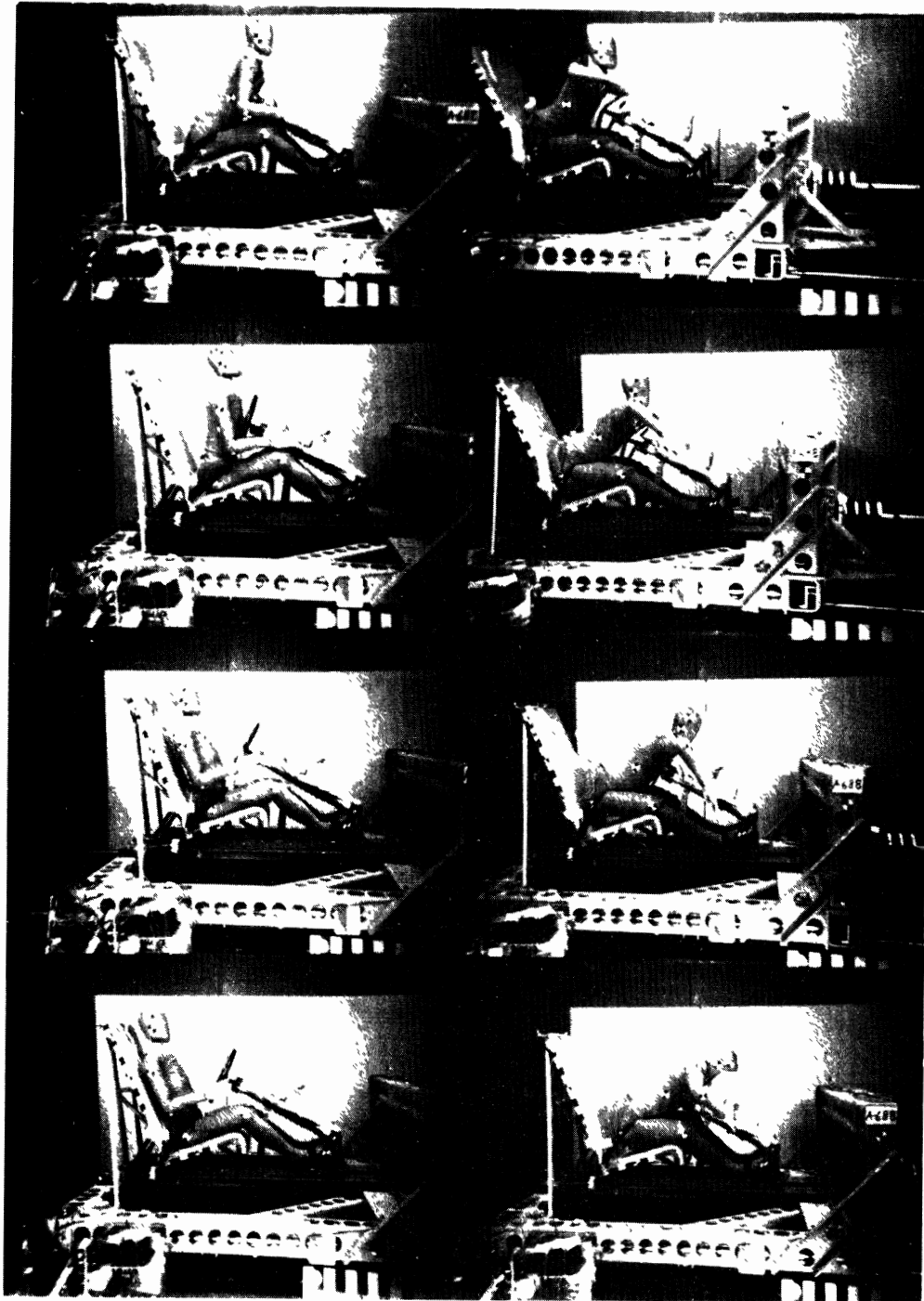
Mean = 115 G Range = 100 - 130 G σ = 9.9

- Head Severity Index:

Mean = 1807 Range = 1540 - 2020 σ = 175.9

- HIC:

Mean = 1439 Range = 1320 - 1561 σ = 86.8



8

1

Figure 80 Mode IV: Sequence Photo of Impact

TABLE 13
DATA SUMMARY: STEERING WHEEL IMPACT TESTS

| Test No. | Dummy No. | Head | | | Chest | |
|--------------------|-----------|--------------------|----------------|------|--------------------|----------------|
| | | Resultant Peak G's | Severity Index | HIC | Resultant Peak G's | Severity Index |
| A-684 | 1 | 130 | 2020 | 1561 | 38 | 240 |
| 685 | 1 | 110 | 1640 | 1370 | 42 | 240 |
| 686 | 1 | 100 | 1540 | 1320 | 46 | 260 |
| 687 | 1 | 118 | 1900 | 1440 | 48 | 280 |
| 688 | 1 | 122 | 1980 | 1540 | 44 | 260 |
| 689 | 1 | 108 | 1760 | 1403 | 46 | 260 |
| Average | | 115 | 1807 | 1439 | 44 | 257 |
| Standard Deviation | | 9.9 | 175.9 | 86.8 | 2.8 | 13.8 |
| A-678 | 2 | 130 | 1660 | 1440 | 56 | 340 |
| 679 | 2 | 96 | 1640 | 1396 | 44 | 260 |
| 680 | 2 | 112 | 1800 | 1410 | 48 | 300 |
| 681 | 2 | 124 | 1900 | 1490 | 38 | 320 |
| 682 | 2 | 108 | 1640 | 1422 | 38 | 220 |
| 683 | 2 | 122 | 2000 | 1580 | 44 | 240 |
| Average | | 115 | 1773 | 1456 | 45 | 280 |
| Standard Deviation | | 11.4 | 139.3 | 63.4 | 6.2 | 43.4 |

- Resultant Peak Chest Acceleration:

Mean = 44 G Range = 38 - 48 G σ = 2.8

- Chest Severity Index:

Mean = 257 Range = 240 - 280 σ = 13.8

See Figures 73 and 74 for typical pre-test and post-test dummy geometry.

Mode IV tests on dummy # 1 followed the six Mode IV tests on dummy # 2, so for A-684 - A-689, test procedures and equipment replacement techniques were well established. Figure 72 shows steering-column and "head-catcher" pad installations. The latter was used for all steering column impact tests after A-678, in which test the head of dummy # 2 flexed forward over the steering wheel and struck the column support structure. (Note the spike in the head acceleration traces for test A-678 in Appendix B.)

Steering column collapse ranged from a maximum of 4.7 inches (A-684) to a minimum of 3.8 inches (A-689); average collapse was 4.2 inches. Although no exact measure of steering-wheel rim deformation was taken, the rims in all tests did deform in the same manner and to approximately the same extent as the rim shown in Figure 74.

Refer to Tables 9 and 13, and to Appendix B, for data summaries and accelerometer traces, respectively, for tests A-684 - A-689.

10.3.4.2 Dummy # 2 Performance: Steering Wheel Impact Tests A-678-A-683.

- Resultant Peak Head Acceleration:

Mean = 115 G Range = 96 - 130 G σ = 11.4

- Head Severity Index:

Mean = 1773 Range = 1640 - 2000 σ = 139.3

- HIC:

Mean = 1456 Range = 1396 - 1580 σ = 63.4

- Resultant Peak Chest Acceleration:

Mean = 45 G Range = 38 - 56 G σ = 6.2

- Chest Severity Index:

Mean = 280 Range = 220 - 340 σ = 43.4

See Figures 73 and 74 for typical pre-test and post-test dummy geometry.

The first six steering-wheel impact tests were run with dummy # 2, and the results of the first test uncovered a minor problem. Despite a lap belt, the dummy moved far enough upward and forward to allow the head to flex over the wheel rim and to strike the column support structure. The solution was the installation of the balsa/styrofoam "head catcher" pad shown in Figures 72 - 74. The purpose of the pad was to provide a repeatable contact surface for the head, and to protect the head from sharp edges and protrusions on the column support structure.

Steering column collapse for the six tests ranged from a maximum of 4.4 inches (A-679 and A-681) to a minimum of 3.8 inches (A-682); average collapse was 4.2 inches. No quantitative measure of rim damage was made, but all deformed in similar fashion to the rim shown in Figure 74.

Following tests A-679, data recording was switched to the Consolidated Electronics Corp. magnetic tape recorder, due to persistent problems with one record channel on the Honeywell recorder. The switchover caused no complications, and all data for tests A-680 - A-689 were recorded with the CEC unit.

Refer to Tables 9 and 13, and to Appendix B, for data summaries and accelerometer traces, respectively, for tests A-678 - A-683.

11.0 MAINTENANCE MANUAL

11.1 Introduction

The HSRI Crash Test Device is designed to assure repeatability and reproducibility of test results. For this reason there are no adjustments required.

In addition, all instrumentation locations are easily accessible. However, in case the results of a particular test are doubtful, the test device should be taken apart and all parts should be inspected for damage. Due to the very demanding environment, it is recommended that periodically all screws and belts should be checked for tightness. This is a simple procedure, once the covering is opened.

It is our intent that based on further experience, to be gained during the coming year, we will recommend more specific maintenance procedures.

In the mean time we suggest periodic total disassembly and inspection of the HSRI Crash Test Device.

This portion of the report is intended to give general guidelines to the user, when he wants to dismantle and reassemble the Crash Test Device for any of the above reasons.

11.2 Instrument Mounting

Specific provisions for instrumentation are in the head, chest and upper legs.

11.2.1 Head

The opening (see Figure 34) in the rear of the head provides easy access to mount either an Endevco Model 7267-C-750 triaxial accelerometer or a Setra Model 113 modular triaxial accelerometer.

To mount the Endevco Triax use two of the four #10-32 tapped holes, located centrally in the mounting surface area of the head (.780 in. apart). For reference see HSRI Drawing number 101-675.

To mount the Setra Triax, first assemble the modular units into mounting bracket (HSRI Drawing number 101-727) using 4 #6-32 x 1.25 in. long socket head cap screws. Then mount P/N 101-727 using 4 #10-32 x 2.0 in. long socket head cap screws into the appropriate threaded holes provided in the head. (See HSRI Drawing number 101-675). Note: There is no room for screws with larger heads.

11.2.2 Chest

The chest instrumentation area can be reached from the back of the crash test device. The recommended procedure is as follows:

Open rear zipper of suit. Remove the 4 #10-32 x 1 3/8 long screws holding the shoulder pad (blue urethane) to the spine.

Folding away the flexible flap of the shoulder pad exposes the spine structure as shown in Figure 49.

Note that the thoracic spine consists of 3 (three) steel boxes interconnected through rubber dampener discs with threaded connecting pins (P/N 100-998-1). See Drawing number 101-729.

Using a standard 1 inch box wrench, reach into the top box (P/N 100-990 and unscrew the top connecting pin (100-998-1). Then remove, through the rear opening of the second box (P/N 101-630) the instrument mounting plate (P/N 101-625 to mount Endevco triax or P/N 101-723 to mount Setra triax).

Note: When reassembling instrument mounting plate make sure that the connecting pin (P/N 100-998-1) is tightened until a solid stop is reached.

11.2.3 Upper Leg

Both upper legs are provided with a femur load-cell blank (P/N 101-746) which can be easily replaced with actual load cells. Each of P/N 101-746 are locked in place using "Adjusto-Fit Blind Bolts. (Adjustable Bushing Corp. P/N ABC 5926) Note: These special bolts require $.500 \pm \begin{smallmatrix} .005 \\ .000 \end{smallmatrix}$ dia holes in the load cell.

The femur load cell is located directly behind the knee joint. One of the special bolts is located in the blue knee cap, the other in the upper leg. Access holes are provided at both locations. (See Figure 81 for locations).

To remove load cell use a long box wrench to loosen nut, while holding the bolt with an allen hex wrench.

Note: do not remove nut completely. When nut is loose, tap bolt lightly to release gripping rings then pull or push out bolt assembly.

When installing load cell, line up through holes in mating parts. Then push the special bolts in as far as nut and washer will allow. To properly tighten Adjusto-Fit Blind Bolts, place allen hex wrench in recess to hold inner bolt from rotating and use a long box wrench to torque nut. As soon as the bushing segments begin to grip bore and inner bolt, hex wrench can be removed to accomodate a torque wrench.

Note: Wrenchings of bolt with hex wrench may result in breaking out hex recess. Bolt should be tightened to a torque value of 450 in-lbs.

11.3 Assembly Procedure

11.3.1 Head

The head itself cannot be taken apart, since as earlier explained, instrumentation is accessible from the outside. The head to neck interface is by means of 4 5/16-18 x 1 3/8 long flat socket head cap screws.

11.3.2 Neck

The neck assembly (see HSRI Drawing No. 101-674) is connected to the torso at the neck adaptor (P/N 100-989) with 4 1/4-28 x 3/4 inch long socket head cap screws.

The neck assembly itself can be disassembled by removing the 1/4 inch diameter spirol pins (4 places). Note: To release shear load on pins, put the whole neck assembly under compression while removing or installing spirol pins.

11.3.3 Covering

The whole crash test device is covered with a one-piece stretch suit. In addition, under the stretch suit, the pelvic region is covered with a vinyl layer. This vinyl layer has a zipper in the back. With the zipper open, the pelvic region covering can be pulled off or put on as a pair of pants.

For easy access to any part of the device, zippers are provided in the following areas of the stretch suit:

A closed ended zipper in the back from the buttocks to the neck.

In the front, the whole chest area of the device can be exposed by opening the zippered flap.

On each side an open ended zipper is located. These zippers start at the wrist, following the underside of the full length of the arm, continue down the side of the torso and along the outside of the legs ending at the ankle.

Finally there is an open ended zipper running from one ankle up along the inside surface of one leg, along the crotch and down the inside surface of the other leg to the ankle.

11.3.4 Arm Assembly

The arm assembly consists of the upper arm, elbow assembly, forearm and the hand. Each arm assembly is connected to the torso with three 5/16-18 x 2 1/2 inch long flat, socket head screws (See Figure 82). These bolts can be reached, after covering is properly opened, by lifting the shoulder pad. When removing arm assembly hold onto the clamp (P/N 100-979) to prevent it from dropping into the chest cavity.

11.3.4.1 The upper arm can be separated from the shoulder plate assembly by removing, on the underside of the shoulder plate, items 6, 7, 8 and 9 of Figure 52 and pulling shoulder plate off the joint shaft. The complete shoulder joint separates from the upper arm by knocking out the 1/4 x 2 inches long roll pin, located about 2 1/2 inches below the shoulder joint, along the upper arm. (Joint assembly procedures are covered in a separate section.)

The elbow assembly slips out of the upper arm after removal of the two 1/4-28 x 1/2 inch long cap screws, located near the upper arm - elbow assembly interface.

11.3.4.2 Elbow Assembly - The elbow is pinned to the forearm with a 1/4 inch diameter pin. After the elbow pivot is separated from the forearm, and the components corresponding to item numbers 6, 7, 8 and 9 of Figure 52 are removed from both sides of the elbow joint, the cast elbow covering can be removed by pushing the elbow pivot (P/N 101-637 through the slot and pulling the elbow joint assembly through the large opening of the cast elbow (P/N 101-714).

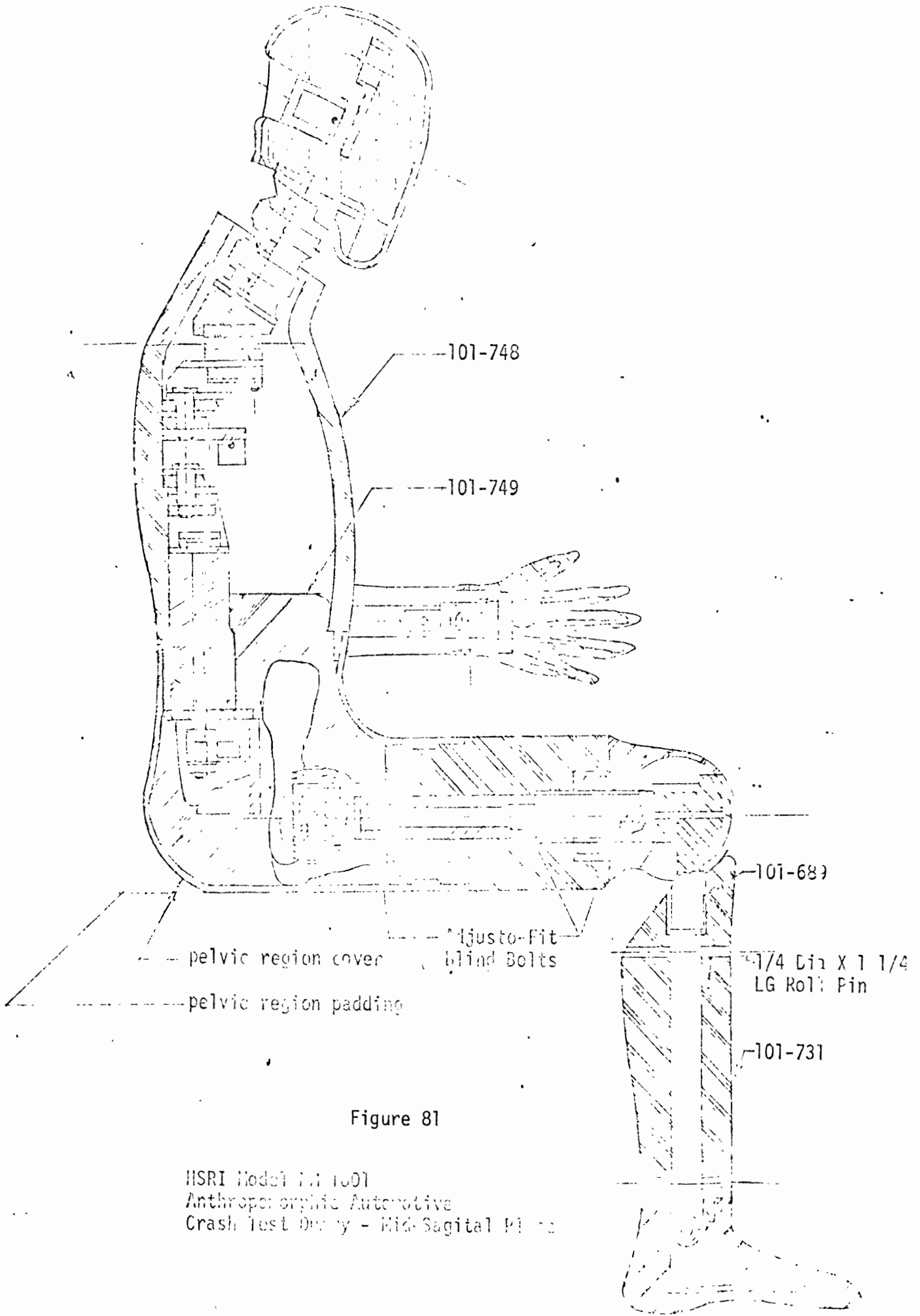


Figure 81

HSRI Model 101-1001
Anthropomorphic Automotive
Crash Test Dummy - Mid-Sagittal Plane

5/16 - 10 x 1/2 10 FL.HD.
SOB. (2 PLCS)
Arm-Torso Connection

134

101-747

1/4 X 2" DILL PIN

100-979 (2 PLCS)

1/4 - 20 X 1/2 - 10
SOC.HD. CAP SOB.

101-714

101-637

101-701

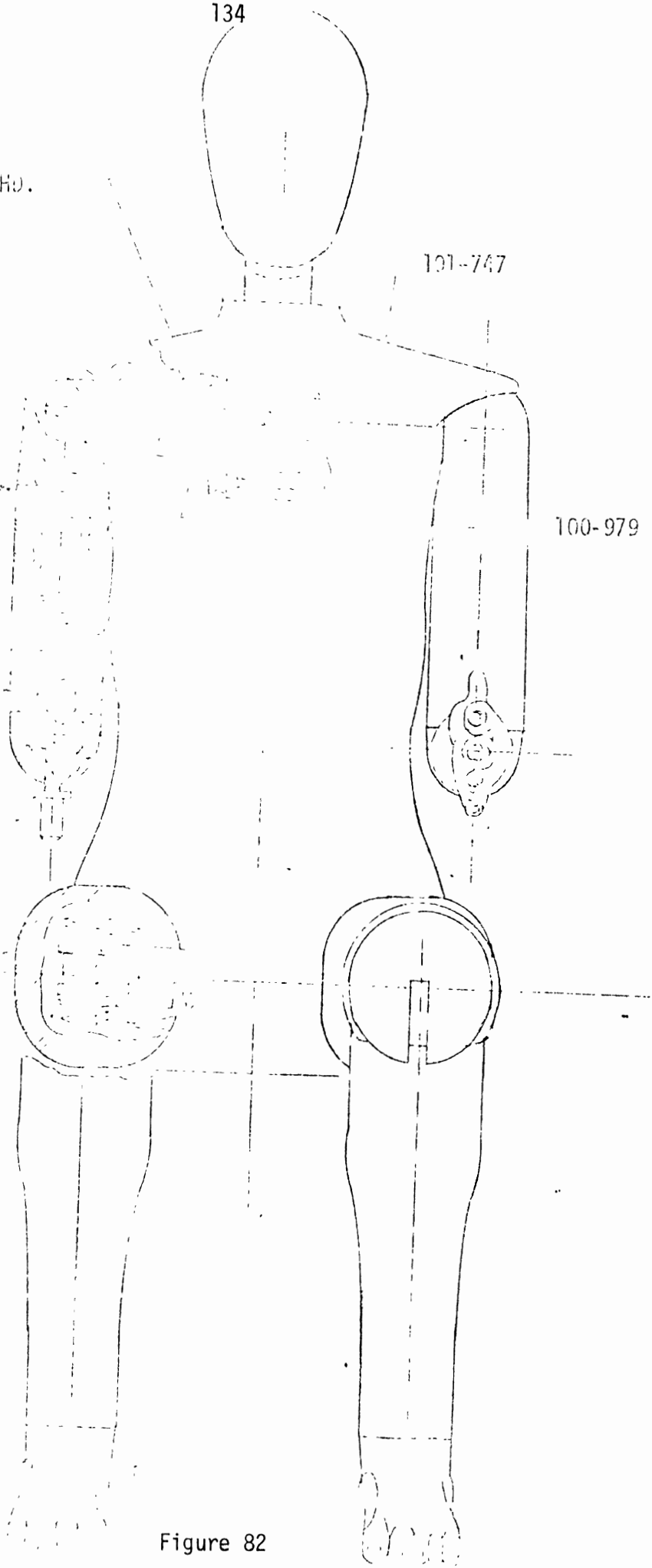


Figure 82

U.S. PATENT OFFICE
Anthropometric Alternative
Chest and Arm - Front View

11.3.4.3 Forearm - The forearm to elbow connection is described in section 3.4.2. The wrist joint and hand is connected with a 1/4 inch pin to the forearm.

11.3.4.4 Hand - The hand can be separated from the wrist joint by dismantling the joint. The joint assembly procedure is described in a separate section.

11.3.5 Leg Assembly

Each leg assembly consists of the upper leg, the load cell (or load cell blank), the knee assembly, the lower leg and the foot. Each leg assembly is connected to the pelvic region of the torso with an "Adjusto-Fit Blind Bolt" specified and described in paragraph 11.2.3 of this maintenance manual.

11.3.5.1 Upper leg - The upper leg can be separated from the load-cell and knee assembly using the procedures outlined in paragraph 11.2.3.2 of this manual. Follow paragraph 11.2.3.3 for reassembly procedures.

11.3.5.2 Load cell - See paragraphs 11.2.3.2 and 11.2.3.3 under instrumentation.

11.3.5.3 Knee assembly - After the load cell (or load cell blank) is removed, this section can be separated from the lower leg by knocking out the 1/4 x 1 1/4 inch long roll pin below the knee joint, where the knee pivot (P/N 101-689) fits into the lower leg (P/N 101-731).

11.3.5.4 Lower Leg - The lower leg can further be separated from the foot assembly by removing the roll pin just above the ankle joint.

11.3.5.5 Foot - It requires total disassembly of the ankle joint in order to separate the foot from the ankle joint. The joint assembly procedure is outlined in a separate section. If desired, however, to keep the ankle joint intact and yet disconnect it from the foot, this can be accomplished

by removing the 1/4 inch roll pin located in the foot assembly 2.08 inches below the ankle joint centerline (For reference see Drawing 101-670).

11.3.6 Torso

The torso consists of the neck adaptor assembly (P/N 100-988), upper spine assembly (P/N 101-729), cast shoulder pad (P/N 101-747) cast ribcage assembly (P/N 101-748), the cast abdomen (P/N 101-749), the lower spine assembly (P/N 101-742), the Pelvis, the hip joint assembly (P/N 101-704) and the pelvic region covering and paddings.

11.3.6.1 Neck Adaptor Assembly - This assembly provides the connection from the neck assembly (P/N 101-674) to the shoulder assembly as shown on Drawing number 100-975, and to the upper spine assembly (101-729). Once the neck assembly is removed as described in paragraph 11.3.2, the heads of the four (4) 5/16-18 x 3 inches long socket head cap screws that hold these components together becomes accessible. The mating nuts, located within the cavity of P/N 100-990, below the rubber shock mount (100-634) and retainer plate (100-992) can be reached from either the front or the back of the test device. Note when reassembling this section that the top shoulder mount (100-978) is different from the next two (2) shoulder mounts (101-737) in shape.

11.3.6.2 Upper Spine Assembly - Drawing number 101-729 well describes this assembly. Note that both spacer pins (100-998-1) should be tightened until their shoulders stop against the retainer (101-629) or mounting plate (101-624) respectively. For proper line-up of the mounting holes of the ribcage and the rib mounting brackets (101-626, 101-632, 101-718) the upper spine assembly should be completely preassembled before the ribcage is mounted.

11.3.6.3 Ribcage Assembly - The ribcage is mounted to the spine assembly with 24 # 10-32 button head, socket screws. These screws pass through the clearance holes in the plastic of the ribcage and press down the cast in spring steel ribs against the rib-mounting brackets. Note the location of the four (4) mounting holes left open (see Figure 49). These mounting holes are used to attach the cast shoulder pad (P/N 101-747) to the torso, using four (4) #10-32 x 1 3/8 long button head cap screws.

11.3.6.4 Lower Spine Assembly - This assembly is shown on drawing number 101-742. The components are assembled to the machined pelvis (101-697). The pelvis adaptor plate (101-739) is mounted onto the pelvis using one 5/8-18 socket head cap screw which is screwed from the underside of the pelvis, through part number 101-740 as shown on drawing 101-742. Part 101-739 contains three (3) 1/2 dia. x 1 1/4 inches long spirol pins, press fitted, to orient the lumbar spine (101-741) with respect to the pelvis. The pelvis adaptor plate is secured in addition, to the pelvis top, using two (2) 1/4-28 x 3/4 inch long socket head cap screws.

Note: Lumbar cable assembly and spacer ring (101-738) has to be assembled into part 101-631 before P/N 101-631 itself is connected to the Upper Spine Assembly (101-729).

It is recommended that the lumbar spine should be compressed so as to expose the threaded end of the cable assembly to enable the assembler to put on the 7/16-70 nut by hand. Once the nut is threaded on far enough, the cable can be held by the wrench flats from twisting.

11.3.6.5 Hip Joint Assembly - To separate the hip joint assemblies (101-704) from the pelvis, release and remove items 6, 7, 8 and 9 of Figure 52 on the inside of the pelvis. Now, with the exception of the hip joint housing, the joint assembly can be pulled out of the pelvis. Next remove the hip joint housings (101-684) by unthreading the 1/4-28 x 5/8 long socket head

cap screws holding it. When assembling the hip joint, follow the procedures outlined in the next section (11.3.7) which are applicable to all joints. However, mount the hip joint housing to the joint before the complete assembly is attached to the pelvis.

Note: Do not completely tighten the belleville washer stack that will be located on the inside of the pelvis. This will allow ease rotation of the hip joint within the joint housing in order to provide access to each of the five (5) screws, per side, attaching the hip joint to the pelvis.

Once the housing screws are in place, the inner hip joint stack can be tightened until item 8 of Figure 52 is bottomed out.

11.3.7 Joint Assembly Procedure

All joints contain basically the same elements. See Figures 52 and 53 to identify the components by the circled numbers in the following description.

11.3.7.1 Joint components - The pivot, 1, is interlocked with the joint pin, 3, using a spirol pin, 2. The bushings, 5 are press fitted into the clevis, 10. The friction washers, 6, are moving with the pivot with respect to the clevis. This is achieved by the square hole in the friction washer interlocking with the square ends of the joint pin. The joint friction is controlled by the force applied by the belleville spring washer or finger spring washer stacks, 7. The spring compression is controlled by tightening the fine threaded screw, 9, until the spring stop, 8, bottoms out against the end surface of the joint pin, 3.

11.3.7.2 Disassembly - Joint Inspection - To inspect a joint for damage, only items 6, 7, 8, 9 and 11 need be removed.

11.7.3 Assembly - Partial - If the joint was dismantled only as far as paragraph 11.3.7.2 shows, follow the appropriate stack configurations of Figure 54 for the spring washers. It is important to properly line up the belleville spring washers. It is therefore recommended that some kind of fixture should be used to align the stack during the tightening process. Always tighten screw until spring stop is bottomed out.

11.3.7.4 Total Disassembly - For easier handling, it is best to separate the complete joint from the limbs by removing the appropriate spirol pin. The appropriate spirol pin locations were described in the paragraphs describing limb assembly procedures. Then follow paragraph 11.3.7.2 as step one. Next remove spirol pins, 2 and push out joint pin, 3.

11.3.7.5 Total Assembly - Push joint pin, 3, through items 1, 4 and 5 (5 pressed into 10) properly lined up as shown in Figures 52 and 53. Line up through holes of items 3 and 1, then press spirol pin, 2 into place. Next assemble exterior components of the joint as described in paragraph 11.3.7.3.

5/16-18X2 1/2 LG FL.HD.
SCW. (6 PLCS)
Arm-Torso Connection

101-747

1/4 X 2" ROLL PIN

100-979 (2 PLCS)

1/4 -- 28 X 1/2
SOC.HD.CAP SCW.

101-714

101-637

101-704

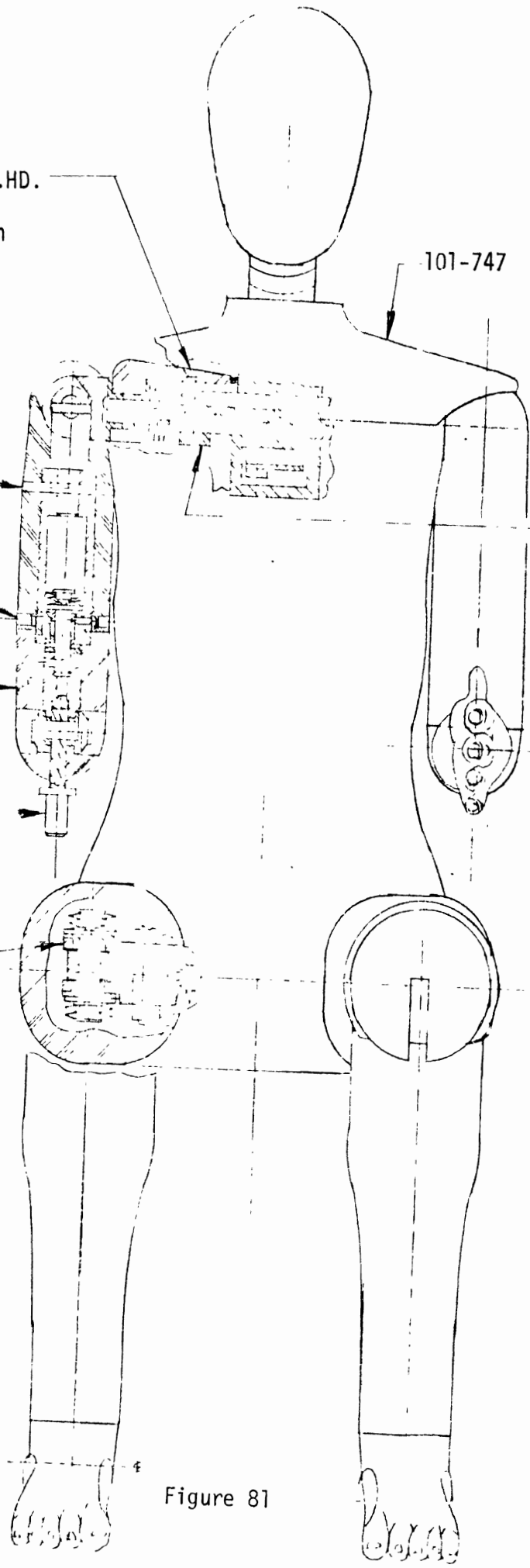


Figure 81

HSRI Model MM 1001
Anthropomorphic Automotive
Crash Test Dummy - Front View

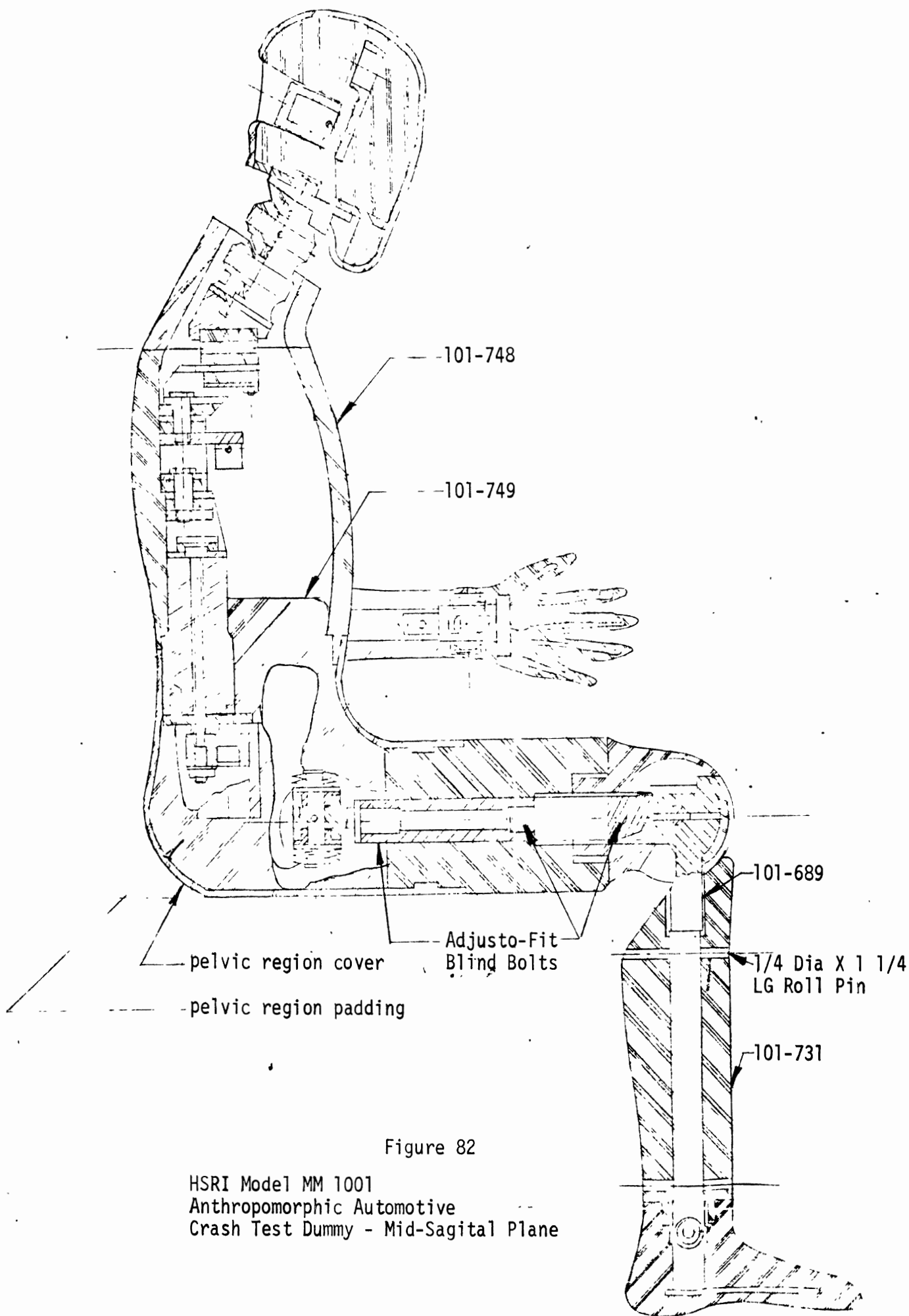
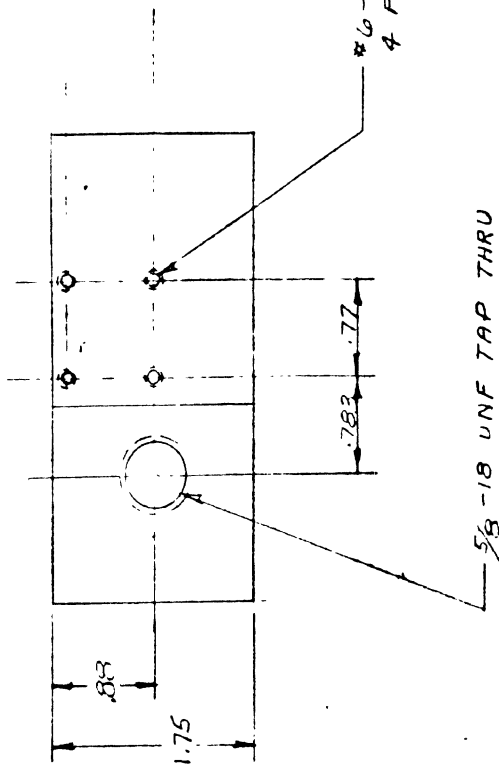
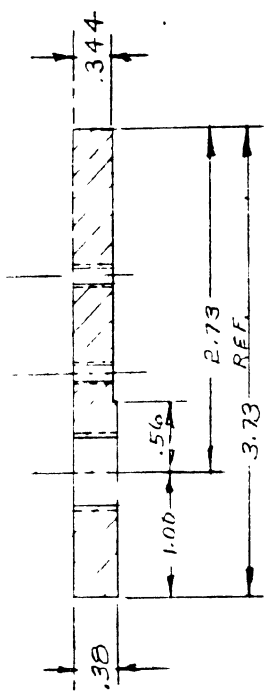


Figure 82

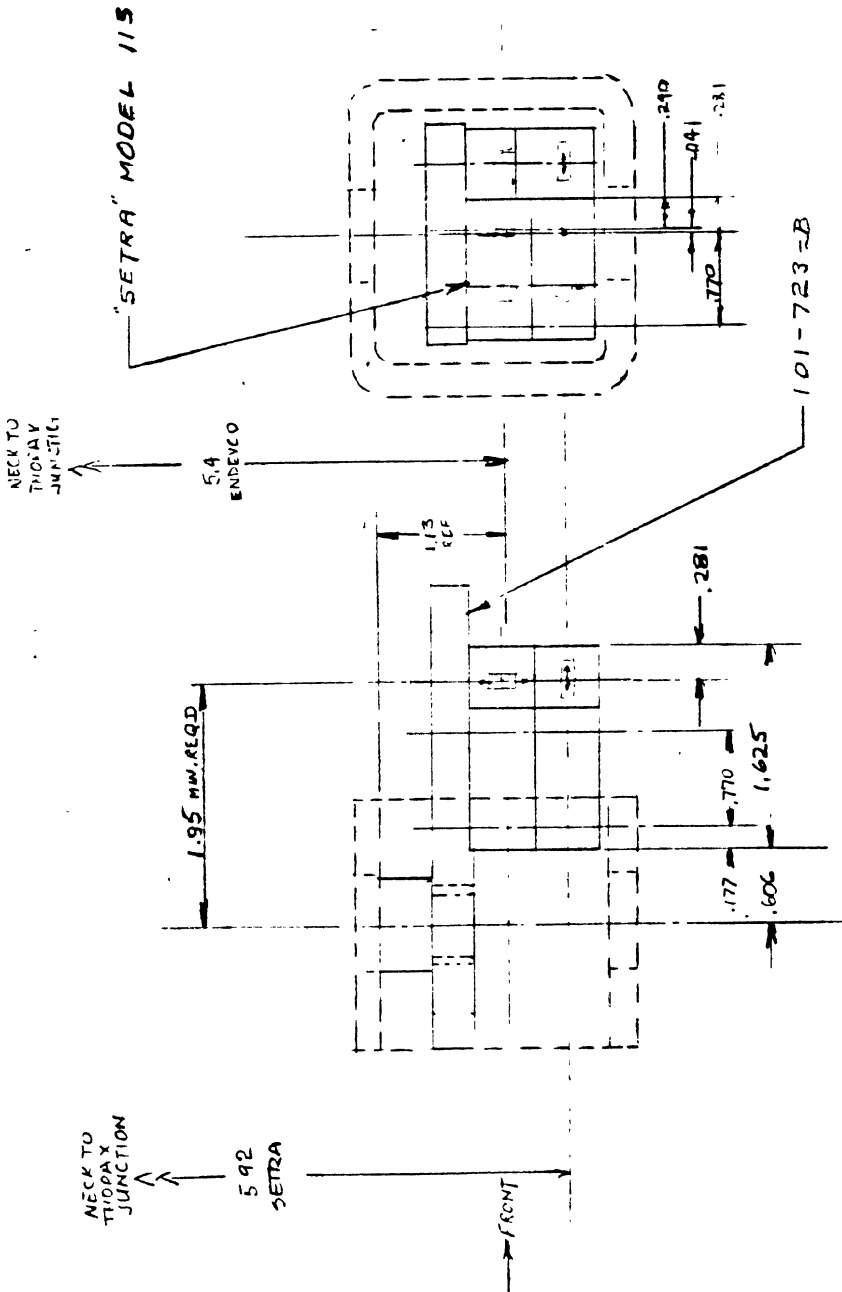
HSRI Model MM 1001
 Anthropomorphic Automotive
 Crash Test Dummy - Mid-Sagittal Plane



TOLERANCES TO BE ± .010, UNLESS OTHERWISE NOTED.
 BREAK SHARP EDGES .010 APPROX.

ALLOWABLE VARIATION IN DIMENSIONS ± .010" UNLESS OTHERWISE SPECIFIED

| | | | |
|---|----------|----------|----|
| DATE | LET | REV | BY |
| | | | |
| HIGHWAY SAFETY RESEARCH INSTITUTE THE UNIVERSITY OF MICHIGAN | | | |
| TITLE | | | |
| 7.0000 | | | |
| MATERIAL SPECIFICATION | SCALE | STARTED | |
| DRAWN | EN | FINISHED | |
| CHECK | APPROVED | W O | |
| PROJECT | DEPT | | |
| MODEL | | | |
| TREATMENT | | | |
| | | | |
| | | | |
| No. 101-725-B | | | |



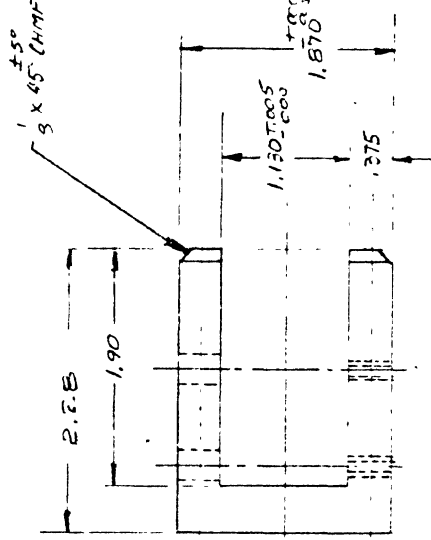
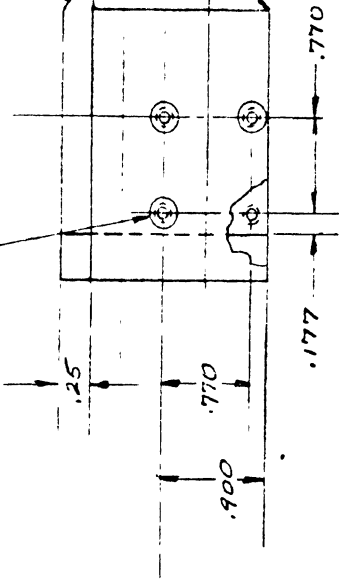
ALLOWABLE VARIATION IN DIMENSIONS ±.010" UNLESS OTHERWISE SPECIFIED

| | | |
|---|---------------|----------|
| DATE | LET | REVISED |
| HIGHWAY SAFETY RESEARCH INSTITUTE THE UNIVERSITY OF MICHIGAN | | |
| TITLE MOUNTING BRACKET FOR SETRA TORSION | | |
| MATERIAL | SPECIFICATION | STARTED |
| SCALE | FULL | FINISHED |
| DRAWN | | APPROVED |
| CHECK | | W. O. |
| PROJECT | | |
| DEPT | | |
| MODEL | | |
| TREATMENT | | |

NO. 101-723-B

.250 DIA. HOLE THRU TOP WALL
#6-32UNC-2B THRD THRU BOTTOM WALL
(TYP) 4 PLCS

1/8 x 45° ± .5° CHAMF

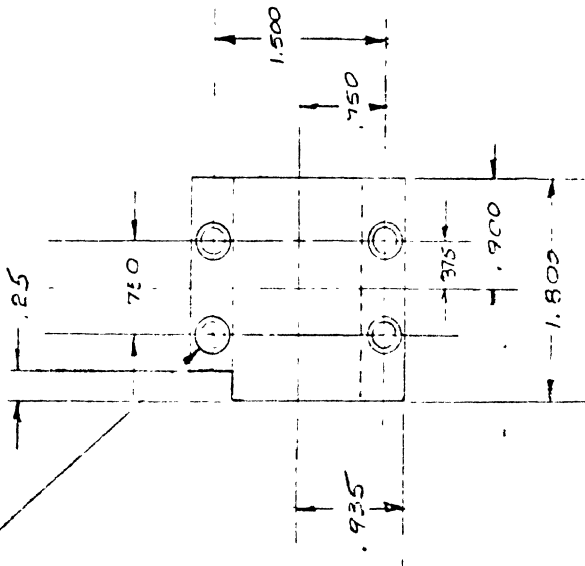


TOLERANCES TO BE ±.010, ±.005
UNLESS OTHERWISE SPECIFIED

SEPAR. SHARP EDGES .010 MIN. DIA.

ALLOWABLE VARIATION IN
DIMENSIONS ±.010" UNLESS
OTHERWISE SPECIFIED

DRILL 1/32 DIA THRU
CO-BORE 5/16 DIA X 1.18 DEEP
(TYP) 4 PLCS



HIGHWAY SAFETY RESEARCH INSTITUTE
THE UNIVERSITY OF MICHIGAN

TITLE

DATE SET UP
BY
F. J. JONES

| | |
|----------|------|
| STARTED | DATE |
| FINISHED | DATE |
| CHECKED | DATE |
| APPROVED | DATE |
| W. O. | |

MODEL

TREATMENT

NO. 1 2 3 4 5 6 7 8 9 10 11 12 13 14 15 16 17 18 19 20 21 22 23 24 25 26 27 28 29 30 31 32 33 34 35 36 37 38 39 40 41 42 43 44 45 46 47 48 49 50

